Bioencapsulation of oxidases and dehydrogenases using electrochemically-assisted sol-gel deposition on the nanoobjects network

Ievgen Mazurenko

U.F.R. FACULTE DES SCIENCES & TECHNIQUES
Secteur Physique, Géologie, Chimie, Mécanique
Ecole Doctorale Lorraine de Chimie et Physique Moléculaires, SESAMES

Thèse
Présentée pour l'obtention du titre de
Docteur de l'Université de Lorraine
Spécialité : Chimie et Electrochimie Analytiques
Par **Ievgen Mazurenko**

Bio-encapsulation de oxydases et déshydrogénases par électrogénération sol-gel sur réseau de nanoobjets

Soutenance publique prévue le 3 Juin 2013 devant le jury composé de :

Rapporteurs :

Prof. Christel Laberty-Robert	Professeur, Université Pierre et Marie Curie, Paris
Dr. Oleg Zuy	Deputy director of the A.Dumansky Institute of Colloid and Water Chemistry, Kiev

Examinateurs :

Dr. Alain Walcarius	Directeur de Recherche, CNRS, Nancy
Prof. Oksana Tananaiko	Professeur, Université nationale Taras Chevtchenko de Kiev, Kiev

Laboratoire de Chimie Physique et Microbiologie pour l'Environnement (LCPME)
Unité mixte de recherche -URM 7564,
405, rue de Vandoeuvre, F-54600 Villers-lès-Nancy (France)

TABLE OF CONTENTS

TABLE OF CONTENTS 2

ABBREVIATIONS 8

INTRODUCTION 9

CHAPTER 1. LITERATURE SURVEY 11

1.1. General overview of amperometric biosensors 11

1.1.1. Concept of amperometric biosensors 12

1.1.2. Enzyme types used in biosensors 15

1.1.3. The methods of biomolecules immobilization on the electrode surface ... 16

1.2. Amperometric SiO_2-based biosensors 18

1.2.1. Biomolecules encapsulation into the silica-matrix on the electrode surface 19

1.2.2. Methods of thin sol-gel films obtaining on the electrode surface 21

1.2.3. Electrochemically-assisted deposition method 23

1.3. Application of nanomaterials in biosensors development 25

1.3.1. General properties of nanomaterials: nanoparticles, nanotubes, nanofibers. 25

1.3.2. Methods of the electrodes modification with carbon nanotubes. Method of electrophoretic deposition 28

1.4. Amperometric biosensors based on SiO_2 and oxidases 30

1.4.1. Overview of oxidases used in amperometric biosensors 30

1.4.2. Problems of electrochemical detection of H_2O_2 33

1.5. Amperometric biosensors based on SiO_2 and dehydrogenases 34

1.5.1. Overview of dehydrogenases used in amperometric biosensors 34

1.5.2. Problems of electrochemical detection of NAD^+/NADH 36
1.6. Conclusions from the literature survey 38
CHAPTER 2. EXPERIMENTAL PART 40
2.1. Chemicals and reagents 40
2.1.1. Enzymes 40
2.1.2. Reagents for sol-gel synthesis. 40
2.1.3. Reagents for voltammetric measurements. 41
2.1.4. Substances studied for interfering influence. 42
2.2. Apparatus 42
2.3. Argumentation of the choice of objects and methods 44
2.3.1. Modification of electrodes by electrochemically-assisted deposition method 44
2.3.2. Modification of electrodes with carbon nanotubes by the electrophoretic deposition method 45
2.3.3. Voltammetric measurements 47
2.3.4. Surface observations 48
2.4. Calculations based on electrochemical measurements 49
2.4.1. Calculation of apparent Michaelis constant 49
2.4.2. Calculation of the electroactive surface area using dye adsorption 50
2.5. Conclusions to the chapter 50
CHAPTER 3. ENCAPSULATION OF OXYDASES BY ELECTROCHEMICALLY-ASSISTED DEPOSITION OF SOL-GEL BIOCOMPOSITE 52
3.1. Immobilization of glucose oxidase into the SiO_2-film on the surface of platinum nanofibers 53

3.1.1. Morphological and electrochemical characteristics of platinum nanofibers network 53

3.1.1.1. Morphological characterization of platinum nanofibers assemblies. 54

3.1.1.2. Electrochemical properties of platinum nanofibers network. 55

3.1.2. Immobilization of glucose oxidase using electrochemically-assisted deposition method 57

3.1.2.1. Voltammetric characteristics of platinum nanofibers modified with SiO_2-glucose oxidase film 58

3.1.2.2. Influence of the duration of electrochemically-assisted deposition on the amperometric response of immobilized glucose oxidase 60

3.1.3. Comparison of platinum nanofibers and platinum macroelectrode for the immobilization of glucose oxidase 64

3.2. Immobilization of choline oxidase into the SiO_2-film 65

3.2.1. Electrochemical generation of the platinum nanoparticles on the surface of glassy carbon electrode for the choline oxidase immobilization 65

3.2.1.1. Optimization of the conditions of the glassy carbon electrode modification with platinum nanoparticles 66

3.2.1.2. Investigation of the stability of amperometric response of glassy carbon electrode modified with platinum nanoparticles 68

3.2.2. The choice of electrode for the choline oxidase immobilization 70

3.2.3. Immobilization of choline oxidase into SiO_2-film on the surface of gold screen-printed electrode 71

3.2.4. Choice of the deposition potential of the SiO_2-choline oxidase film 72

3.2.5. Investigation of the response stability of gold screen-printed electrode modified with SiO_2-choline film 74

3.2.6. Dependence of the amperometric response of the gold screen-printed electrode modified with SiO_2-choline oxidase film from the choline concentration 77

3.3. Conclusions to chapter 3 78

CHAPTER 4. IMMOBILIZATION OF SORBITOL DEHYDROGENASE ON THE ELECTROPHORETICALLY-DEPOSITED CARBON NANOTUBES 80

4.1. Characterization of the electrophoretically deposited carbon nanotubes layers 81

4.1.1. Morphological characteristics 81

4.1.2. The influence of the duration of deposition on the CNT-layer thickness .. 82

4.1.3. Measurement of the electroactive surface area of CNT-layer 84

4.2. Electrocatalytic properties of CNT assemblies towards NADH oxidation 87

4.2.1. Comparison of the voltammetric characteristics of NADH oxidation on the modified with CNT and non-modified glassy carbon electrods 87

4.2.2. Stability of the NADH voltammetric response 89

4.3. Electrochemically-assisted deposition of SiO_2-sorbitol dehydrogenase film on the CNT-modified electrode 91

4.3.1. Optimization of the parameters of the biocomposite film 94

4.3.2. Analytical performance of the modified electrode 97

4.4. Electrophoretic deposition of macroporous CNT-assemblies for electrochemical applications 98

4.4.1. Fabrication of macroporous CNT-layers on the electrode surface 99

4.4.1.1. Optimization of PS-beads concentration in the suspension 103

4.4.1.2. Methylene green adsorption and electrochemical characterization . 105

4.4.2. Functionalization of the macroporous CNT electrode for (bio)sensing applications 106

4.4.2.1. CNT assembly modification with Pt-nanoparticles for the detection of H_2O_2 106

4.4.2.2. Electrochemical response of NADH on the macroporous CNT-assembly 109

4.5. Co-immobilization of sorbitol dehydrogenase and coenzyme on the macroporous CNT-assembly 111

4.6. Conclusions to chapter 4 113

CHAPTER 5. APPLICATION OF MODIFIED ELECTRODES AS SENSITIVE ELEMENTS OF BIOSENSORS FOR THE DETERMINATION OF SORBITOL AND CHOLINE 115

5.1. Determination of sorbitol using glassy carbon electrode modified with CNT and SiO_2-sorbitol dehydrogenase film 116

5.1.1. Procedure of the amperometric determination of sorbitol using the glassy carbon electrode modified with CNT and SiO_2-sorbitol dehydrogenase film... 117

5.1.2. Interference of some substances on the determination of sorbitol 118

5.1.3. Determination of sorbitol in the food and cosmetic samples 120

5.1.4. Comparison of the standard methods of sorbitol determination with the developed technique 122

5.2. Determination of choline using gold screen-printed electrode modified with film SiO_2-choline oxidase 125

5.2.1. Procedure of amperometric determination of choline using gold screen-printed electrode modified with film SiO_2-choline oxidase 126

5.2.2. Interference of some substances on the determination of choline 127

5.2.2.1. Elimination of interfering influence of ascorbic acid 129

5.2.3. Determination of choline in food products 131

5.2.4. Comparison of the standard methods of choline determination with the developed technique 133

5.3. Conclusions to chapter 5 136

CONCLUSIONS 138

APPENDICES 140

Appendix A 140

Appendix B 140

Appendix C 141

Appendix D 141

Appendix E 142

Appendix F 143

Appendix G 144

REFERENCES 146

ABBREVIATIONS

Pt-Nfb	platinum nanofibers
Pt-NPs	platinum nanoparticles
Tris-HCl	Tris buffer solution
AFM	atomic-force microscopy
CNT	carbon nanotubes
EAD	electrochemically-assisted deposition
GOx	glucose oxidase
GPS	3-glycidoxypropyltrimethoxysilane
AuSPE	gold screen-printed electrode
MG	methylene green
NAD^+	nicotinamide adenine dinucleotide, oxidized form
NADH	nicotinamide adenine dinucleotide, reduced form
PDDA	poly(dimethyldiallylammonium chloride)
PS-beads	polystyrene beads
GCE	glassy carbon electrode
SDH	sorbitol dehydrogenase
SEM	scanning electronic microscopy
ChOx	choline oxidase
CTAB	cetyltrimethylammonium bromide
PBS	phosphate buffer solution
TEOS	tetraethoxysilane

INTRODUCTION

The progress of modern analytical chemistry is closely associated with the increase of sensitivity and selectivity of the analysis, as well as with the development of new equipment that would allow quick and easy analysis of complex objects outside laboratory. These requirements have led to the emergence of a new trend in analytical chemistry – chemical sensors. One of the most promising types of chemical sensors is biosensors, containing bio-recognition element.

Biosensors can be characterized, above all, by extraordinary selectivity due to the high specificity of bio-recognition element, such as an enzyme, allowing in some cases separate identification of stereoisomers. Secondly, biosensors demonstrate fast response time that allows express analysis. Thirdly, the analysis with biosensors is highly sensitive because, in most cases, it refers to the kinetic methods based on measuring of reaction rate.

Biosensors are particularly promising in the analysis of organics, including biologically active substances. Acute need for such analysis is associated with high demands for quality control of food, medicines. It associated also with the importance of the definition of such substances in biological fluids for the purposes of diagnosis of large number of diseases. However, routine analysis of the above objects is complicated by the presence of large variety of components inside the matrix. That leads to the analysis with reduced sensitivity and selectivity. In fact, nowadays only chromatography allows to analyze such objects with confidence, suffering from such disadvantages as long duration and high cost of analysis, complex procedure of sample preparation and high demands for the purity of the reagents. Considering the absence of these disadvantages, biosensors are real alternative to the chromatographic methods in the analysis of organic substances in complex objects.

The research conducted so far for the development of new biosensors is limited, in most cases, to the glucose oxidase as a bio-recognition element. This enzyme allows to implement different approaches for enzyme immobilization on the

electrode surface due to its high activity and stability. At the same time, other available enzymes from the oxidoreductases class, offer more opportunities for the selection of analyte and object of analysis. However, these enzymes can often be characterized by worse stability and activity that prevents the application of traditional immobilization approaches and directs research efforts to finding of new matrices for bio-encapsulation.

One of the promising methods of enzyme immobilization is their encapsulation in thin SiO_2 film on the electrode surface by sol-gel technology. This allows to keep them active and to ensure unhindered access of substrate molecules to the enzyme, increasing the sensitivity of the modified electrodes. The electrodeposition method acquired good reputation for deposition of such films on the electrode surface, allowing to obtain uniform and homogeneous coating. This method was previously proposed in our laboratory for encapsulating of glucose and hemoglobin. Another pathway for increasing of the biosensors sensitivity consists in the use of metallic and carbonaceous nanomaterials, which can be characterized by high surface area and catalytic properties.

CHAPTER 1. LITERATURE SURVEY

1.1. General overview of amperometric biosensors

Development of electrochemical sensors is one of the most popular areas of analytical chemistry, widely developed in recent years. The electrode is used as a transducer in such sensors contributing to their cheapness and availability. Owing to easy registration of electrical signal, electrochemical sensors first reached commercialization and are widely used in clinical, industrial, agrochemical and environmental analysis [1].

Electrochemical biosensors combine the analytical power of electrochemical techniques with unprecedented specificity of biological processes of recognition. The general idea of such sensors is appropriate immobilization bio-recognition element in close proximity to the electrode surface and generating electrochemical (more often amperometric or potentiometric) signal, the magnitude of which depends on the concentration of the analyte. The level of development of modern technologies can get tiny, cheap and easy to use biosensors, which are already exploited in many fields of analytical chemistry - analysis of food [2, 3], the environmental [4] and clinical analysis [5]. Unanimously adopted by the world scientific community as a powerful analytical methods, biosensors own chapters in modern textbooks about analytical chemistry [6–8].

The term "biosensor" usually refers to the use of any material of biological origin as a recognition element. Microorganisms, organelles, nucleic acids, antibodies, they all find their application in biosensors. However, the most popular are biosensors, containing an enzyme (s). This is because of relative simplicity of their preparation and the fact that enzymes, conceived as natural catalysts, are characterized by high specificity, efficiency and response rate. Therefore, below the term “biosensors” will refer to enzyme-based biosensors.

1.1.1. Concept of amperometric biosensors

Unlike many chemical reactions, electrochemical processes always occur at the interface between the electrode and the solution. Depending on conditions, the electrochemical measurements can be carried out in potentiometric (equilibrium) or potentiostatic (nonequilibrium) modes. In the first case, the experiment is carried out in static mode with no current flowing through the electrochemical cell. The established potential of electrode allows to determine the concentration of analyte in solution. Potentiometry - an important method in analytical chemistry, and new ion-selective membranes that have been developed over the past 10-20 years, allow direct monitoring of many ions in complex samples using this method [9].

Potentiostatic or voltammetric methods of analysis are based on dynamic non-equilibrium situation, when applied to the electrode potential induces electrochemical reactions at the electrode-solution boundary. The electric current passing through the cell is different from zero. This current can be used for the characterization of occurring reaction and for detection any electroactive substances in solution. The advantages of voltammetry are a high sensitivity and selectivity, wide linear range, portable and cheap equipment, and a large number of different available electrodes [10].

Immobilized on the electrode enzyme catalyzes some reaction, which can be schematically represented as follows:

$$\text{Substrate + Co-Reactant(coenzyme)} \xrightarrow{enzyme} \text{Product + Co-Reactant(coenzyme)'},$$

Therefore the choice of transducer depends primarily on the enzymatic system that is used in each case. For example, the enzymatic reaction of urease leads to changes in pH, so the best choice is pH-sensitive electrodes, while decarboxylase initiating carbon dioxide release can be used together with potentiometric gas sensors. However, the use of voltammetry is advantageous for most enzymes, because of release or consumption of electroactive substances easily detectable with electrodes.

Historically amperometric biosensors can be divided into three generations [11] (Fig. 1.1):

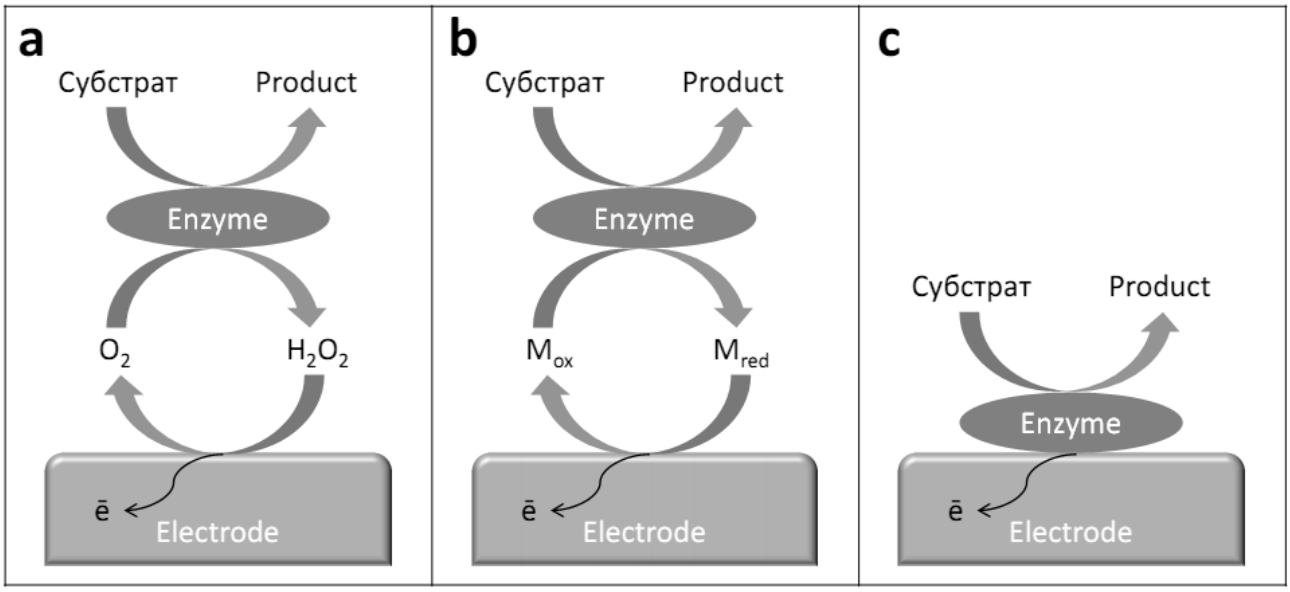

Fig. 1.1. Schemes of amperometric biosensors of 1st (a), 2nd (b) and 3d (c) generations.

1) In the first-generation biosensors (Fig. 1.1a) the enzymatic oxidation of the substrate involves participation of dissolved oxygen. The first such biosensor was developed on the basis of glucose oxidase and Clark oxygen electrode [12]. It allowed to measure the concentration of glucose by detecting the decrease in the concentration of dissolved oxygen consumed as a result of enzymatic reaction [13]. However, these biosensors have significant limitations invoked by the need to maintain a constant concentration of dissolved oxygen and very low potential of its reduction (-0.7 V). Therefore, cathodic reduction of oxygen has been replaced by anodic oxidation of hydrogen peroxide released as a result of the reaction.
2) The second generation biosensors (Fig. 1.1b) uses so-called mediator or electrons-carrier involved in the enzymatic reaction. Mediators are usually molecules that can be easily and reversible oxidized and reduced on the electrode at low potential (e.g., ferrocene and ferrocyanides). Their role is electron transfer from the molecule of the enzyme to the electrode, inducing current, which depends on the substrate concentration. The use of mediators

gave a significant boost to the development of new types of biosensors, while the problems remain such as an effective mediator immobilization on the electrode surface and very strict demands to the molecule (low redox potential, pH independence, lack of reaction with other components of biosensors) [14].

3) Third-generation biosensors (Fig. 1.1c) operate on the basis of direct electron transfer between the electrode and the active center of the enzyme. This approach makes possible getting rid of any intermediary molecules and almost directly converts the concentration of the substrate on the measurable electrochemical signal. However, the design of such biosensors is not easy task, especially because the electrochemically-active group of the enzyme is usually located deep inside of the protein molecule beyond the shield protein groups [15].

Regardless of biosensor's generation, the enzyme must be firmly fixed in close proximity to the electrode, and the unobstructed diffusion of substrate to the enzyme as well as the reaction products to the electrode must exist.

As noted above, the concentration of analyte in solution is determined by the amount of current flowing through the working electrode. There are two methods of its measurement that can achieve the best results. The voltammograms (linear or cyclic) are being obtained by gradual change of the potential at the working electrode at a certain rate. The electrochemical reaction occurs at some point characterized by increased current and peak appearance at the voltammogram. The value of the peak is proportional to the concentration of electrochemically-active substances according to the equation of Randles-Sevcik [11] (see Appendix B)

However, the methods with potential scanning is not very practical for the applications in biosensors due to the impact of charging current of the electrical double layer [16] and the considerable time required for one scan. A more convenient method is amperometry, where a constant potential is applied to the working electrode inducing an electrochemical reaction. At such conditions current firstly

decreases sharply due to the depletion of near-electrode layer, and then goes to the constant value, which can be calculated from the modified equation Cottrell (see. Appendix B). The value of quasistationary current under these conditions depends on the concentration of electrochemically-active substances, and the use of stirred solution reduces the thickness of the diffusion layer and leads to increased current.

1.1.2. Enzyme types used in biosensors

Enzymes – substances of protein nature that catalyze chemical reactions in living systems. At present several thousands of individual enzymes existing in living organisms are known [17]. The International Union of Biochemistry and Molecular Biology has developed a 4-levels system of their classification and nomenclature in accordance with the type of reaction accelerated by corresponding enzyme [18]. According to this classification oxidoreductases are the first, and probably one of the largest classes among 6 types of enzymes. Such enzymes catalyze biological redox reactions that transfer electrons from one molecule to another. These enzymes are ideal for the creation of electrochemical biosensors given that all enzymatic reactions of oxidoreductases involve the electron transfer from one molecule to the other.

Oxidoreductases class can be divided into two subclasses, depending on the type of oxidant used. If molecular oxygen acts as an electron acceptor, thus turning into a molecule of hydrogen peroxide, these enzymes belong to oxidases. If a special molecule (coenzyme) acts as oxidant, these enzymes belong to the subclass of dehydrogenases. Among the variety of coenzymes (PQQ, FMN, TPP, Coenzyme A etc.), the two of them are most widespread in the oxidoreductase class: the nicotinamide adenine dinucleotide (NAD or NADP) or flavin adenine dinucleotide (FAD). These molecules are able to be oxidized and reduced in a reversible redox process.

The wide popularity of oxidases as biosensors sensitive elements is primarily evoked by relative ease of electrochemical detection of hydrogen peroxide at metallic electrodes. The electrochemical detection of dehydrogenases coenzyme

NAD^+/NADH is complicated (see paragraph 1.5.2), but they are also widely used in the development of biosensors.

1.1.3. The methods of biomolecules immobilization on the electrode surface

Biomolecules such as enzymes may lose their activity quickly in aqueous solutions because of their gradual oxidation or destruction of quaternary structure on the edge of the liquid/air [19]. Given the relatively high cost of pure enzyme preparations their cost-beneficial use requires the reusability of enzyme based biosensors. For this reason, the use of enzymes in solution is an exception, and research efforts are aimed at finding new ways of enzyme immobilization, i.e. attachment to the surface.

When choosing an immobilization method one should pay attention to the retention of enzyme activity and conformation of the active center. In addition, enzyme should be in biocompatible environment protected from microbial attack and pollutants. Substrate molecules should be able to diffuse freely to it from the external solution [20, 21]. Biosensors characteristics are very dependent on the method of enzyme immobilization. The purpose of this immobilization is to ensure close contact between the enzyme and the transducer, while maintaining (and sometimes even improving) stability of the enzyme. There are physical and chemical methods of immobilization, which consist in the following [22, 23]:

1) Adsorption. A simple and cheap method, but it is often reversible, i.e. enzyme gradually desorbs from the surface during measurements. This leads to poor stability of biosensors.
2) Micro-encapsulation using solid or liquid membranes. This method is often used in first biosensors, it allows to place the biomolecules inside the semipermeable membrane in close contact with the transducer. The disadvantage of this method is the complexity and high cost of such membranes, and, most importantly, complicated diffusion of reactants through the membrane.

3) Encapsulation. The enzyme is mixed with a solution of polymer and then the polymerization is initiated. The result is a gel containing encapsulated enzyme. The absence of chemical bonding and biocompatible environment makes the enzyme more active. Unfortunately, enzyme can leach from the gel over time, resulting in signal loss.
4) Crosslinking. The enzyme is bound using so-called bifunctional reagents such as glutaraldehyde, which could form a Schiff base with aminogroups of the protein. The mild binding method almost does not change steric configuration of the enzyme, but such electrodes are characterized by low mechanical properties and diffusion of the substrate through the material is rather slow.
5) Covalent binding. The chemical binding of the enzyme to the carrier by a variety of functional groups is used. This method provides the best stability of the immobilized enzyme, however, it is difficult and tedious, with a lack of results reproducibility. In addition, the chemical binding leads to disruption of steric configuration of the enzyme molecule, which leads to the degradation of its activity and denaturation.

Summing up the above, the choice of method of immobilization depends on the each particular case [24]. However, it can be concluded that very tough or very weak binding of the enzyme does not lead to good results because of a lack of the electrode activity or stability respectively. In search of the optimal immobilization method the preference should be given to a "golden mean" – an encapsulation and cross-linking methods, they could provide a strong enzyme fixing together with the preservation of its activity [21].

One of these soft methods is the encapsulation of enzyme in a polymer film of silicon oxide (SiO_2). Such material is biocompatible, has a high porosity and several other important advantages making promising the development of SiO_2-based biosensors [25].

1.2. Amperometric SiO_2-based biosensors

Hybrid silica materials obtained by the sol-gel technology are widely used in electroanalytical chemistry [26]. Interest to these materials is due to ease of synthesis, and their unique properties, including a variety of chemical compositions and structure (in the form of monoliths or thin films). Being solid inorganic substances, they have a high specific surface area (200-1500 m^2/g) at the same time and three-dimensional structure, consisting of a large number of open interconnected pores. It provides a high diffusion rate of analytes inside. Together with lots of available active sites this is a key factor in the development of highly sensitive electrochemical sensors [27]. Another advantage of silica-based materials is the ease of modification with various mediators that can alter their characteristics, increasing the selectivity analysis or providing electrocatalytic properties [27, 28].

Recently it was shown that these materials can also be used to encapsulate biomolecules preserving their activity [29–31]. Silica-materials possess several key characteristics that make them promising for bioencapsulation. Simple low-temperature synthesis method avoids protein denaturation and unique approach of polymer chains formation around the enzyme molecule, does not lead to a violation of its steric configuration [25]. These materials may contain a high amount of water in the structure that improves the long-term stability of immobilized biorecognition elements [32]. In addition, silica-materials have excellent biocompatibility and ability to protect against microbial attack [33].

However, the SiO_2-based materials have several shortcomings that need to be removed. First, it is a gradual leaching of modifier molecules from the film and the destruction of the film. This problem can be solved by the introduction of the structuring and stabilizing agents (e.g., surfactants and polyelectrolytes) [34–36]. Secondly, it is a need for a uniform distribution of enzymes in the film (without the formation of conglomerates), that can be achieved by selecting the appropriate method of SiO2-film obtaining.

1.2.1. Biomolecules encapsulation into the silica-matrix on the electrode surface

In general, the sol-gel method involves hydrolysis of the precursor (alkoxide) in acidic or alkaline medium with subsequent condensation and polycondensation of monomers leading to the formation of porous gel [37]:

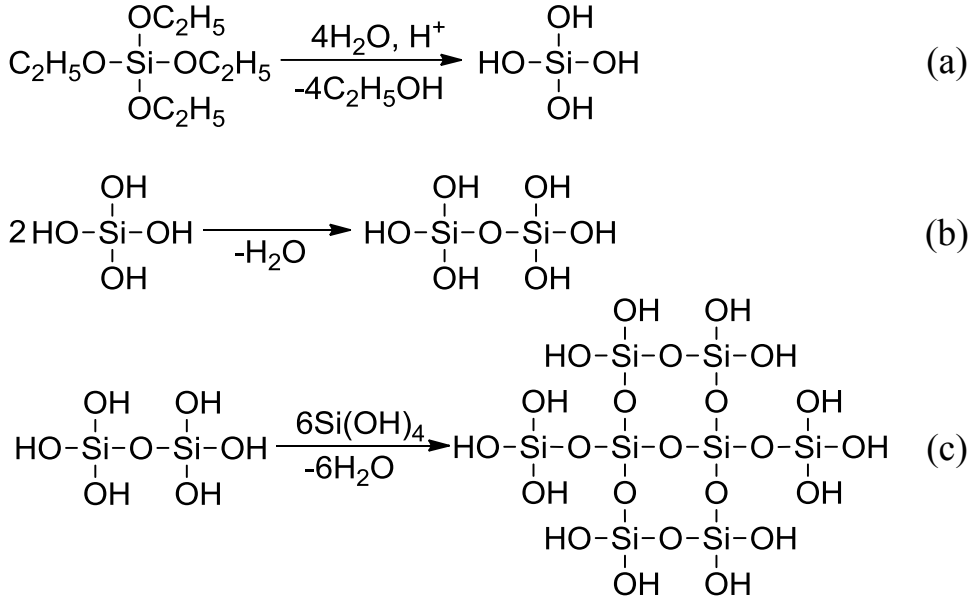

Fig. 1.2. Scheme of reactions occurring during the sol-gel synthesis (on the example of TEOS): hydrolysis (a), condensation (b), polycondensation (c).

The properties of the formed gel, such as porosity, surface area, polarity, hardness, largely depend on the rate of hydrolysis and condensation reactions (Fig. 1.2), as well as on the choice of the precursor, molar ratio, choice of solvent, temperature, processes drying and aging [38]. Moreover, the process of aging may occur long time after the formation of the gel, forming additional bonds inside sol-gel matrix. During the aging process the solvent can be removed from the pores, which leads to a change in polarity and viscosity and to reduction of the pores diameter [37, 39].

For analytical purposes, sol-gel materials can be obtained either as monoliths or thin films [25]. Monoliths can be from hundreds of micrometers to several centimeters of thickness and can effectively immobilize large number of

biomolecules that are kept inside because of its size and molecular weight. However, the main drawback of monoliths is very large response time due to slow diffusion. In addition, they usually do not find their use in electrochemistry due to lack of conductivity of thick layers of silica. One way to solve this problem can be the creation of composite bioelectrode [38] by mixing the sol-gel precursor with enzyme and conductive materials – carbon paste [40], graphite [41] or metal particles [42].

At the same time, thin sol-gel films with thickness less than one micrometer offer significantly faster diffusion of analyte to biorecognition centers guarantying fast response. Therefore they are considered more promising for application in electrochemical sensors [31].

There are several ways of enzyme immobilization within the sol-gel film on the electrode surface:

Covalent binding of the enzyme to the SiO_2-matrix (Fig. 1.3) by carbodiimide coupling reaction was used for glucose oxidase [43] and lactate dehydrogenase [44], but this method has not gained widespread use due to the loss of enzyme activity as result of binding to hard matrix.

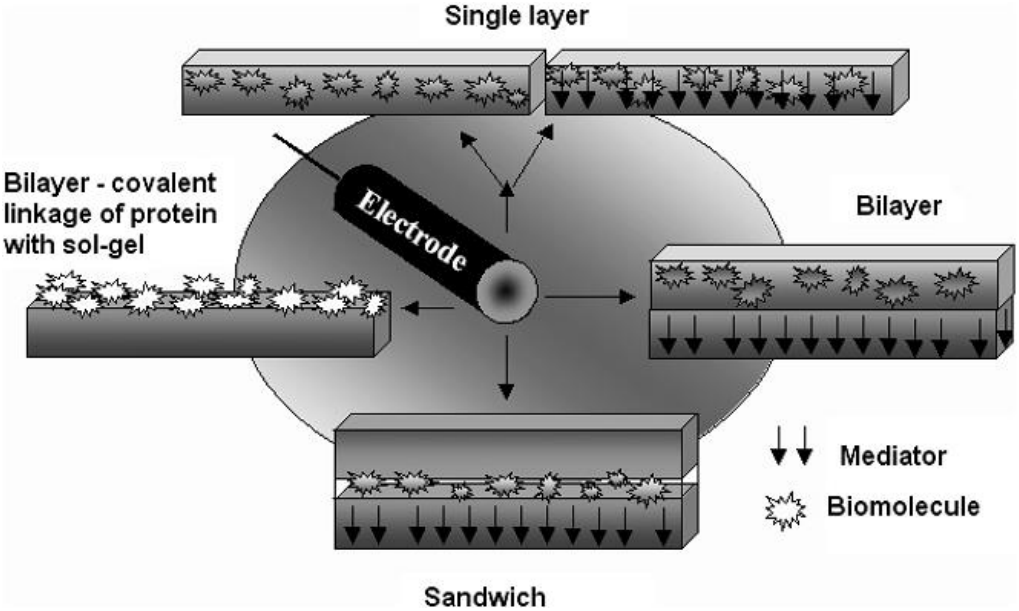

Fig. 1.3. Scheme of different biosensor configurations based on the sol-gel-materials [33].

The so-called «sandwich»-configuration (Fig. 1.3) imply enzyme placing between two layers of sol-gel film. Such configuration have been used for the first time for glucose oxidase in work [45] and shown higher activity and fast response compared to conventional methods. Later it was also used for lactate dehydrogenase [46, 47]. Unfortunately, the result of this configuration is uneven distribution of the enzyme throughout the film-modifier reducing the reproducibility of the analytical response.

Double-layer SiO_2-film (Fig. 1.3) was used for immobilization of lactate oxidase [48] and peroxidase [49, 50], together with the osmium redox mediator. But the enzyme and the mediator in this configuration may contact only at the boundary between two layers, making efficiency of such biosensors significantly lower.

The encapsulation of enzyme in whole thin SiO_2-film (with or without a mediator) is one of the most popular methods. Thus, a uniform distribution of modifier-molecules in the film and close contact with the electrode can be achieved. The important key factors of thin film formation are homogeneity and thickness of the film, adhesion to the electrode, resistance to cracking and minimization of possible enzyme leaching. The film thickness is a major parameter for the obtained modified electrodes, as its increase slows diffusion of the analyte to the active centers inside the film, reducing the response [33]. However, the amount of immobilized enzyme is low in very thin films, which also leads to the signal drop.

1.2.2. Methods of thin sol-gel films obtaining on the electrode surface

The main methods for the obtaining of thin sol-gel coatings on the surface of the electrodes is dip-coating and spin-coating [51], less common methods are drop-coating and spray-coating (Table 1.1).

Table 1.1

Main methods of sol-gel films obtaining

Method	Advantages	Drawbacks

Drop-coating	Simplicity	Impossibility of the thickness control, irregularity of drying, cracking
Spray-coating	Possibility of complex morphology objects modification	Impossibility of the thickness control, irreproducibility
Dip-coating	Homogenous coatings, possibility of the thickness control	Impossibility of complex morphology objects modification
Spin-coating	Reproducible coatings, possibility of the thickness control	Impossibility of complex morphology objects modification

Despite the variety of methods for the obtaining of thin sol-gel films several difficulties need to be got round on the road to a successful application of such films in biosensors [25]. Firstly, most of the techniques do not allow to reproducibly modify surfaces with complex morphology, such as fibers. Second, for achievement of measurable signal level, thin films require large biomolecules content, and this can create problems for the enzymes that are insoluble or precipitate in the sol. Thirdly, homogeneous films often require the presence of significant amounts of alcohol as a viscosity modifier, that can lead to denaturation of immobilized biomolecules. Finally, unlike the monoliths with slow processes of drying and aging, these processes for thin films occur simultaneously and very fast. This could potentially lead to the film cracking and dehydration of immobilized biomolecules.

Thus, the researchers face with the task of developing new, simple and effective ways of electrodes modification with bio-composite films SiO_2-enzyme that would allow to solve the above problems. One of the promising methods that can be used for this purpose is electrochemically-assisted deposition.

1.2.3. Electrochemically-assisted deposition method

The method of electrochemically-assisted sol-gel deposition (EAD) is a relatively new way for getting thin coatings, it was first described in 1999 [52]. This method now can be applied only to the conductive surfaces, but can solve the basic problem of the traditional methods of sol-gel processing – impossibility of modification of surfaces with complex morphology and small size [53].

This method consists in immersion of the electrode in a solution of pre-hydrolyzed sol-gel precursor and application of sufficient negative potential (EAD at positive potential is also possible [54]) over some time (Fig. 1.4):

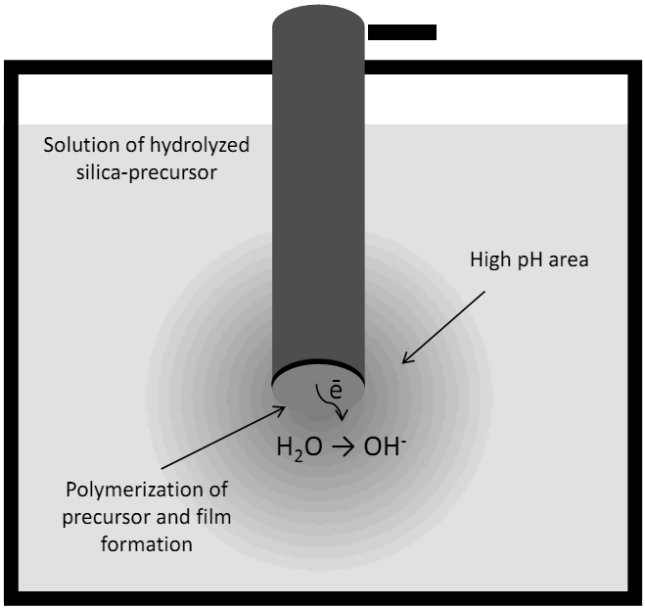

Fig. 1.4. Scheme of electrochemically-assisted deposition.

When applying a negative potential to the electrode the reactions of water (and oxygen) reduction are occurring according to the scheme [55]:

$$2H_2O + 2\bar{e} \rightarrow 2OH^- + H_2$$
$$O_2 + 2H_2O + 4\bar{e} \rightarrow 4OH^- \quad (1.1)$$
$$O_2 + 2H_2O + 2\,\bar{e} \rightarrow H_2O_2 + 2OH^-$$

Hydroxyl-ions generated by these reactions, enhance pH in the near-electrode area, significantly accelerating the polycondensation reaction of SiO_2-precursor (Fig. 1.2b, c) and the formation of SiO_2-film on the electrode surface. Since the time of

potential application is typically less than a few minutes and even seconds, it does not lead to significant changes in the overall pH of the whole solution. Thickness of the formed film can be easily changed by controlling the value [52] and time [56] of negative potential applying. This affects the amount of the formed catalyst (OH^--ions) and thus – the rate of the precursor polycondensation. In particular, the EAD method was used to obtain ultra-thin SiO_2-films with ordered vertically-oriented pores [57].

Since the gelation and drying processes during EAD occur independently of each other, coatings obtained by this method are much more porous than ones obtained by classical methods of sol-gel deposition [26, 54]. The higher number of pores facilitates diffusion of reactants through the film increasing the sensitivity and response time, which is especially important for electrochemical sensors. The addition to the sol-gel solution during EAD can be used for the formation of films containing encapsulated mediators such ferrocenedimethanol and ruthenium bipyridyl [55].

The EAD method is also suitable for the encapsulation of biomolecules, particularly due to lower amount of produced alcohol [54, 55], which is formed during deposition and can lead to denaturation of proteins. It was used for the immobilization of biomolecules such as glucose oxidase [58–60], hemoglobin [36, 60], peroxidase [61]. These biomolecules are among the most stable and can withstand relatively harsh chemical conditions, so widely used in the development of new types of biosensors [62]. However, the application of EAD method for the immobilization of other types of enzymes is still unresolved and poorly researched issue. In addition, owing to the vast possibilities of the thickness control of the formed film this method is of interest for the modification of nanostructured electrodes [53, 56, 63, 64].

1.3. Application of nanomaterials in biosensors development

Nanomaterials having the size less than 100 nm in at least one dimension, are widely used in modern analytical chemistry, particularly in the field of chemical sensors. Their uniqueness is associated with significant differences in the properties of nanosized particles from those of macrosize made from the same material [65]. This creates the possibility of modification of the nanomaterials properties by varying their size [66]. They have exceptional thermal and electrical properties, high activity and surface area, thus can be used to improve the sensitivity and response time of (electrochemical) sensors [67]. Nanosize materials were used for the achievement of direct electron transfer between the electrode and the enzyme, for acceleration of electrochemical reaction, for amplification of the biorecognition element signal etc. [68].

1.3.1. General properties of nanomaterials: nanoparticles, nanotubes, nanofibers.

Nanomaterials that have found application in the development of sensors can be classified by the dimensionality [69, 70]:

zero-dimensional (0D) nanomaterials. These include particles with the size in all three dimensions less than 100 nm, nanoparticles and quantum dots;

one-dimensional (1D) nanomaterials. These particles have a size larger than 100 nm in only one dimension, the two others do not exceed 100 nm. These include a variety of nanofibers, nanotubes, nanowires;

two-dimensional (2D) nanomaterials. Such materials have a size greater than 100 nm in two dimensions, representing a variety of nanosheets and nanofilms with thickness less than 100 nm. In recent years, rapid development of sensors based on this type of material is associated with the discovery of graphene [71, 72].

Although nanomaterials may be made of any material, only metal or carbon nanomaterials and conductive polymers are mainly used in electrochemistry, because of their high electrical conductivity.

Gold and platinum nanoparticles are the most widely used type of nanomaterials for the development of amperometric biosensors [73]. Several layers of nanoparticles deposited on the electrode lead to the formation of porous layer with large surface area, which can adsorb and concentrate a large number of substances [74]. They can also be considered as an array of nanoelectrodes with own advantages [75]. Gold nanoparticles are able to provide stable immobilization of enzymes while preserving their activity, to achieve the direct electron transfer between the electrode and the enzyme without addition of mediators [76, 77]. Platinum nanoparticles are mainly used in amperometric biosensors based on oxidases, due to their ability to greatly facilitate oxidation and reduction of hydrogen peroxide and oxygen [78–80].

However, of the greatest interest in the development of electrochemical biosensors are zero-dimensional materials [67, 70]. Due to the considerable length-to-diameter ratio, they can act as nanowires, increasing conductivity of film-modifier and connecting the electrode surface with molecules encapsulated in the film [67]. Metal nanofibers can be used for direct detection of biological and chemical substances[81], but their use in the design of enzymatic biosensors, except several examples [82, 83], is not enough explored.

Among carbon nanomaterials carbon nanotubes (CNT) attract great interest since their discovery [84]. Single-walled CNT consist of a monatomic layer of graphite rolled into a cylinder, which has a large length-to-diameter ratio. Multi-walled CNT consist of several cylinders of different diameters, placed one inside another (Fig. 1.5).

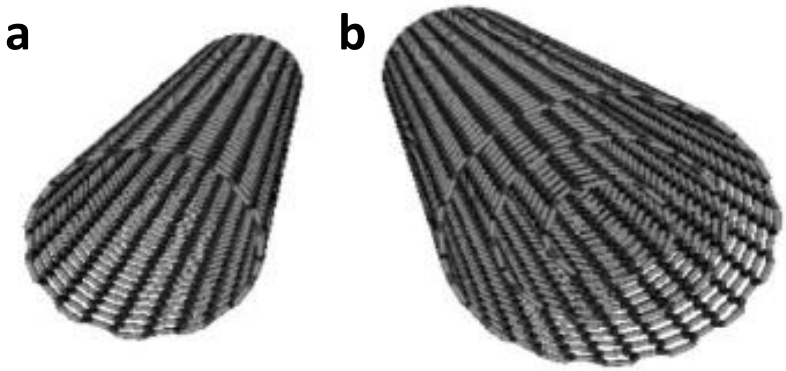

Fig. 1.5. Structure of single-walled (a) and multi-walled (b) carbon nanotubes [85].

CNT have unique electrical, mechanical and structural properties that make them very attractive for use in electrochemical sensors [85, 86]. High sensitivity of CNT conductivity to the adsorbed molecules allows their use as nanoscale DNA-sensors, and the ability to accelerate the electron transfer of many important biomarkers can significantly improve the characteristics of CNT-based enzyme electrodes [87]. Also CNT can accumulate important biomolecules (e.g., nucleic acids [88]), and neutralize the process of the electrode surface poisoning by reaction products [89].

Possibility of H_2O_2 and NADH detection at low potential and limited surface passivation during the oxidation of NADH makes CNT an ideal material for use in amperometric biosensors based on oxidases and dehydrogenases [87] . Moreover, studies have shown that vertically-oriented CNT can be used as a direct conductor between the electrode and the active center of the enzyme (which is usually located deep inside the molecule and isolated by protein chains) that covalently bound to the end of nanotube [90, 91].

1.3.2. Methods of the electrodes modification with carbon nanotubes. Method of electrophoretic deposition

Successful implementation of CNT in amperometric biosensors requires adequate control of their chemical and physical properties, their functionalization and immobilization on the surface [87]. Simple mixing CNT with a solution of the enzyme in most cases leads to very low final concentration of nanotubes and often to enzyme denaturation or aggregation of CNT.

There are two basic approaches for surface modification with CNT: direct synthesis of CNT from metal catalysts located on the electrode surface, or surface modification with pre-synthesized CNT obtained by various techniques. Direct methods of synthesis allow to obtain a big number of firmly fixed on the electrode surface CNT and sometimes even to get vertically-oriented CNT [92]. However, the most synthesis methods require high temperatures, pressures and sophisticated equipment, which limit their use in ordinary laboratories. Therefore most of modified electrodes are being obtained by deposition of CNT dispersion and subsequent drying or preparation of composite electrodes based on CNT mixed with carbon paste [93, 94], teflon [95], polymers [96], ceramics [97].

Because the synthesized CNT usually contain many impurities of other allotropic modifications of carbon their purification before use by treating with acid-oxidants is often necessary [98]. Besides elimination of impurities, this treatment also aims to create carboxyl functional groups on the places of defects in the structure of CNT. The presence of these groups enables covalent immobilization of biorecognition molecules or integration of CNT in polymer structure [99].

The limitation on the way of broad application of CNT in the development of biosensors is their negligible solubility in most solvents (including complete insolubility in inorganic solvents) [100], which makes the preparation of composite electrodes with high content of CNT quite challenging. Moreover, the difficulties of CNT manipulating are related to their small size and tendency to aggregation that prevents the formation of homogeneous and reproducible coatings on the electrode

surface [101]. Therefore, the additives are often used to improve the dispersion of CNT in solvents such as surfactants, nafion, chitosan, DNA and others [102].

Two conditions are desirable for fabrication of enzyme electrodes based on CNT: a) a sufficiently high content of CNT in the final film-modifier in order to take full advantage of their properties, and b) the biocompatibility and mild conditions of bio-composite electrode fabrication to ensure the retention of the enzymatic activity (hence the undesirability of organic solvents and a large quantity of surfactants). Given this, it would be optimal simultaneous deposition and concentration of CNT from the aqueous solution.

Method of electrophoretic deposition (EPD) is widely used in the development of new types of ceramic and biocoatings [103, 104]. It is based on the motion of charged particles in a constant electric field and their deposition on the one of the electrodes (Fig. 1.6). Recently this method has been proposed as a simple and versatile method for the obtaining of homogeneous and reproducible coatings based on CNT [105–107].

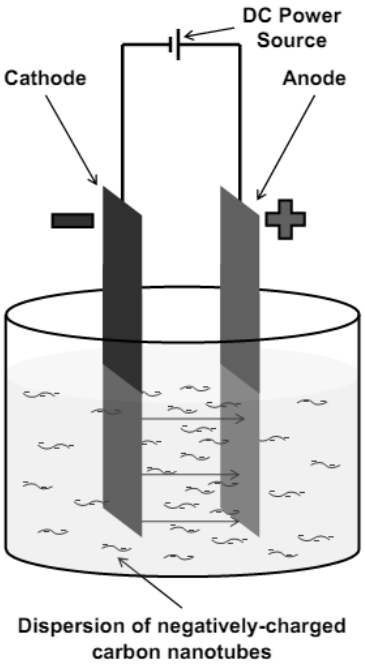

Fig. 1.6. Scheme of electrophoretic deposition of CNT.

To date, CNT-coatings, obtained by this method are mainly used for the creation of new composite materials [108], field emission devices [109, 110], supercapacitors [111, 112], fuel cells [113–115], and for biomedical applications [116–118]. However, the EPD method, due to inherent advantages such as the possibility of CNT deposition from low-concentrated aqueous solutions can be used for the fabrication of CNT-matrix for amperometric biosensors. Currently, in the literature there are only a few examples of electrophoretically-deposited CNT application (as a part of CNT-polyaniline composite) for construction of biosensors based on cholesterol oxidase [119] and glycerol dehydrogenase [120], but the influence of the characteristics of CNT layer in the above works is not discussed.

1.4. Amperometric biosensors based on SiO_2 and oxidases

1.4.1. Overview of oxidases used in amperometric biosensors

Oxidases subclass contains more than 100 enzymes that catalyze specific oxidation of many important biologically-active organic compounds by molecular oxygen [87]. In most cases, enzymatic reactions catalyzed by oxidases are following:

$$Substrate + O_2 \xrightarrow{oxidase} Product + H_2O_2 \quad (1.2)$$

The enzyme glucose oxidase (GOx) – “pioneer” in the field of amperometric biosensors, the rapid development of this industry began from a message about the first GOx-based biosensor [121]. The reason of its popularity is in the spread of diabetes disease, which affects the people around the globe. The regular screening of glucose concentration in the blood becomes for them a daily routine task and amperometric biosensors may be the solution of this problem [122]. However, the popularity of GOx is also linked to its unique properties – a high specificity, activity and stability [62]. That is the reason for its applicability for testing new methods of immobilization, mediators and electrodes. The number of publications that report the use of GOx in biosensors development for the last five years exceeded 2000 [123].

Lactate oxidase – an enzyme that catalyzes the oxidation of lactate to pyruvate and H_2O_2. Determination of lactate in the blood is necessary as a marker during anoxia, shock, breathing problems and heart failure [124]. In addition, monitoring of lactate in the blood is important in sports medicine to assess the physical conditions of athletes [125]. In the food industry it can be determined as an indicator of enzymatic processes associated with freshness and storage conditions of products [126]. However this enzyme is unstable, much less stable than glucose [127], so the search of suitable immobilization methods that could improve long-term stability of lactate oxidase-based biosensors is in progress [128].

Choline oxidase (ChOx) - an enzyme that catalyzes the oxidation of quaternary ammonium salt - choline, which is an important nutrient and involved in the synthesis of the neurotransmitter acetylcholine. Thus, ChOx-based biosensors are used to determine choline in the food – infant formula, vitamins, sports medicine [129] and biological fluids [130]. Its conjunction with the enzyme acetylcholinesterase can be also applied for the determination of acetylcholine levels [131] and pesticides (inhibitory effect) [132, 133].

Tyrosinase and laccase belong to the group of phenol oxidases that catalyze the oxidation of various mono-and biphenyls by molecular oxygen. These enzymes are characterized by low specificity, and by the formation of water molecules instead of hydrogen peroxide in the reaction, making impossible the use of electrodes sensitive to H_2O_2. Another problem is the formation of insoluble products of enzymatic reactions that can be adsorbed on the electrode surface and cause inactivation of enzymes [134]. However, amperometric biosensors based on these enzymes are used to determine the total content of phenol compounds in natural waters [135], polyphenol index in wine [136] and pesticides [137].

Cholesterol oxidase - an enzyme catalyzing the oxidation of cholesterol, is the second most popular enzyme (after GOx), which is widely used in clinical practice [138]. Such biosensors allow to analyze cholesterol in blood plasma. Cholestirol is important because of its involvement in the development of diseases such as

atherosclerosis, coronary heart disease, hypertension and cerebral thrombosis [119, 139, 140]. However, this enzyme should be used in conjunction with cholesterol esterase for the determination of total cholesterol, which is in partially esterified form in the blood [141].

Amine oxidases - this group includes several enzymes from various sources that are specific to low-molecular amines, such as histamine, which is being released during decomposition of amino acids [142]. Biosensors based on this enzyme are used to evaluate the freshness of many food products, including meat and fish [143, 144].

Alcohol oxidase - an enzyme that catalyzes the oxidation of low-molecular monohydric alcohols (especially methanol) to the corresponding aldehydes. Given the necessity of ethanol and methanol identification [145], biosensors based on this enzyme can be used in a clinical [146], judicial, food [147, 148] and agrochemical analysis [149]. The drawback of alcohol oxidase is much lower stability and selectivity compared with other enzyme that can be used for the same purpose – alcohol dehydrogenase [150].

Glutamate oxidase catalyzes the oxidation of glutamic acid and its salts that are often used as a flavor enhancer. Nevertheless, besides food analysis [151], biosensors based on this enzyme are used in clinical analysis [152, 153], since glutamate is also an important mediator linked to the one of the reasons of Alzheimer's and Parkinson's diseases [154].

In addition to the above, there are existing biosensors based on xanthine oxidase, ascorbate oxidase, bilirubin oxidase, lysine oxidase and other enzymes [1].

There is a considerable number of works about the immobilization of mentioned enzymes into SiO_2-film by sol-gel method for the development of amperometric biosensors. This particularly concerns cholesterol oxidase [139, 141, 155–157], lactate oxidase [48, 126, 158, 159], tyrosinase [160–163], glucose oxidase [45, 60, 164–167]. Among other types of enzymes choline oxidase has an important substrate – choline, the determination of which is necessary in biomedical practice as

well as in the analysis of food. In addition, this enzyme can be used to analyze important inhibitors – pesticides. However, in the literature we found only a few reports of the ChOx immobilization in SiO_2-film [168, 169]. Taking into account the mentioned above properties of SiO_2-materials, the development of ChOx- and SiO_2-based biosensors is a promising possibility.

1.4.2. Problems of electrochemical detection of H_2O_2

As noted above (see section 1.1.1) the indicator reaction of the first-generation oxidases-based biosensors may be electrochemical detection of consumed oxygen by its reduction on the electrode at potential –0.7 V. Although the first known biosensors used this principle, this approach has some significant drawbacks leading to its renunciation. First, this is significant variation of oxygen content depending on pH, temperature and composition of the solution, and secondly, it is the simultaneous reduction of hydrogen peroxide at the same potential. Therefore the electrochemical detection of hydrogen peroxide, which is one of the products of enzymatic reactions of almost all oxidases, is considered more promising [170]. The detection can be performed by its oxidation at potential about 0.6 V – the dissolved oxygen does not interfere with the reaction under these conditions.

However, the use of such biosensors in the analysis of real objects faces the problems associated with side reactions that may occur at the electrode at this potential. For example the analysis of biological fluids is complicated due to a lot of components may be oxidized at the electrode at potential 0.6 V, such as ascorbic acid, dopamine, bilirubin and some others [11].

Possible solutions of this problem include the separation of interfering substances by semi-permeable membranes [171, 172], pre-xidation [173–175] or impact accounting [176]. The use of semipermeable membranes typically reduces sensitivity and does not guarantee the complete elimination of interfering substances [177, 178], other methods also do not give reliable results. Another possible way to solve this problem is to use mediators that reduce the oxidation potential of H_2O_2

[170] or peroxidase enzyme [179], which is a natural catalyst of the H_2O_2 reduction. However, their use significantly complicates the design of biosensors and leads to non-reproducible results. Therefore, the most promising is the potential decrease of H_2O_2 detection by using specially-structured electrodes [180].

In addition to "classical" electrodes for the detection of hydrogen peroxide – platinum [181] and gold [182], the point of interest is the use of electrodes modified with nanomaterials – nanoparticles [183, 184] and nanotubes [87, 100]. In particular, platinum nanoparticles deposited on carbon electrodes can significantly reduce the potential of hydrogen peroxide oxidation [185], and carbon nanotubes deposited from dispersion in nafion on the surface of glassy carbon electrode increases the rate of response and sensitivity of the modified electrode to hydrogen peroxide at potential +0.2 V [186].

1.5. Amperometric biosensors based on SiO_2 and dehydrogenases

1.5.1. Overview of dehydrogenases used in amperometric biosensors

Dehydrogenases subclass includes more than 300 enzymes that use coenzyme NAD^+/NADH (or its modification $NAD(P)^+$/NAD(P)H) as an electron acceptor. Dehydrogenases can (due to reversibility of NAD^+/NADH) also catalyze the reverse reaction in most cases [187]. In general, the enzymatic reaction of dehydrogenases can be represented as:

$$Substrate + NAD^+ \overset{dehydrogenase}{\longleftrightarrow} Product + NADH \quad (1.3)$$

The number and diversity of dehydrogenases provide more choices for the construction of various amperometric biosensors. The absence of oxygen in the enzymatic reaction scheme can eliminate most of the disadvantages associated with it (difficulty of detecting. interfering influence, etc.) [188]. The reversibility of enzymatic reactions allows to expand analytical applications with the ability to determine the reaction product instead of the substrate. Nevertheless, biosensors

based on dehydrogenases are much less common than ones on the basis of oxidases. This is associated with the difficulty of electrochemical detection of NAD^+/NADH (see paragraph 1.5.2)

The most widespread enzymes from the dehydrogenases subclass used in the development of biosensors (alcohol dehydrogenase, glucose dehydrogenase, lactate dehydrogenase, glutamate dehydrogenase) more or less duplicate the functions of the corresponding enzymes of oxidases subclass (see paragraph 1.4.1) and their applications. However, alcohol dehydrogenase is used more than analog from oxidases due to its higher activity and stability in the sensors and much higher specificity towards ethanol [145]. Lactate dehydrogenase is also characterized by higher selectivity than lactate oxidase [189].

(Form)aldehyde dehydrogenase - an enzyme that catalyzes the oxidation of formaldehyde to formic acid. Besides the coenzyme NAD^+, the reaction also requires the presence of coenzyme glutathione. Biosensors based on this enzyme can be used to determine the formaldehyde having allergic, mutagenic and toxic effects in the food, pharmaceutical and cosmetic industries [190–193]. The disadvantage of this enzyme is low activity, high cost and difficulty of application due to the need of two coenzymes [193].

Glycerol dehydrogenase provides oxidation of glycerol by coenzyme NAD^+. Biosensors based on this enzyme may be useful for wine quality control during fermentation [194, 195] as well as in clinical analysis of blood [196]. At the same time, the lack of selectivity of this enzyme and reversibility of enzymatic reaction are reported [197].

Sorbitol dehydrogenase (DSDH) - an enzyme that catalyzes the conversion of polyhydric alcohol sorbitol to fructose. Measurement of sorbitol content is important in the analysis of diabetic food and clinical analysis to prevent the development of diabetes. To date there are only several reports on the biosensors development based on this enzyme [198–201], among them only in work [198] it was used for the real

objects analysis. In addition, immobilized DSDH can be used for the design of the bioreactor for electro-enzymatic synthesis [202, 203].

Malate dehydrogenase catalyzes the oxidation of malic acid and its salts. Biosensors based on this enzyme can be used to determine the malic acid in food: fruits, juices and wines, where it affects the organoleptic [187, 204, 205].

3-hydroxybutyrate dehydrogenase can be used in the biosensors for clinical analysis of blood, where the determination of 3-hydroxybutyrate is important to avoid life-threatening diabetic ketoacidosis in diabetic patients [206–208].

As mentioned above, the data mainly is missing in the literature about the immobilization of dehydrogenases in SiO_2-film by sol-gel method and the development of amperometric biosensors based on such modified electrodes. Among all the above enzymes such procedure has been described only for lactate dehydrogenase [209–211] and malate dehydrogenase [212]. Given the small number of publications and the importance of substrate the point of interest is the development of biosensor based on sorbitol dehydrogenase immobilized in SiO_2-film.

1.5.2. Problems of electrochemical detection of NAD^+/NADH

The coenzyme NAD^+ serves as an electron acceptor in most enzymatic reactions of dehydrogenases, turning to the reduced form NADH. Due to the electrochemical activity of pair NAD^+/NADH the amperometric detection of concentration changes of any component of this pair could be linked to the initial concentration of the substrate-analyte. However, the NADH interacts with the electrode, causing the dependency of the position and height of the peak on the material and the structure of the electrode as well as on the pH and the buffer solution [213]. Although the formal redox potential of pair NAD^+/NADH is quite low (approximately –0.515 V vs. Ag/AgCl [213–215]), the process is characterized by significant overvoltage on conventional electrodes (0.7 V - on platinum, 1.0 V - on gold) because of irreversible oxidation of NADH [215]. Electrochemical detection at such high potentials would have led to significant interfering effect from other

electroactive substances and even water electrolysis, preventing any analytical application of such biosensors.

The electrochemical oxidation of NADH at carbon electrodes has been reported to lead to the electrode poisoning due to contamination of surface by reaction products [216], including adsorbed NAD^+ dimers [217]. This leads to a decrease of the anodic current of NADH oxidation and consequently to the loss of electrode sensitivity with time, greatly complicating the development of stable biosensors.

Therefore, research efforts are aimed at searching of new materials and ways of NADH oxidation potential reduction. The carbon nanotubes established a reputation as a promising material for such enzyme electrodes [87, 100]. Thus, the use of an electrode modified with carbon nanotubes reduces the potential of NADH oxidation by almost 0.5 V compared to the unmodified carbon electrode [89]. Even better results can be obtained by performing pre-activation of carbon nanotubes by anodic oxidation [218] or microwave processing [219]. This treatment leads to partial destruction of the nanotubes structure and the emergence of highly-active centers [217, 218] as well as to the appearance of quinone-like groups on the surface of the nanotubes, which act as mediators [219, 220].

Another way to solve the problem of high oxidation potential of NADH may be the use of electrochemical mediators, including various quinones, aromatic diamines, phthalocyanine, ruthenium complexes and other [215, 221]. Scheme of such mediators application may include simple addition to the solution or immobilization on the electrode by adsorption, covalent binding or (electro)polymerization [221, 222]. Phenothiazine and phenoxazine redox dyes [223] attract attention as mediators due to the high rate of heterogeneous electron transfer reactions of NADH and are considered as one of the most promising electrochemical mediators for coenzyme oxidation [222, 224]. The biosensors based on such dyes have already been developed: Meldola Blue [225, 226], Nile Blue [227], Methylene Blue [228–230] and Methylene Green [231, 232].

A particular interest is the presence of well-developed aromatic system in phenothiazine dyes that determines their ability to be easily and firmly adsorbed on carbon surfaces, including carbon nanotubes [233, 234]. Such combination of nanostructured electrode and mediator leads to a synergistic effect – the potential decrease and the increase of the sensitivity and stability NADH detection [235, 236]. This allows to apply this approach in the development of dehydrogenase-based biosensors [189, 237–239].

1.6. Conclusions from the literature survey

Analysis of the literature data has shown that electrochemical biosensors is a promising branch of the sensor development. An approach that deserves attention for the immobilization of biomolecules on the electrode surface is their encapsulation into a thin polymer film of silica, due to the large porosity and biocompatibility of the latter. However, there are unresolved issues about the use of such bio-composite films in the biosensors development, e.g., the achievement of strong enzyme fixing in the film, as well as maintaining its sufficient activity. In addition, the fabrication of SiO_2-films by traditional methods does not always lead to reproducible results.

The method of electrochemically-assisted deposition is an alternative to this methods allowing to obtain reproducible porous films with controlled thickness. On the example of glucose oxidase and hemoglobin this method was successfully applied also for bioencapsulation, but information about its application for other types of enzymes, particularly dehydrogenases, is absent in the literature.

The use of nanomaterials can significantly improve the analytical characteristics of biosensors based on oxidases and dehydrogenases, including sensitivity and selectivity. The platinum nanoparticles are promising for the choline oxidase immobilization, since they can increase the sensitivity of detection of hydrogen peroxide. Carbon nanotubes are suitable for the stable and low potential detection of coenzyme NADH, so they can be used for the immobilization of sorbitol

dehydrogenase. However, there is not much information in the literature about the selection of nanomaterials and the methods of their immobilization.

CHAPTER 2. EXPERIMENTAL PART.

2.1. Chemicals and reagents

2.1.1. Enzymes

Three enzymes from the oxidoreductases class were used in this work:

- Glucose oxidase (GOx, EC 1.1.3.4, «Sigma») from *Aspergillus niger* ($M_w \approx$ 160000, activity 15 – 50 units/mg). Isoelectric point 4,2;
- Choline oxidase (ChOx, EC 1.1.3.17, «Sigma») from *Alcaligenes sp.* ($M_w \approx$ 95000, activity $\geq$ 10 units/mg). Isoelectric point 4,1;
- D-Sorbitol dehydrogenase (DSDH, EC 1.1.1.15), synthesized at the Department of Microbiology of the University of Saarland (Germany). Solution with concentration 10 mg/mL (activity 100 units/mg). Isoelectric point 4,3.

Enzyme solutions (except DSDH) were prepared by dissolving an appropriate amount (final concentration 10 mg/mL) in 0.067 M PBS (pH 6.0) and stored at 4°C when not used.

2.1.2. Reagents for sol-gel synthesis.

For the synthesis of SiO_2-based sol the tetraethoxysilane (TEOS, 98%, «Alfa Aesar»), concentrated hydrochloric acid (HCl, 36%, «Prolabo») and deionized water from a «Purelab Option» water purification system were used.

The polyelectrolytes and surfactants were added to the sol as additives: poly-(dimethyldiallylammonium chloride) (PDDA, low molecular weight, 20 wt% in water, «Aldrich»), poly-(ethyleneimine) (PEI, high molecular weight, water-free, «Aldrich»), and cationic surfactant cetyltrimethylammonium bromide (CTAB, «Sigma»).

Addition of positively-charged polyelectrolytes and surfactants was intended for improvement of the enzyme interaction with silica-groups of the sol-gel film.

Silaca-groups are negatively charged at the pH used during the sol-gel synthesis (5 - 7) due to their deprotonation [240]. This results in electrostatic repulsion taking into account the negative charge of the enzyme molecules at such pH. Therefore, the use of positively-charged polyelectrolyte, that plays a role of stabilizing agent between SiO_2 and protein, leads to significant improvements of the enzyme encapsulation [241]. In addition, cationic surfactants, such as CTAB, improve structure of the sol-gel film and can enhance the response stability of the encapsulated in SiO_2-film biomolecules due to their inclusion into micelles [34, 36].

While immobilizing coenzyme NAD^+ into SiO_2-film 3-glycidoxypropyl-trimethoxysilane (GPS, 98%, «Sigma») was used as bonding agent. It is able to bind the adenine residue in the coenzyme molecule and react with silanol-groups in the condensation reaction [203].

2.1.3. Reagents for voltammetric measurements.

All solutions were prepared using deionized water by dissolving of accurate amounts and/or appropriate dilution. Standardization of solutions was performed using titrimetry.

1,1'-Ferrocenedimethanol (98%, «Aldrich»), hydrogen peroxide (H_2O_2, 35%, «Acros»), oxidized and reduced forms of β-nicotinamide adenine dinucleotide (NAD^+/NADH, 98%, «Sigma») were used as electrochemical probes.

Glucose («Acros»), D-sorbitol (98%, «Sigma») and choline chloride (97%, «Fluka») were used as substrates of the corresponding enzymes. Solutions of glucose were left to mutorotate at least for 24 h before using.

The voltammetric measurements were conducted using phosphate and Tris-HCl buffer solutions as background electrolytes unless otherwise specified. Acidity and composition of buffer solutions were chosen taking into consideration optimal pH of enzymatic activity and the absence of interfering influence of solution components for the substrate determination.

The adsorption of dye methylene green (MG, >80%, «Sigma») was used for the determination of electroactive surface area of electrodes.

2.1.4. Substances studied for interfering influence.

To investigate the interfering effect on the determination of sorbitol the number of carbohydrates that can be found in the food was chosen as well as representatives of the homologous series of polyhydric alcohols, including sorbitol stereoisomer (mannitol). The components that can be part of cosmetic products (glycerol, sodium lauryl sulfate) and biological fluids (ascorbic acid, urea) were tested as well. All solutions were prepared by dissolving accurate amounts of substances or by dilution of initial solutions. Iron(III) nitrate, acidified to prevent its hydrolysis, was used for ascorbic acid masking.

To investigate the interfering effect on the determination of choline we studied mono- and disaccharides that can be part of the food (glucose, sucrose, lactose), substances that are part of the biological fluids (uric and ascorbic acid, urea), ethanol and some metal ions (Pb (II), Zn (II), Cu (II), Fe (III)), which are classical inhibitors of enzymes. All solutions were prepared by dissolving accurate amounts of substances or by dilution of initial solutions.

2.2. Apparatus

All electrochemical experiments were carried out on potentiostat/galvanostat PalmSens («Palm Instruments BV», Netherlands) potentiostat EmStat2 («Palm Instruments BV», The Netherlands) and bipotentsiostat/galvanostat μStat 400 («DropSens», Spain). The three-electrode cell was used containing (except gold screen-printed electrode) corresponding working electrode, an Ag/AgCl reference electrode (Ag / AgCl, 3 M KCl, «Metrohm», Germany) and a platinum auxiliary electrode. Data from the potentiostat was transferred to a personal computer and processed using software «PSTrace», «DropView» and «Origin».

Following electrodes were used as working:

- Platinum nanofibers (Pt-Nfb) were synthesized and deposited on the surface of the glass substrate in Physico-Chemical Institute of the University of Giessen (Germany) by the method of electrospinning [242]. There were one-, two-, and four-layers Pt-Nfb with resistance 10, 2 and 0.5 kΩ accordingly;
- Glassy carbon electrode (GCE) in the form of plates (Sigradur ®, «HTW Hochtemperatur-Werkstoffe», Germany), modified with CNT;
- Gold screen-printed electrode (AuSPE) («DropSens», Spain). This type of electrode contained both gold working electrode, silver reference electrode and gold auxiliary electrode.
- For the purpose of comparison platinum and gold macroelectrodes were useds.

For Pt-Nfb and GCE a specially designed Teflon cell were used in which the working electrode is located on the bottom side, and its required surface area is limited by rubber ring (ø = 6 and 9,5 mm). The electrode was connected to the potentiostat using copper wire and silver glue (див. Scheme 2.1 для Pt-Nfb).

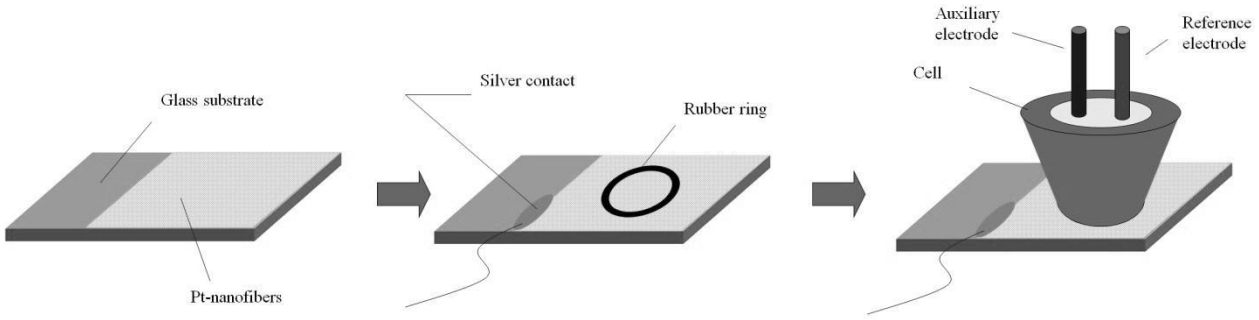

Scheme 2.1. The connection way of Pt-Nfb to electrochemical cell.

For electrophoretic deposition of CNT a specially designed device was used consisting of a DC source of alternating voltage and two steel plates-electrodes that were placed strictly parallel to each other at a distance of 6 mm (Fig. 1.6). Plate, which acted as an anode, was shorter providing possibility of GCE connection.

The study of electrodes surface was carried out by method of scanning electron microscopy (using commercial microscope Hitachi FEG S4800, SCMEM, University

of Nancy) and by atomic-force microscopy (using a microscope Asylum Research MFP-3D-Bio).

To ensure continuous mixing of solutions magnetic stirrers with adjustable speed was applied. Acidity of the solution was checked using pH-meter Mettler Toledo S220 and Piccolo HI 1290.

2.3. Argumentation of the choice of objects and methods

2.3.1. Modification of electrodes by electrochemically-assisted deposition method

The modification of electrodes with SiO_2-film was performed by electrochemically-assisted deposition method using alcohol-free sol composition, which does not inhibit the enzyme activity [60].

- For the preparation of the sol for GOx immobilization 2.28 mL of TEOS, 2.0 mL of H_2O, and 2.5 mL of 0.01 M HCl were mixed with a magnetic stirrer for 16 h. Then, prior to introduction of the enzyme in the medium, 1.66 mL of 0.1 M NaOH was added to neutralize the sol (to avoid possible enzyme denaturation in acidic medium). The enzyme solution (50 μL of PBS (0.067 M, pH 6.0) and 100 μL of 10 mg/mL GOx solution) was added to 0.5 mL of the hydrolyzed sol and left to stay for 1 h.
- For the preparation of the sol for ChOx immobilization 0,21 mL of TEOS, 0,15 ml of H_2O and 0,26 mL of 0,01 M HCl were mixed with a magnetic stirrer for 12 h. Prior to EAD 0,4 mg of CTAB, 0,03 mL of 0,067 M PBS (pH 6,0) and 0,01 mL of ChOx solution (10 mg/mL) were added to 0.5 mL of the hydrolyzed sol.
- For the preparation of the sol for DSDH immobilization 2.28 mL of TEOS, 2.0 mL of H_2O, and 2.5 mL of 0.01 M HCl were mixed with a magnetic stirrer for 16 h. The final sol was diluted three times with pure water and, then, a 100 μL

aliquot of this solution was mixed with 100 μL of PDDA (20 wt% in water) and 100 μL of DSDH solution.

- For the preparation of the sol for co-immobilization of DSDH and NAD+ [203] 2.28 mL of TEOS, 2.0 mL of H_2O, and 2.5 mL of 0.01 M HCl were mixed with a magnetic stirrer for 16 h. The sol was diluted five times with water and its 20 μL aliquot was mixed with 10 μL of 20% PEI-solution, 10 μL ofNAD^+-GPS solution (prepared by mixing 25 mg of NAD^+ and 37.6 mg of GPS in 400 μL of Tris-HCl buffer solution pH 7.5 for 14 h at room temperature) and 20 μL of DSDH-solution.

Prepared sol was introduced in the electrochemical cell where some negative potential was applied to the working electrode in order to initiate the generation of OH-ions (typically from -1.1 to -1.3 V). Potential and/or duration of its application were optimized for each individual case.

After electrodeposition the working electrode was kept in the sol for 5 minutes, then gently washed with water and dried at room temperature for 1 hour before use.

2.3.2. Modification of electrodes with carbon nanotubes by the electrophoretic deposition method

This work used single-walled carbon nanotubes functionalized carboxylic groups (CNT, > 90%, 4-5 nm × 0,5-1,5 microns, 1-3 atom.% COOH-groups, «Sigma»). The presence of carboxyl groups improves dispersancy of CNT in water and gives them a negative charge required for their movement in a constant electric field. For the suspension preparation the appropriate amount of CNT was weighed on an analytical balance (considering concentration 0.1 mg/mL), then deionized water was added, and the suspension was treated in ultrasonic bath for 12 hours.

Glassy carbon plates were polished before the modification by wet emery paper 4000 with Al_2O_3 powder (0.05 micron, «Buehler»). The same procedure was used to renew the electrode surface after suc- cessful modification and measurements.

The two parallel electrodes were introduced in a 4-mL aliquot of the dispersion and a constant potential difference of 60 V (corresponding to the magnitude of the electric field between the electrodes 100 V/cm) was applied for required time usually from 5 to 120 seconds. The optimal applied voltage of 60 V was used throughout because it constitutes a good compromise between a high speed of deposition and limited decomposition of ultra-pure water (which would generate oxygen bubbles that may affect CNT assembly). The level of electrodes dipping was kept constant in order to ensure the same area (1 cm^2) of their contact with dispersion and reproducibility of deposition. After deposition, the glassy carbon plate was carefully removed from the remaining dispersion, gently washed in water, first dried horizontally at room temperature and then put in an oven at 450◦C for 1 h. The

For the preparation of macroporous CNT-layers the mixture of CNT (0,1 mg/mL) and polystyrene beads (0.05 mg/mL to 0.5 mg/mL) was used. It was obtained by adding to the suspension of CNT certain aliquots of concentrated (5%) suspension of polystyrene beads (PS-beads, 500 nm), obtained by the method [243]. Polystyrene was chosen because of facility of homogeneous beads synthesis and their removal by heating. This mixture was stirred, brought into the cell and applied to EPD as was described above. After the deposition electrode was carefully removed from the suspension and left at room temperature until dry. The template removal was carried out in an oven at 450 C for 1 h with 15 C/min ramp.

For the purpose of comparison, GCE was also modified with CNT-layer by drop-coating method. The CNTs were deposited from aqueous solution, by dropping 10 μL of the same water suspension as for EPD and left to dry completely.

For electrochemical generation of platinum nanoparticles on the surface of CNT we used technique described in [64]. Electrode was dipped in the solution of 1 mM $Pt(NO_3)_2$, that also contained 0.1 M $NaNO_3$, and was exposed to a series of pulses. The sequence of pulses in each series was as follows: 0.035 V for 1 s, –0.7 V for 0.2 s, 0.035 V for 1 s. The electrochemical reduction of platinum and the formation of nanoparticles occurs during the application of negative potential.

Application of the positive potential was used for dumping, it does not happen any electrochemical reaction at such potential. The choice of the number of series of pulses is justified in section 3.2.1.1.

2.3.3. Voltammetric measurements

To study the properties of modified electrodes we used methods of cyclic and linear voltammetry, amperometry and hydrodynamic voltammetry.

All voltammogramms were obtained using saturated silver chloride electrode (Ag/AgCl), all potentials are mentioned versus it. All voltammogramms were obtained in buffer solutions of appropriate pH (unless otherwise specified) in static mode (without stirring). Potential scan rate varied from 20 to 100 mV/s, in some cases the extended range from 5 to 200 mV/s was used. Coenzyme NAD^+ (1 mM) was added into solution during measurement in the study of the voltammetric characteristics of immobilized DSDH.

Amperograms were obtained at constant stirring, applied potential was kept constant throughout the measurement. At the beginning of the measurement dumping time was at least 200 s.

Hydrodynamic voltammetry was carried out in the dynamic mode (with constant stirring). Potential changed stepwise with interval 50 mV every 30 s. The equilibrium current at the end of the time interval was measured.

If necessary voltammetric measurements were performed in an anaerobic mode. Oxygen removal for the anaerobic experiments was achieved by bubbling argon for 15 min prior to experiment and this atmosphere was kept in the cell during the whole measurement.

The sensitivity of the modified electrode to the substrate was calculated as the slope of a graph current-substrate concentration [244].

2.3.4. Surface observations

Investigation of the surface of modified electrodes by scanning electron microscopy (SEM) was carried out by connecting the modified electrode with substrate using a special conductive tape. Since the conductivity of the electrodes was sufficient spraying metal plating wasn't used. Energy of scanning electron beam ranged from 1 to 15 kV, magnification – from 1,000 to 400,000 times. If necessary, the electrode was placed at a certain angle to the electron beam.

Investigation of the surface by atomic force microscopy (AFM) was conducted in the temperature-controlled room using V-shaped silicon nitride probe (MLCT-EXMT-BF, «Veeco Instruments», USA) with a radius of curvature 50 nm and a constant of elasticity 0.1 N/m. Scanning was carried out in contact mode, the speed ranged from 0.5 to 2 Hz, the data was captured from laser optical detector. A thin scratch was made with a needle for profile and film thickness measurements. AFM images were captured on the border of scratches, allowing to estimate the difference in film thickness. Processing of AFM images was carried out using software WSxM 5.0 («Nanotec Electronica SL», Spain) [245].

Scanning electrochemical microscopy (SECM) with a special device developed on the basis of commercial appliance Sensolytics (Germany) was used to study the conductivity of bio-composite films. The measurements were performed using a platinum microelectrode (ø = 25 microns) in a solution containing 0.1 M KCl, 1 mM ferrocenedimethanol. Profilometry with SECM was also applied to study the morphology of the layers of CNT with a thickness greater than 500 nm, in this case a glass needle was used, measuring the distance from it to the surface using piezoelectric sensors [246].

For electrochemical studies of electroactive surface area the dye methylene green was adsorbed on the electrode surface by immersion of the electrode in a 1 mM solution of the dye and stirring on a magnetic stirrer for 12 hours. Then the electrode was washed thoroughly with water and dried at room temperature.

2.4. Calculations based on electrochemical measurements

2.4.1. Calculation of apparent Michaelis constant

The apparent Michaelis constant was calculated in order to determine the degree of the relationship of the corresponding enzyme to substrates, as well as to determine the upper limit of the linear range of modified electrodes. The assumption was made that the enzymatic reaction is one-substrate or the concentration of the second substrate (in the case of coenzyme) is saturating, that allows to apply the Michaelis-Menten kinetics to it [247]:

$$V = \frac{V_{max} \times S}{K_M + S} \tag{2.1}$$

wh. V – the rate of enzymatic reaction;

V_{max} – the maximum rate of enzymatic reaction at such conditions;

S – equilibrium concentration of substrate, mM;

K_M – Michaelis constant, mM.

The current flowing through the electrochemical cell with a known concentration of the substrate was taken as rate of enzymatic reaction. In this case, the graph of V–S relation for equation (2.1) has the form of hyperbole that approaches to a straight line $V = V_{max}$. The processing of such curves is difficult (although possible with modern software) so the linearization of this equation was performed by the method of Lineweaver–Burk [248]:

$$\frac{1}{V} = \frac{1}{V_{max}} + \frac{K_M}{V_{max} \times S} \tag{2.2}$$

In the coordinates 1/V – 1/S the graph of the equation (2.2) has the form of a straight line that intersects the abscissa at the point $-1/K_M$ making possible finding Michaelis constant.

Further, in all cases apparent Michaelis constant was found out from the equation of the graph 1/V against 1/S, calculated by the method of least squares, and the point of intersection of this line with the abscissa. As an alternative method direct processing of the V–S graph with filter «Hill» in software «Origin 8.5» was used.

2.4.2. Calculation of the electroactive surface area using dye adsorption

The adsorption of the dye methylene green (MG) was used for the calculation of approximate electroactive surface area of electrodes modified with CNT. It was assumed that the dye molecules form a monolayer on the surface of nanotubes [234]. The area of anodic or cathodic peak of adsorbed dye on voltammogram of modified electrode was calculated using computer program «Origin 8.5» (e.g. Fig. 4.5a). Electroactive surface area calculation was performed using the formula:

$$S_{el.act} = \frac{S_{peak} \times 6{,}24 \cdot 10^{18} \times S_1}{\nu \times n} \qquad (2.3)$$

wh. S_{peak} – area of the MG peak on the voltammogram, A·V;

ν – potential scan rate, V/s;

n – number of electrons transferred in the electrochemical reaction (n = 2 for MG);

$6{,}24 \cdot 10^{18}$ – number of electrons for the charge of 1 C;

S_1 – area occupied by one adsorbed molecule of dye (for MG 0,8 nm^2, or $8 \cdot 10^{-13}$ mm^2 [249]), mm^2.

2.5. Conclusions to the chapter

The chapter lists and argues the choice of reagents and methods for carrying out the necessary experiments, describes the objects of study.

The choice of interfering substances investigated in developing amperometric methods for detection of sorbitol and choline was argued. The techniques of sol-gel proceeding and generation of bio-composite SiO_2-films on the electrode surface by electrodeposition method were described. The method of the formation of CNT-coatings by electrophoretic deposition on the surface of glassy carbon electrode was defined, including macroporous CNT-layers. The techniques of voltammetric measurements, spectroscopic studies and formulas for calculations were listed.

CHAPTER 3. ENCAPSULATION OF OXYDASES BY ELECTROCHEMICALLY-ASSISTED DEPOSITION OF SOL-GEL BIOCOMPOSITE

One of the needs of electroanalytical chemistry is the development of new, simple and effective methods of enzyme immobilization on the surface of electrodes. The EAD method allows to encapsulate biomolecules in SiO_2-film on the electrode surface by simple one-step process, which has currently been applied only for certain enzymes. Meanwhile, the immobilization of less active enzymes, such as ChOx, requires ways to increase the sensitivity of such modified electrodes.

As it was mentioned in the literature survey (paragraph 1.4.2), the general feature of all oxidases is release of hydrogen peroxide in the enzymatic reaction. The initial concentration of the substrate can be determined by registering the change of the H_2O_2 concentration. One of the best materials for electrochemical detection of H_2O_2 is platinum [250]. The oxidation of hydrogen peroxide on platinum surface occurs with high signal reproducibility and at low potential due to the catalytic action of platinum oxides. This fact can be exploited to avoid interfering effects of reductants, increasing thereby the selectivity of platinum electrodes in comparison with other types of electrodes [251]. However, even with relatively low reaction potential [252], one would desire further reduction of the H_2O_2 oxidation potential. One possible approach for achievement of this goal is use of platinum-based nanomaterials, including nanoparticles and nanofibers [82, 253]. Such materials can exhibit electrocatalytic properties towards hydrogen peroxide oxidation due to their small size and large surface area.

This chapter covers the results of the EAD method application for the immobilization of oxidases in bio-composite SiO_2-film on electrode surface. It was shown the prospects of the combination of this method with nanomaterials to improve the sensitivity of modified electrodes. The influence of platinum nanostructured materials on the analytical signal of modified electrodes was studied.

3.1. Immobilization of glucose oxidase into the SiO_2-film on the surface of platinum nanofibers

Platinum nanofibers (Pt-Nfb), forming a conductive network with a large number of intersections can be quite easily obtained by the method electrospinning, which allows to control the thickness and density of the network [242, 254, 255]. Despite the attractive characteristics such as small diameter and high density of fibers there is no information in the literature about the use of electrospun Pt-Nfb for the development of biosensors. The first part of this section presents the results of modification of Pt-Nfb with bio-composite SiO_2-film, containing an enzyme from the class of oxidases.

As a model, we have chosen the enzyme glucose oxidase (GOx), which is often used in amperometric biosensors [122]. This is due to the acute need of quick monitoring of the glucose concentration in the blood (and food) for people with diabetes. Another reason for the popularity of GOx is its high stability, which allows application of different ways of immobilization without loss of enzyme activity. Given this, we have chosen this particular enzyme as a model, to verify the applicability of Pt-Nfb network for the oxidases immobilization in the SiO_2-film by electrochemically-assisted deposition method. In this case, the advantage of this method is the ability to selectively modify only Pt-Nfb, without affecting the glass substrate.

3.1.1. Morphological and electrochemical characteristics of platinum nanofibers network

Given that electrospun Pt-Nfb was not previously used as an electrode, we have investigated their morphological and electrochemical properties, as well as response of hydrogen peroxide on the electrodes of this type.

3.1.1.1. Morphological characterization of platinum nanofibers assemblies.

Fig. 3.1 depicts typical microscopic characterization data of the Pt-Nfb assemblies. SEM (Fig. 3.1a) and AFM (Fig. 3.1b) imaging reveals that the diameter of individual fibers is in the range 30–60 nm. Under the conditions used here, the overall thickness of the two- layers assembly remains limited to ca. 100 nm, as shown in the AFM profile (Fig. 3.1b). Platinum nanofibers deposited by electrospinning are highly interconnected, forming a 2Dnetwork of Pt nanoelectrodes on the glass substrate, suggesting good conductivity. This is indeed the case, as the conductivity of the assembly varied typically from 0.5 to 10 kΩ/cm (two points measurement), depending on the film density (which can be tuned by adjusting either the deposition time and/or the number of deposited layers). As also shown, individual Pt nanofibers can be easily evidenced by AFM, and their diameter can be evaluated quite accurately when they are deposited directly onto the glass support (see the two first features around X =1 μm in the line scan in Fig. 3.1b).

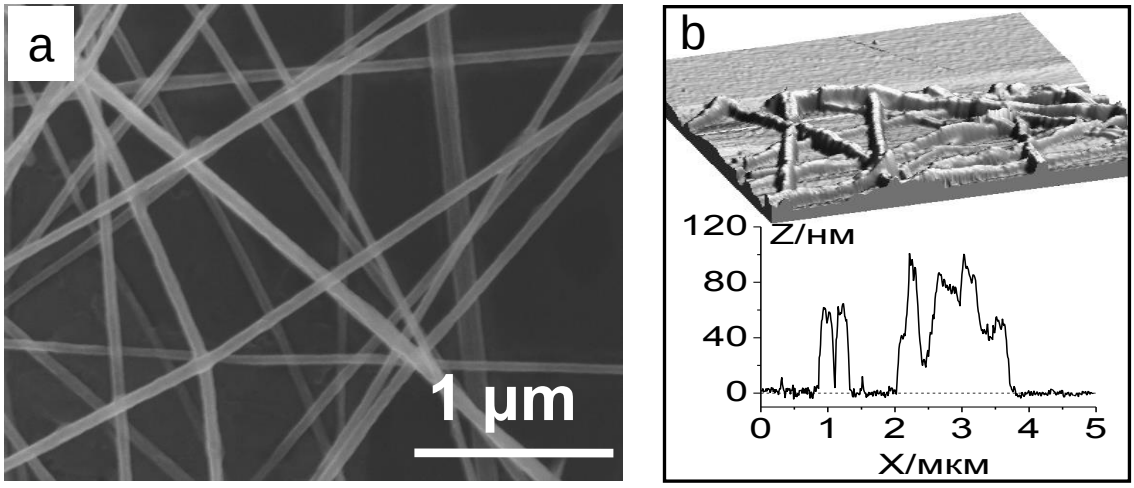

Fig. 3.1. Characterization of platinum nanofibers. (a) SEM picture; (b) AFM pictures of fibers with scratch and cross-section profile.

3.1.1.2. Electrochemical properties of platinum nanofibers network.

The mechanical stability of the assembly is good enough in solution to perform electrochemical measurements. As shown in Fig. 3.2, the fiber density affects the electroactive surface area. Samples displaying various densities of Pt nanofibers have been characterized by cyclic voltammetry in sulfuric acid solution [256]. The electroactive surface area measurement was performed by the area calculation of anodic oxidation peak of adsorbed hydrogen (Fig. 3.2a, shaded), which corresponds to the charge, using the formula:

$$A = \frac{Q_H}{Q_H^s} \tag{3.1}$$

wh. A – electroactive surface area, cm^2;

Q_H – charge of the hydrogen oxidation, μC;

Q_H^s – constant for platinum, 210 μC /cm^2.

The estimation made from the integration of the hydrogen desorption peak shows that one fiber layer exhibits an electroactive surface area (0.29 cm^2) similar to the geometric surface area defined by the O-ring of the electrochemical cell (0.28 cm^2). Comparing to the SEM image (showing much incomplete coverage of the underlying glass support; see Fig. 3.1a), this result confirms the interest of nanoobjects/ nanostructuration to improve the electrochemical performance. The electroactive surface area increases proportionally to the number of layers (Fig. 3.2b), reaching almost 1.2 cm^2 for a four-layers sample.

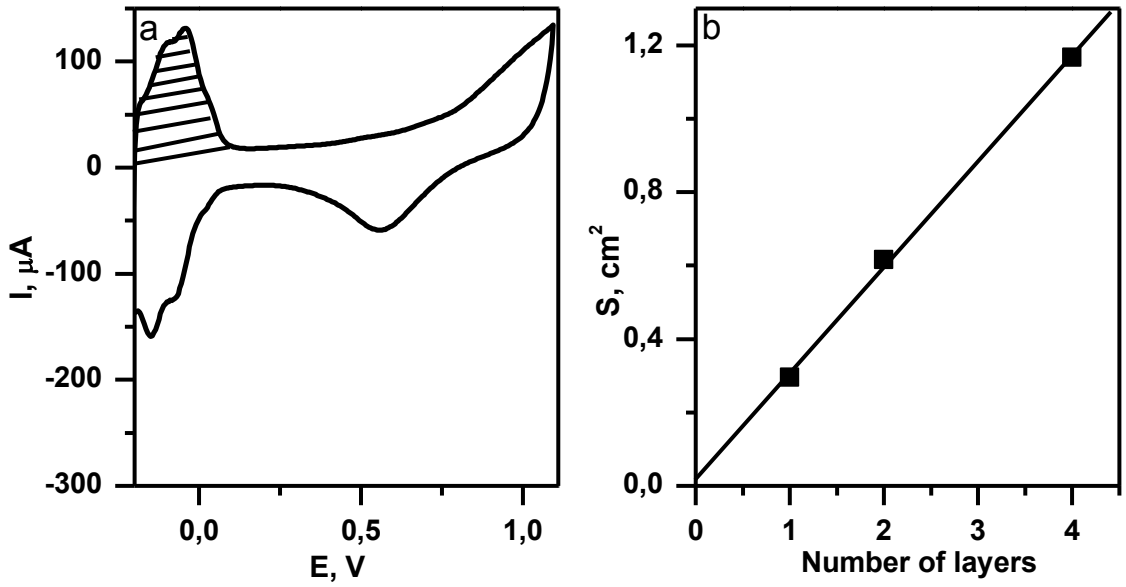

Fig. 3.2. Cyclic voltammogram of Pt-Nfbs in 0.5 M H_2SO_4 solution. Scan rate 100 mV/s; (b) Dependence of estimated electroactive surface area of Pt-Nfbs as a function of the number of nanofibers layers.

The situation is very different for the probes with slow electron transfer rate, for example H_2O_2 (Fig. 3.3). As predicted in the works [257, 258] the reduction and oxidation currents of hydrogen peroxide are strongly affected by the number of nanofiber layers at slow scan rates (compare curves 2, 3, and 4 of Fig. 3.3 that correspond, respectively, to one, two, and four Pt-Nfbs layers). Moreover, Pt-Nfbs display in these conditions a better electrochemical detection than the bare Pt electrode (curve 1 of Fig. 3.3). The platinum nanofibers show behavior typical of ensemble of 1-D nanoelectrodes, having advantages only for the detection of substances with low electron transfer rates.

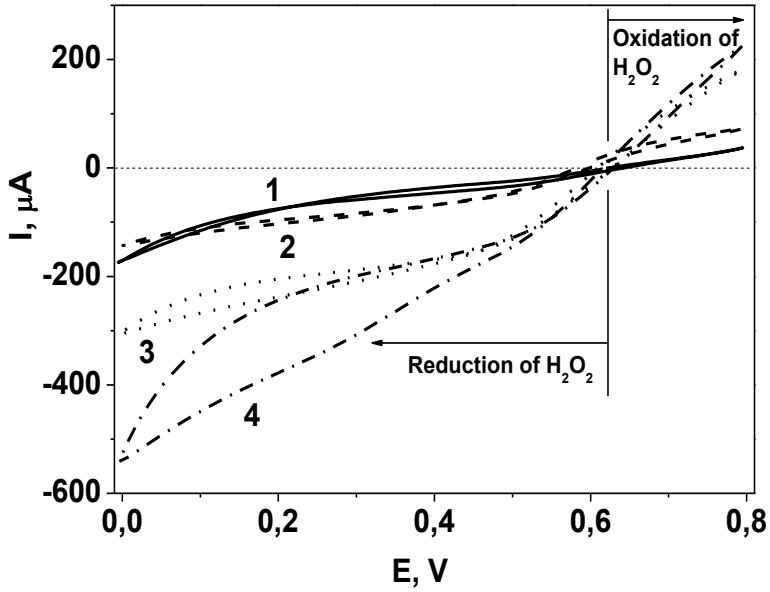

Fig. 3.3. Cyclic voltammogram of Pt-Nfbs in 0.1 M H_2SO_4 solution containing 50 mM H_2O_2 for (1) Pt-bare electrode, (2) 1-layer Pt-Nfbs, (3) 2-layers Pt-Nfbs, (4) 4-layers Pt-Nfbs, scan rate 10 mV/s.

Thus, Pt-Nfbs are much more active upon oxidation and reduction H_2O_2 than conventional platinum electrode. This allows to consider them as promising for use as a matrix for the immobilization of oxidases.

3.1.2. Immobilization of glucose oxidase using electrochemically-assisted deposition method

In an attempt to cover only the surface of Pt-Nfb sol-gel electrochemically-assisted deposition was preferred over the classical evaporation method, which is basically restricted to film deposition onto flat surfaces. We carried out an immobilization of model enzyme GOx on the surface of Pt-Nfb by EAD method, and the influence of EAD parameters on the thickness of the formed SiO_2-film and the electrochemical response of immobilized enzyme was studied.

3.1.2.1. Voltammetric characteristics of platinum nanofibers modified with SiO_2-glucose oxidase film

The cyclic voltammogram of Pt-Nfb in phosphate buffer has a complex shape, inherent in platinum electrodes (Fig. 3.4, curve 1). The current increase is noted in the anodic region at potential 0.7 V, which can be attributed to the formation of oxides of platinum. The significant peak at the potential of 0.0 V in the cathodic region can be noticed caused by several reactions, including the reduction of platinum oxides and reduction of dissolved oxygen [259].

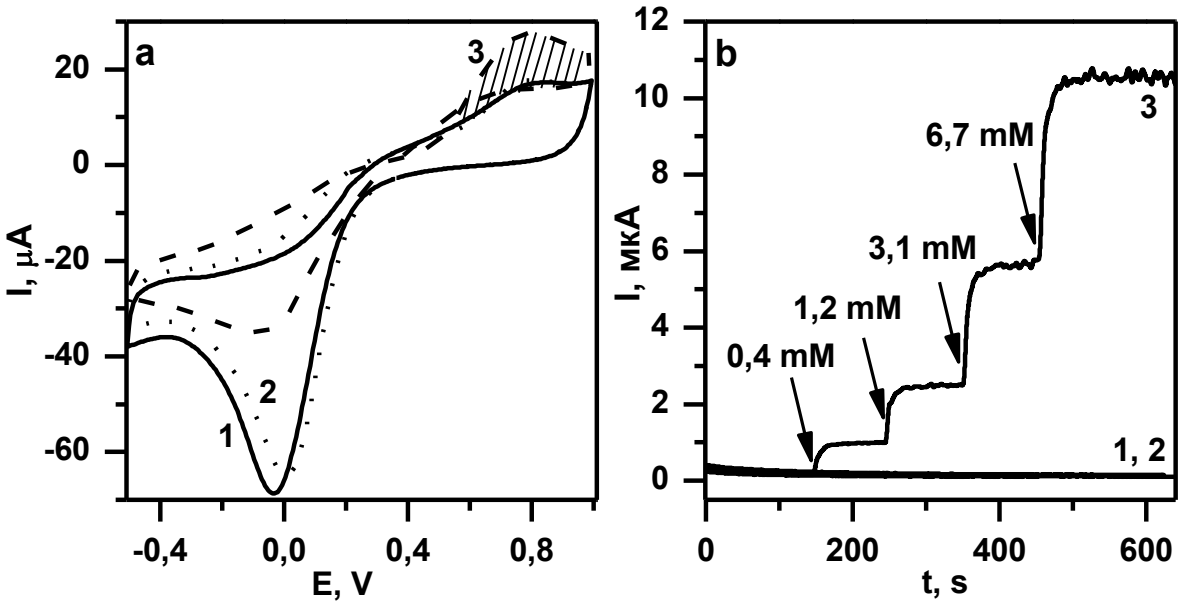

Fig. 3.4. (a) Cyclic voltammograms of Pt-Nfb (1), Pt-Nfb-SiO_2 (2) and Pt-Nfb-SiO_2-GOx(3) in PBS (pH 6,0) containing 10 mM glucose (2, 3). Scan rate 20 mV/s; (б) Amperometric response of Pt-Nfb (1), Pt-Nfb-SiO_2 (2) and Pt-Nfb-SiO_2-GOx (3) to the additions of glucose (on the graph). Supporting electrolyte: PBS pH 6,0. Applied potential +0,6 V.

The voltammogram of Pt-Nfb modified with SiO_2-film in the absence of GOx in solution of glucose (Fig. 3.4, curve 2) is similar to voltammogram of unmodified Pt-Nfb. This suggests, first, the expected absence of electrochemical activity of glucose on Pt-Nfb in this range of potentials, and, secondly, that the film does not prevent the diffusion of reagents to the electrode. At the same time, the

voltammogram of Pt-Nfb modified with SiO_2-GOx film in the presence of glucose in solution (Fig. 3.4, curve 3) displays increasing of anodic current from 0.5 V, which can be attributed to the oxidation of hydrogen peroxide at surface Pt-Nfb in the reaction:

$$H_2O_2 \rightarrow O_2 + 2H^+ + 2e^- \quad (3.2)$$

Hydrogen peroxide is formed in the enzymatic reaction, indicating the preserving of activity of immobilized GOx, which catalyzes the oxidation of glucose by oxygen:

$$\text{D-Glucose} + O_2 \rightarrow \text{D-gluconolactone} + H_2O_2 \quad (3.3)$$

It should be noted that the above equation oxidation of hydrogen peroxide (equation (3.2) is simplified, the mechanism of oxidation of H_2O_2 on the surface of platinum is much more complicated and involves intermediate stages of the formation of platinum oxides [250].

Detection of glucose using Pt-Nfb-SiO_2-GOx is also possible in the amperometric mode at a potential of 0.6 (Fig. 3.4b), which was selected in previous studies as one that meets the highest current value and the smallest existing noise. While Pt-Nfb and Pt-Nfb-SiO_2 (Fig. 3.4b, curves 1 and 2) do not show a significant response to additions of glucose in solution, the amperogram of Pt-Nfb-SiO_2-GOx (Fig. 3.4b, curve 3) demonstrates significant increase in current, which is proportional to the change of glucose concentration in the solution. Amperometric response is stable and reproducible.

As mentioned in the literature survey (paragraph 1.2.3), the properties of the formed film, and therefore the response of immobilized enzyme are affected by electrochemically-assisted deposition parameters, such as potential and duration. Therefore, further optimization of EAD duration was conducted to achieve the best response of immobilized enzyme.

3.1.2.2. Influence of the duration of electrochemically-assisted deposition on the amperometric response of immobilized glucose oxidase

To assess the optimal conditions for obtaining electrogenerated film SiO_2-GOx, we investigated the relationship of modified electrode amperometric response to glucose with the duration of EAD at a constant potential of -1.2 V. At 1-2 s the response is negligible, further signal sharply increases for the duration of electrodeposition 3 s, and then the sensitivity gradually decreases, approaching zero at 10 s (Fig. 3.5).

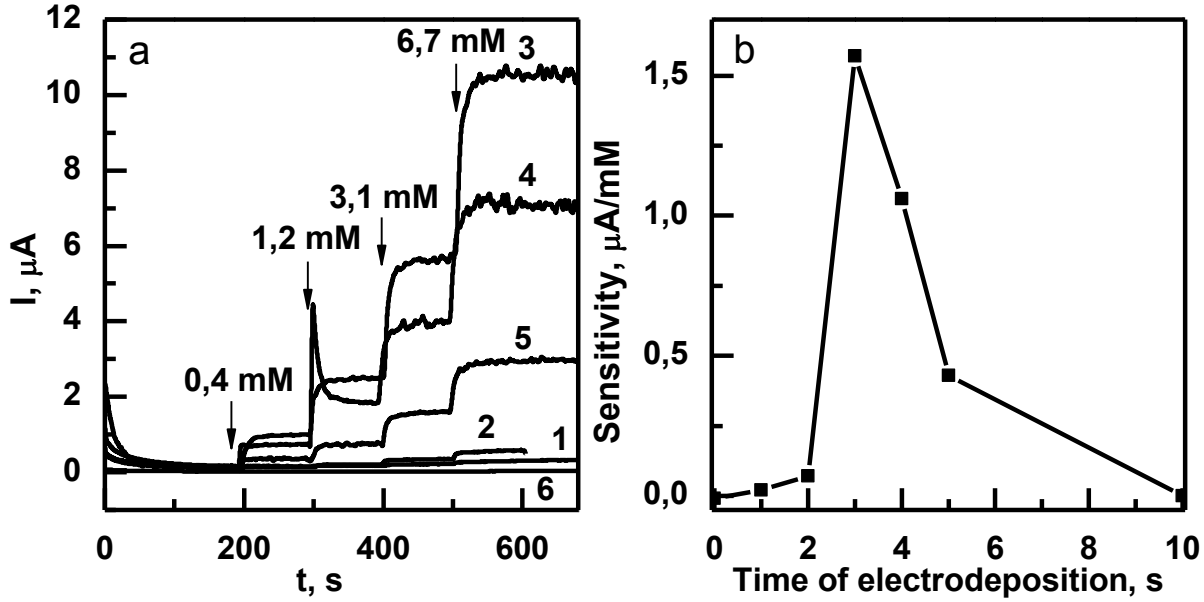

Fig. 3.5. (a) Amperometric response of Pt-Nfb-SiO_2-GOx, modified with time of EAD 1 s (1), 2 s (2), 3 s (3), 4 s (4), 5 s (5) and 10 s (6) to the additions of glucose (on the graph). Supporting electrolyte: PBS pH 6,0. Applied potential +0,6 V; (b) Dependence of electrode Pt-Nfb-SiO_2-GOx sensitivity on glucose at potential +0,6 V as a function of time of sol-gel electrodeposition.

To explain the reasons for such a complex dependence of sensitivity on the duration of EAD, the surface of modified Pt-Nfb was investigated by SEM and AFM methods.

AFM allows monitoring, step-by-step, the electrochemically-assisted deposition of silica on the platinum nanofiber assembly. Both the image and a

selected profile permit the visualization of the unmodified fibers and their packing on the glass substrate (Fig. 3.1b). Fig. 3.6 reports the AFM analysis of Pt-Nfb assemblies after electrochemically-assisted deposition for 1 s, 2 s, 3 s, 4 s, 5 s, and 10 s. In addition, high resolution SEM imaging of selected samples (Fig. 3.7) has been performed to confirm and complete AFM data. When applying deposition times less than 5 s, the Pt nanofibers remain visible on the AFM images and the corresponding height profiles. The SEM observation (top-view) shows that a thin layer of material is effectively deposited onto the whole surface of the fibers after 1 s (Fig. 3.7a) and 3 s (Fig. 3.7c). The thickness of such a silica layer cannot be determined accurately, but one can estimate values of about 7-8 nm and ~15 nm, respectively, for 1 and 3 s deposits.

The depth profile of the deposits is difficult to analyze from SEM pictures, but it can be evaluated from AFM data obtained on scratched samples, pointing out peculiar features as a function of the deposition time. Whereas no silica deposit can be observed in between the individual fibers for 1 and 2 s deposition (the film was only present on the Pt-Nfb surface; see Fig. 3.6a,b), such an "inter-fiber" film started to grow on the glass support from 3 s deposition and beyond. The presence of this additional deposit for longer deposition times can be explained by the fact that the OH^- catalysts are generated not only in the close vicinity of the Pt-Nfb surface, but also in the diffusion layer located at the electrode/solution interface, which is growing with time. The thickness of the deposit increases with the deposition time from 20 nm (3 s) to 80nm (4 s). It becomes thicker and starts to cover both the glass and the Pt nanofibers for 5 s deposition, the Pt- Nfb becoming completely encapsulated with 10 s deposition (Fig. 3.6f) or more (not shown). The corresponding SEM picture of the same sample prepared with 10 s electrolysis (Fig. 3.7d) confirms that the Pt nanofibers are embedded within a textured material, the silica-GOx composite (note that a better magnification could not be obtained here due to the insulating property of this layer).

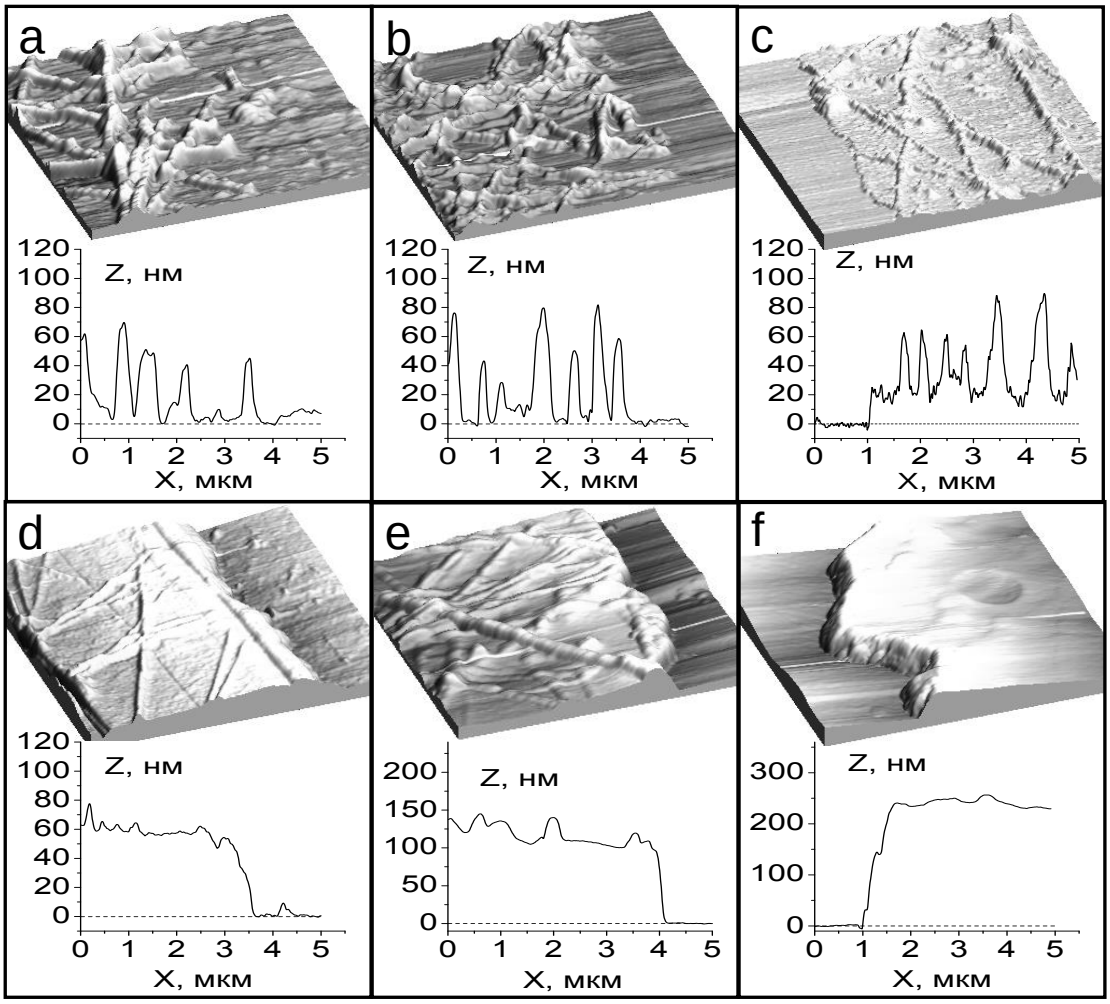

Fig. 3.6. AFM images and cross-section profiles (along white lines shown in the images) of silica-modified Pt-Nfbs prepared with using increasing electrolysis times: 1 s (a), 2 s (b), 3 s (c), 4 s (d), 5 s (e) and 10 s (f).

To conclude this section, it can be stated that silica deposition occurs essentially on the Pt nanofibers for very short deposition times (<3 s). More prolonged electrolysis resulted in larger amounts of OH^- catalyst diffusing onto the overall surface, thereby inducing film formation on both the platinum nanofibers and the glass substrate, which can then lead to the full encapsulation of the fibers into the silica material. Such morphological variations affect the electroactivity of the immobilized GOx.

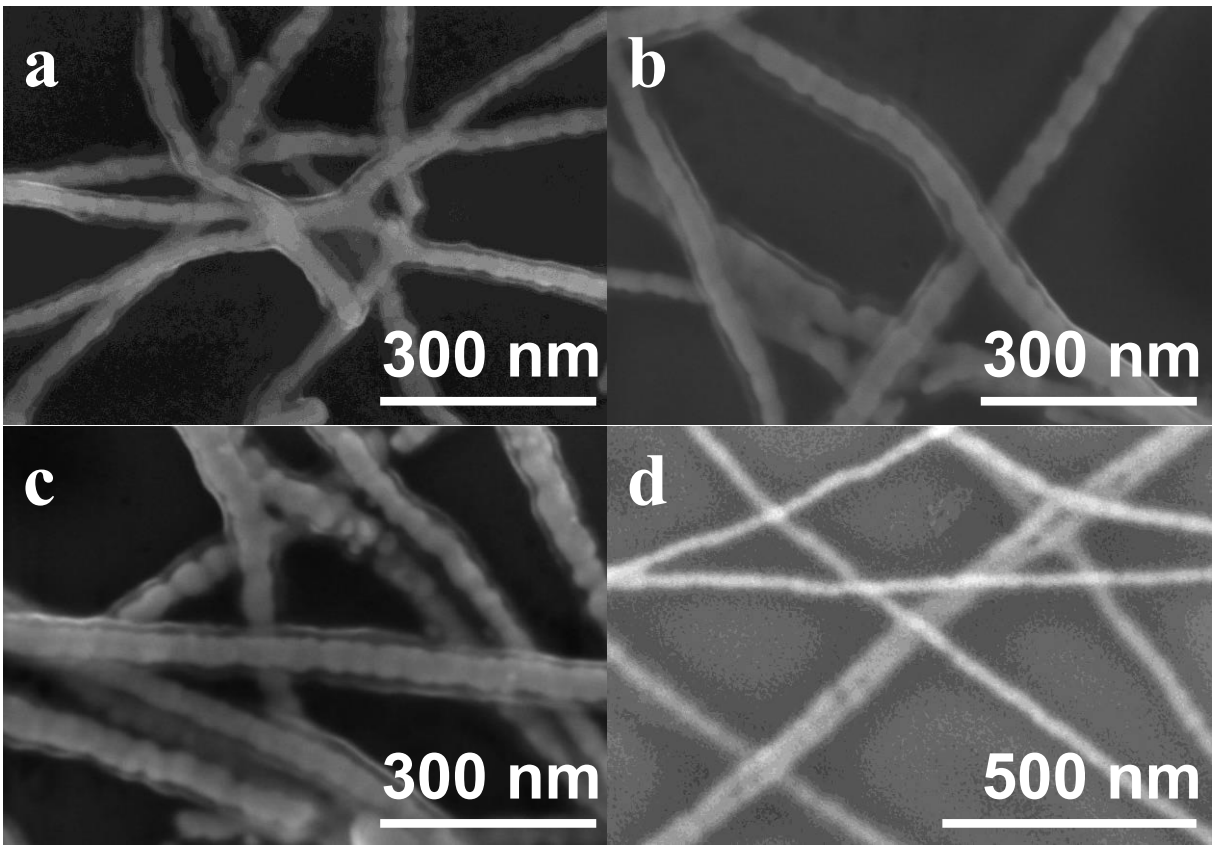

Fig. 3.7. SEM images of silica-modified Pt-Nfbs prepared for various electrodeposition times: 1 s (a), 2 s (b), 3 s (c) and 10 s (d).

The low sensitivity of the sensors prepared from 1 and 2 s deposition can be explained by the low amount of glucose oxidase immobilized in the ultrathin films covering Pt-Nfb. The best case in terms of high sensitivity (3 s deposition) corresponds to the transition between silica covering all fibers and starting to grow on the neighboring areas (Fig. 3.6c). The important stock of enzyme in this sample thus permits us to produce a sufficient amount of H_2O_2 that can be detected on Pt-Nfb without significant resistance to mass transport. On the other hand, films obtained for 4 and 5 s deposition resulted in progressive loss of sensitivity. In these cases, the thicknesses of the silica layer located in the intra-Pt-Nfb region become of the same order of magnitude as the nanofibers size (Fig. 3.6d,e), and this starts to hinder the diffusion of reactants to the Pt-Nfb surface and thus the detection of glucose. When

the biocomposite film totally covers the nanofiber assembly (i.e., 10 s deposition, Fig. 3.6f), it totally blocks the electrochemical detection of glucose.

3.1.3. Comparison of platinum nanofibers and platinum macroelectrode for the immobilization of glucose oxidase

A comparison was performed with Pt-Nfbs and bare Pt electrode with using 3 s electrochemically-assisted deposition in the same conditions. Similar results were obtained which suggests that here the electrochemical response of the assembly is mainly limited by diffusion of glucose in the sol-gel layer (Fig. 3.8). At these conditions Pt-Nfbs behave as partially-blocked electrode [257] and diffusion layers of individual nanofibers overlap to form a common layer, similar to the diffusion layer of macroelectrode [258, 260, 261].

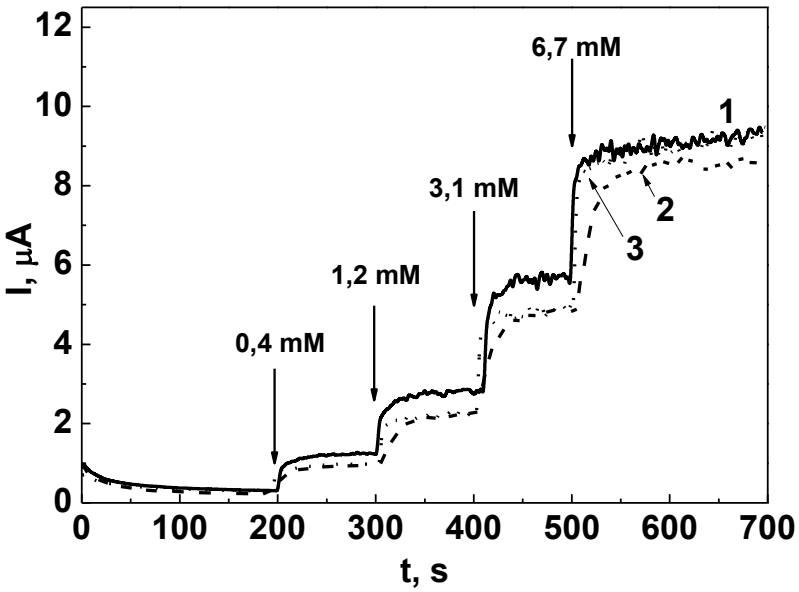

Fig. 3.8. Amperometric response of Pt-bare electrode (1), 2-layers Pt-Nfb (2) and 4-layers Pt-Nfb (3) modified with SiO_2-GOx film by EAD method (-1,2 V, 3 s), to the additions of glucose (on the graph). Supporting electrolyte: PBS pH 6,0. Applied potential +0,6 V.

However, such a control experiment has to be taken into account very carefully as the electrolysis of the sol occurs at more negative potential on the Pt bare electrode than on Pt-Nfbs, potentially affecting the thickness of the deposit. In any case, these results highlight the interest of the low-dimensional Pt-Nfbs and well-controlled sol-gel electrochemically assisted deposition to improve the response of biomolecule-doped thin silica films produced by the electrochemically-assisted deposition method.

3.2. Immobilization of choline oxidase into the SiO_2-film

Choline oxidase (ChOx), as well as glucose oxidase, belongs to the class of oxidases, which makes possible the use of common approach of sensitive hydrogen peroxide detection to develop a biosensor based on it. However, unlike GOx, ChOx is characterized by much lower stability, which makes necessary finding ways to increase its stability in the immobilized state. Thanks to biocompatibility of SiO_2-based materials, they are promising for use as a matrix for encapsulation of the enzyme on the surface of the electrode. The use of rapid one-step EAD method allows immobilization in mild conditions and shortening of the time of unfavorable conditions exposure on the enzyme molecule.

3.2.1. Electrochemical generation of the platinum nanoparticles on the surface of glassy carbon electrode for the choline oxidase immobilization

Pt-Nfb did not demonstrate significant advantages of sensitivity and selectivity compared with planar platinum electrode and method for their preparation requires sophisticated equipment. Therefore, in order to obtain choline-based biosensor, we decided to investigated another type of electrode –glassy carbon electrode modified with platinum nanoparticles (Pt-Nps). Nanoparticles were chosen due to the fact that they can be easily obtained on the electrode surface by electrochemical generation. At the same time, the size of such particles can be much smaller than the diameter of Pt-

Nfb, which may contribute to an increase of electrocatalytic effect, compared with nanofibers.

3.2.1.1. Optimization of the conditions of the glassy carbon electrode modification with platinum nanoparticles

We used a method described in work [64] for electrochemical generation of nanoparticles on the surface of GCE, which involves alternation of reducing and dumping pulses of short duration. While imposing negative potential the reduction of platinum precursor occurs on the electrode surface, which leads to the formation of platinum nanoparticles, at dumping pulse no electrochemical reaction occurs. SEM-image of modified electrode (Fig. 3.9a) reveals a presence of nanoparticles that are uniformly distributed over the electrode surface.

The confirmation of the fact of Pt-NPs formation is possible also electrochemically. We have investigated the electrochemical response of GCE modified with Pt-NPs (GCE-Pt-NPs) to hydrogen peroxide, and compared it with unmodified GCE (Fig. 3.9b,c)

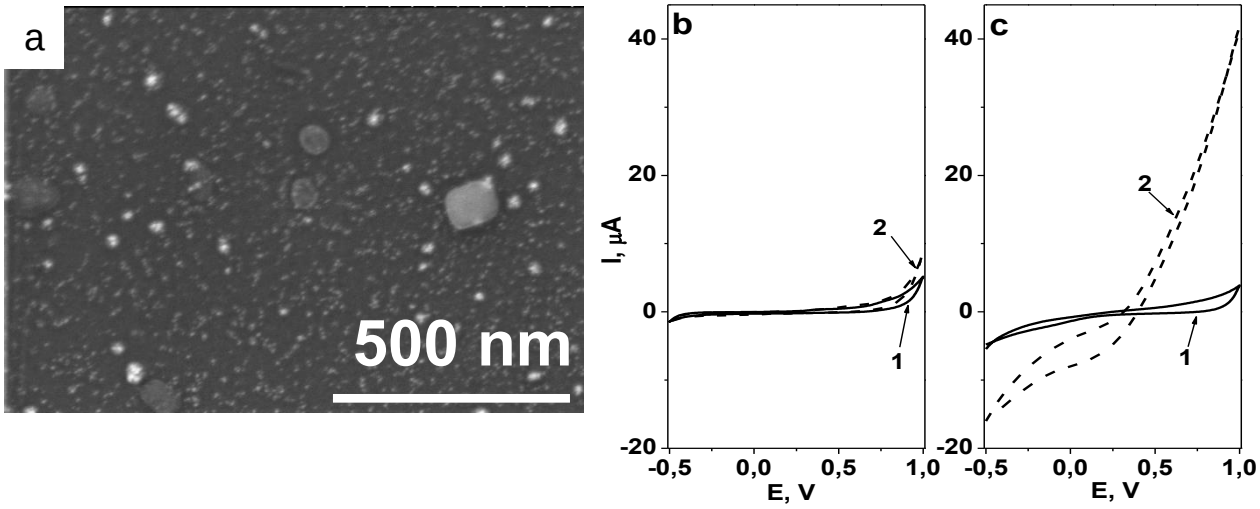

Fig. 3.9. (a) SEM-image of GCE, modified with with Pt-Nps by means of electrochemical generation; (b, c) Cyclic voltammograms of GCE (b) and GCE-Pt-Nps (c) in 0.025 M PBS (pH 7.0) in the absence (1) and presence of 3 mM H_2O_2 (2). Scan rate 50 mV/s.

It is noticeable that unmodified GCE is almost inactive to hydrogen peroxide in the range of potentials -0.5 – 1.0 V. There is no difference in voltammograms of this electrode in the presence and in the absence of H_2O_2 (Fig. 3.9b, curves 1,2). A slight increase of current is seen from the potential 0.9 V you, which apparently precedes the peak of H_2O_2, oxidation observed at potentials higher than 1 V. In contrast, the voltammogram of modified GCE-Pt-NPs in the presence of hydrogen peroxide is significantly different from voltammogramms in the buffer solution (Fig. 3.9c). Two half-wave, cathodic and anodic, are visible at potential about 0.35 V corresponding to the reduction and oxidation of hydrogen peroxide, respectively (Fig. 3.9). They appear due to the presence of platinum nanoparticles on the surface of GCE, catalyzing the electrochemical reaction of H_2O_2. Thus, the electrodeposition of Pt-NPs on the surface of GCE significantly shifts the potential of H_2O_2 oxidation in the negative direction and improves the electrochemical response. Such behavior makes the electrode a promising sensor for hydrogen peroxide.

The assumption can be made that the pulse duration affects the size of nanoparticles and the number of pulses affects their quantity. The change of these parameters may affect their catalytic properties. Therefore, to increase the sensitivity of GCE-Pt-NPs to hydrogen peroxide the number and duration of pulses have been optimized. Sensitivity was calculated as described in paragraph 2.3.3). The results are shown in Table 3.1.

Table 3.1

Influence of the duration (1) and number of pulses (2) of Pt-Nps electrogeneration on the sensitivity of GCE-Pt-Nps to H_2O_2

1		2	
Pulse duration, s	Sensitivity to H_2O_2 at 0.7 V, μA/mM	Number of pulses (0.3 s)	Sensitivity to H_2O_2 at 0.7 V, μA/mM
0*	0.19	0*	0.19

0.3	**1.27**	1	1.27
0.5	0.55	**3**	**4.08**
0.8	0.46	5	2.18
1.5	0.33	7	0.77

* nonmodified GCE

The obtained data indicate that the highest sensitivity of modified electrode to H_2O_2 is observed at the shortest pulse duration, i.e., the formation of smaller particles. This can be explained by the fact that smaller particles are likely to exhibit stronger catalytic properties. Sensitivity also increases with the number of pulses from one to three, and further increase leads to a decrease in the signal, possibly due to the formation of a large number of particles forming agglomerates. Thus, the optimal parameters of electrochemical generation of Pt-NPs were three pulses of 0.3 sec each.

3.2.1.2. Investigation of the stability of amperometric response of glassy carbon electrode modified with platinum nanoparticles

In addition to high sensitivity to hydrogen peroxide electrochemical transducer must demonstrate the stability and reproducibility of the response. Therefore, we have tested the stability of amperometric and voltammetric responses of GCE-Pt-Nps to hydrogen peroxide (Fig. 3.10).

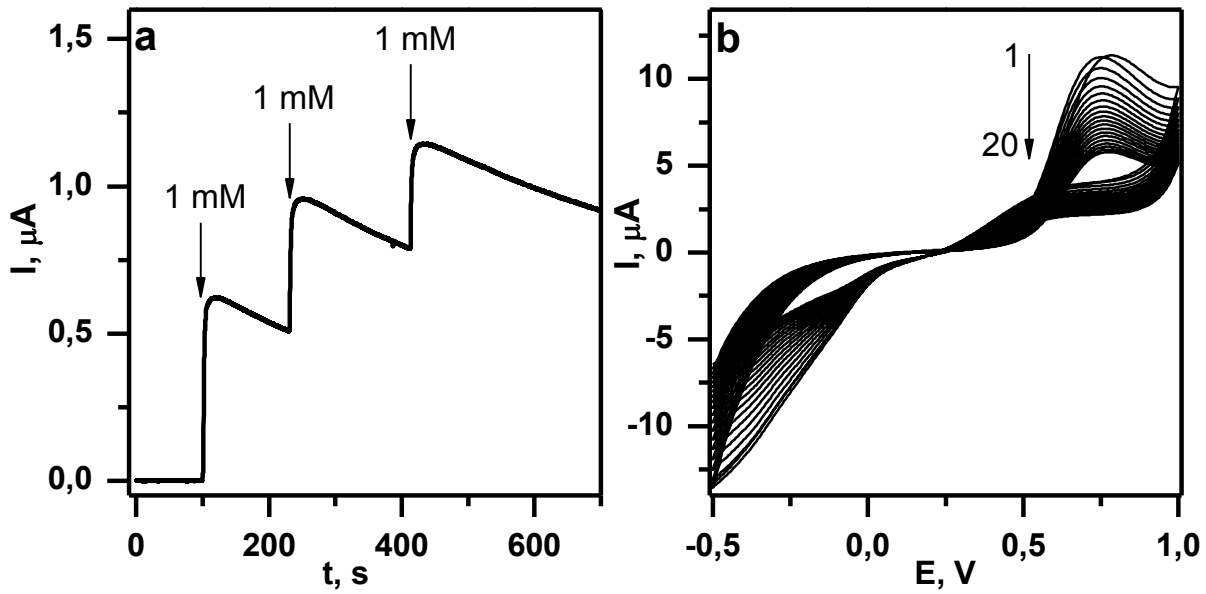

Fig. 3.10. (a) Amperometric response of GCE-Pt-Nps to the additions of H_2O_2 (on the graph). Supporting electrolyte: 0.025 PBS (pH 7.0), applied potential +0.7 V; (b) Cyclic voltammograms (20 cycles) of GCE-Pt-Nps in the presence of H_2O_2 (1 mM). Supporting electrolyte: 0.025 PBS (pH 7.0), scan rate 50 mV/s.

The amperogram of GCE-Pt-Nps at potential 0.7 V demonstrates clear response to additions of hydrogen peroxide (Fig. 3.10a). However, the magnitude of this response differs for three consecutive additions of the same amount of H_2O_2, indicating poor reproducibility. But most important is that the response is not stable over time – the current value after each addition does not remain stable, but gradually and continuously decreases (Fig. 3.10), reaching only 50% of the original after 200 seconds of experiment. A similar situation is observed on a cyclic voltammogram of GCE-Pt-Nps in the solution containing hydrogen peroxide (Fig. 3.10b). Each scan reduces the size of anodic peak at potential 0.7 - 0.8 V, its value remains only at 50% level from initial after the 20-th scanning.

In the efforts to improve stability and to prevent leaching of nanoparticles from the electrode surface we have coated the GCE-Pt-Nps electrode with biocomposite film SiO_2-ChOx with the same parameters of electrodeposition as explained in

section 3.1. This modified electrode was active to choline (Appendix C), but its stability was still quite low.

Thus, the glassy carbon electrode modified with platinum nanoparticles is characterized by poor stability of the response. This situation can be explained by the gradual leaching of platinum nanoparticles from the electrode surface or their deactivation. Therefore, given the high demands on the stability of amperometric sensors, GCE-Pt-NPs was not desirable for using as a transducer in amperometric sensor for choline.

3.2.2. The choice of electrode for the choline oxidase immobilization

Given the poor stability of nanoparticles a comparative study of the other types of electrodes was conducted in order to find a new type of transducer for the immobilization of ChOx (Fig. 3.11).

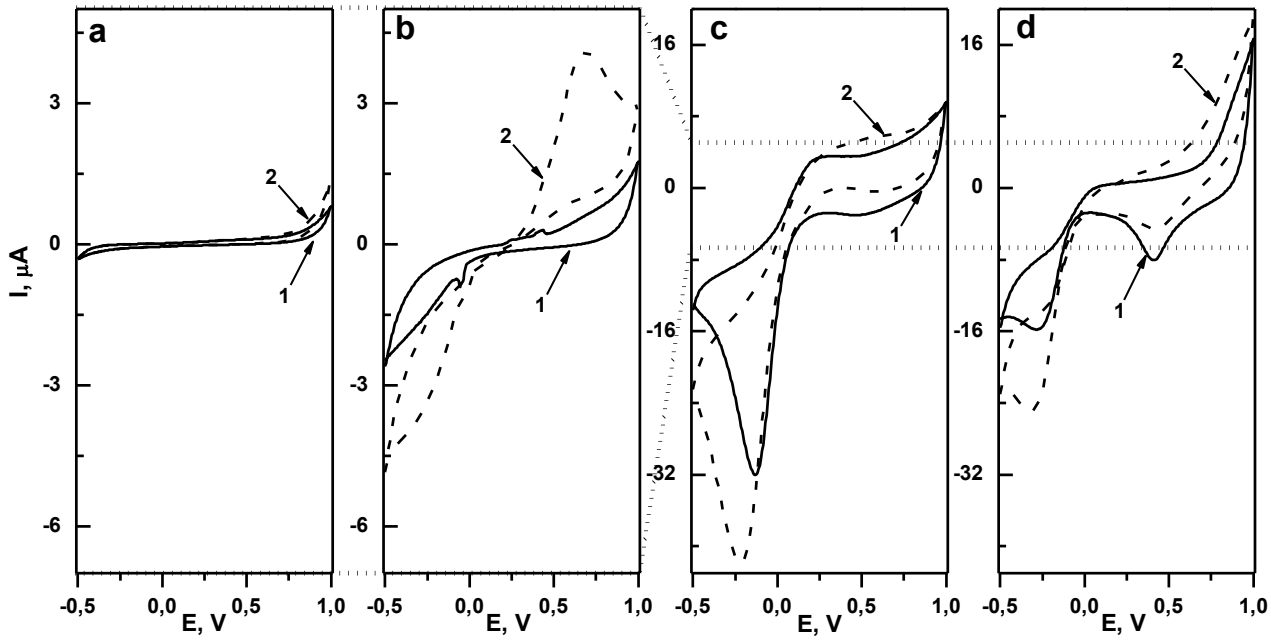

Fig. 3.11. Comparative cyclic voltammograms of GCE (a), GCE-Pt-Nps (b), platinum (c) and gold (d) screen-printed electrodes in the absence (1) and presence (2) of 1 mM H_2O_2. Supporting electrolyte: 0.025 PBS (pH 7.0), scan rate 50 mV/s. The dotted line shows proportionality of scales of (a, b) and (c, d).

As objects of comparison we selected screen-printed electrodes as they have low cost and easy fabrication, as well as small size including both working, auxiliary and reference electrodes. At the same time, specially designed for use in the sensors, they usually have high electrochemical activity. The type working electrode material (gold and platinum) was chosen because of their high sensitivity to H_2O_2.

Cyclic voltammograms of platinum (Fig. 3.11c) and gold (Fig. 3.11d) screen-printed electrodes (AuSPE) shows active oxidation of hydrogen peroxide on them – the current increase in both cases is noticeable starting from potential 0.2 V (Fig. 3.11c, d curve 2). The value of current is approximately the same for these two electrodes and commensurate with the current on GCE modified with platinum nanoparticles (Fig. 3.11b). Given this, any of the two screen-printed electrodes can be used as a transducer for the immobilization of ChOx. However, taking into account the slightly higher response to H_2O_2, lower cost and advantages of gold electrode [251], we have chosen the AuSPE for the immobilization of ChOx.

3.2.3. Immobilization of choline oxidase into SiO_2-film on the surface of gold screen-printed electrode

For the one-step immobilization of ChOx in the SiO_2-film on the surface of AuSPE the EAD method was proposed with parameters similar to those used for the immobilization of GOx on the surface of Pt-Nfb. However, to achieve a significant response the duration of deposition has been increased to 20 seconds.

The AuSPE modified with film SiO_2-ChOx demonstrates significant increase of anodic current on the voltammogram in the presence of choline (Fig. 3.12a).

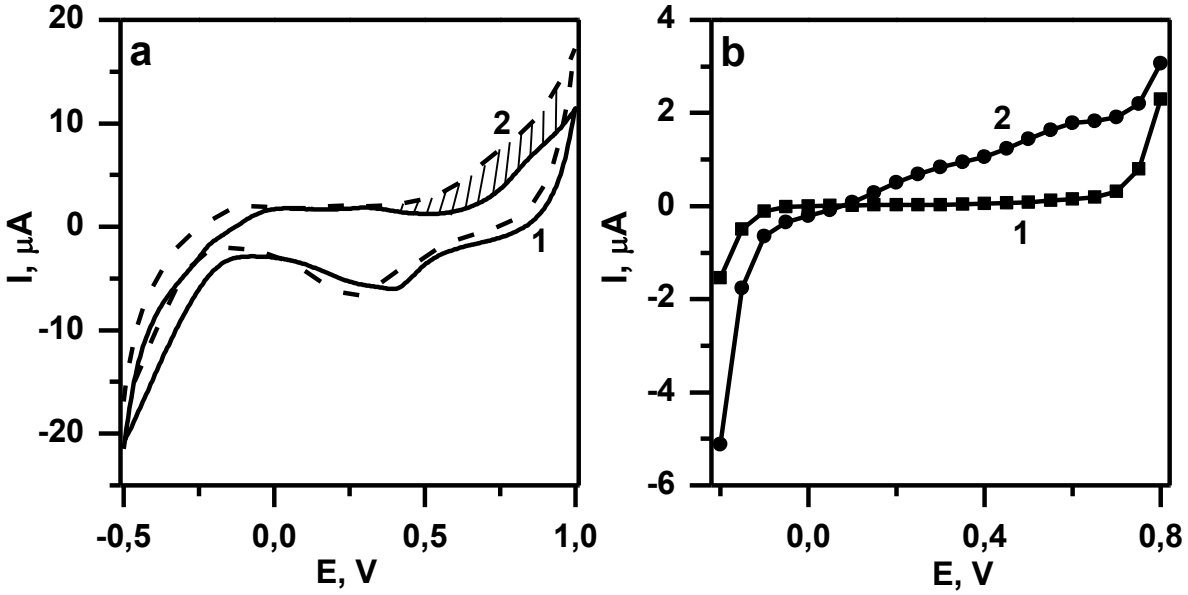

Fig. 3.12. Cyclic voltammograms (a) and hydrodynamic voltammograms (b) of AuSPE modified with SiO_2-ChOx film in the absence (1) and presence (2) of 2 mM choline. Supporting electrolyte: 0.025 M PBS (pH 7.5), scan rate 50 mV/s.

The current increase is due to the oxidation of H_2O_2 (Equation (3.2)), which is formed during the passing of enzymatic reactions involving ChOx:

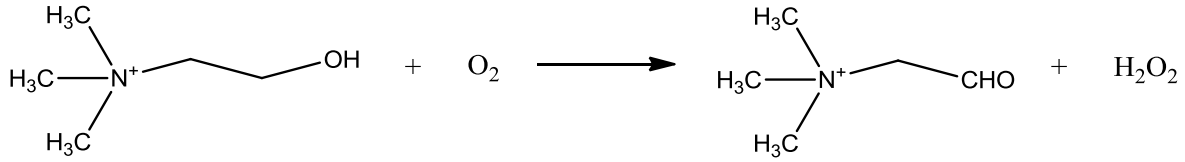

(3.4)

The method of hydrodynamic voltammetry (Fig. 3.12b) confirms this finding. Indeed, the voltammogram of AuSPE-SiO_2-ChOx in the presence of choline (Fig. 3.12b, curve 2) depicts two half-waves, whose presence can be explained by a complex mechanism of hydrogen peroxide oxidation on gold electrodes [262]. From this voltammogram the optimum working potential (0.7 V) was selected.

3.2.4. Choice of the deposition potential of the SiO_2-choline oxidase film

Negative potential imposed during EAD, affects the rate of formation of electrogenerated catalyst affecting the parameters of formed SiO_2-films, such as thickness and porosity. In turn, these characteristics influence the response of

immobilized enzyme. Therefore, we have investigated the influence of the electrodeposition potential on the sensitivity of AuSPE-SiO_2-ChOx, obtained at constant duration of deposition 20 s.

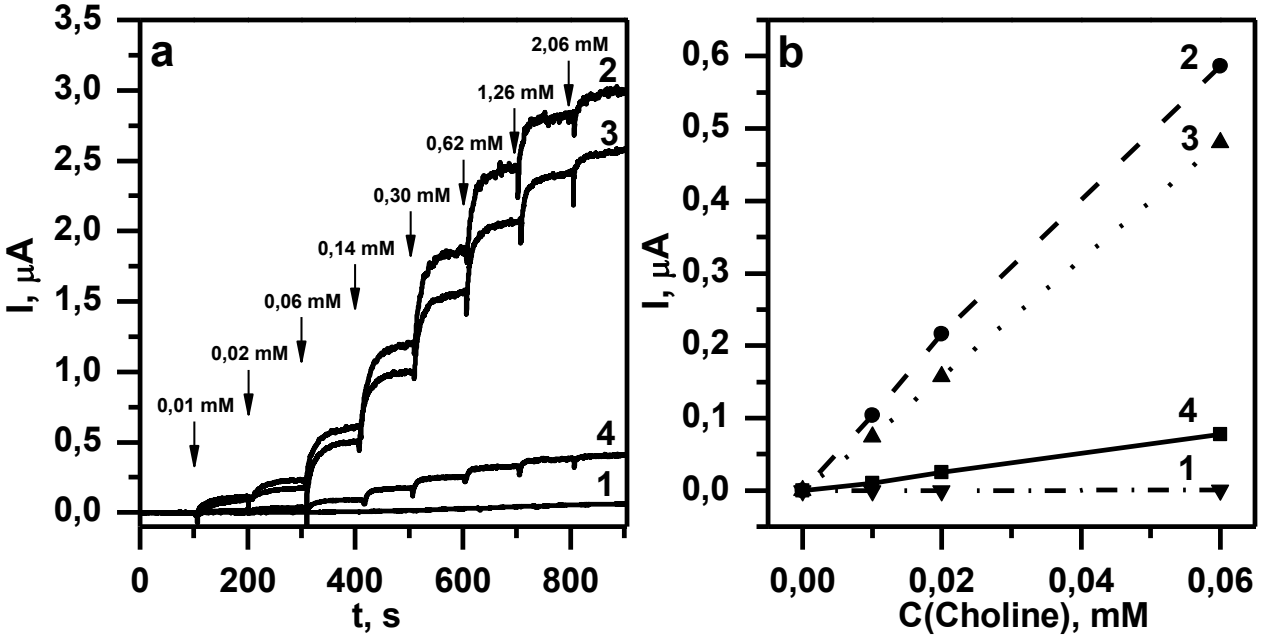

Fig. 3.13. Amperometric curves (a) and corresponding dependences of current from choline concentration in the initial range (b) for AuSPE-SiO_2-ChOx, obtained at potential -1.0 (1), -1.1 (2), -1.2 (3), -1.3 (4) V and time of deposition 20 s. Supporting electrolyte: 0.025 M PBS (pH 7.5), applied potential +0.7 V.

The results shown in Fig. 3.13 indicate that the change of deposition potential leads to changes in the sensitivity of the modified electrode. The greatest response observed for the EAD at potential -1.1 – 1.2 V, which correlates with the optimal parameters of deposition of GOx-containing film on the surface of Pt-Nfb (section 3.1). At the same time, at higher potential (Fig. 3.13b, curve 1) the response is almost absent due to slow speed of electrogeneration resulting in the absence of SiO_2-film on the electrode. However, more negative potentials (-1.3 B) (Fig. 3.13b, curve 4) lead to a too violent reaction of electrolysis of water and active hydrogen bubbles formation which prevent the formation of the film, causing its destruction.

3.2.5. Investigation of the response stability of gold screen-printed electrode modified with SiO_2-choline film

Stability is an important parameter of biosensors, so we performed a study of long-term stability of AuSPE-SiO_2-ChOx. The study was conducted by recording the calibration curves every 4 days for 2 weeks and comparing the sensitivity of the modified electrode to choline relative to the initial value immediately after modification.

As known, the main causes of sensitivity loss of biosensors is inactivation of enzymes in the film, as well as their leaching, including as a result of the film destruction. The presence of surfactants in sol during EAD significantly affects the last factor, enhancing the interaction of the enzyme with silanol groups of film as well as acting as structuring agent and improving its morphological properties (paragraph 1.2, 2.1.2). Therefore, we have investigated the effect of concentration of CTAB in the sol on the long-term stability of AuSPE-SiO_2-ChOx.

To assess the stability of the biosensor the relative sensitivity of the electrode modified with film SiO_2-CTAB-ChOx was calculated, using the formula:

$$S = \frac{S_x}{S_1} \times 100\% \qquad (3.5)$$

wh. S – relative sensitivity, %;

S_1 – sensitivity of the electrode to substrate at first day after modification, μA/mM;

S_x – sensitivity of the electrode to substrate at x-th day after modification, μA/mM.

The modified electrode was stored in a refrigerator at +4 C in the interim between experiments. It should be noted that the free enzyme in buffer solution under these conditions completely lost the activity in week, which contrasts with preservation of activity of immobilized enzyme. The data presented in Table 3.2.

Table 3.2

Influence of CTAB concentration in the sol on the long-term response stability of AuSPE-SiO_2-ChOx

C (CTAB), mM	Relative sensitivity in two weeks, %
0.0	< 1
6.1	9.8
12.2	52.7
21.3	18.9
42.7	8.5

The data obtained shows that the biggest stability of modified electrode is observed at concentrations of CTAB in sol 12.2 mM, which is much greater than its CMC in aqueous solutions (≈ 1 mM [35]). This correlates with data on a range of CTAB concentrations in sol with the highest analytical response of immobilized biomolecules [34, 36]. High concentrations of CTAB leads to a high foaming and flotation effect, and may lead to the restructuring of micelle and film structure reducing amperometric response of immobilized enzyme.

The operational stability of AuSPE-SiO_2-ChOx which is necessary during continuous operating of biosensor was investigated in voltammetric and amperometric modes at optimum concentration of CTAB in sol (Fig. 3.14). The first cycle of potential scan at cyclic voltammogram of AuSPE-SiO_2-ChOx in the presence of choline slightly differs from others with higher current (Fig. 3.14, curve 2), which can be explained by leaching out the surface layer of weakly bound enzyme not captured by film. At the same time, the 10th, 20th and 30th cycles are almost identical and constant (Fig. 3.14, curves 3-5), indicating a high operational stability.

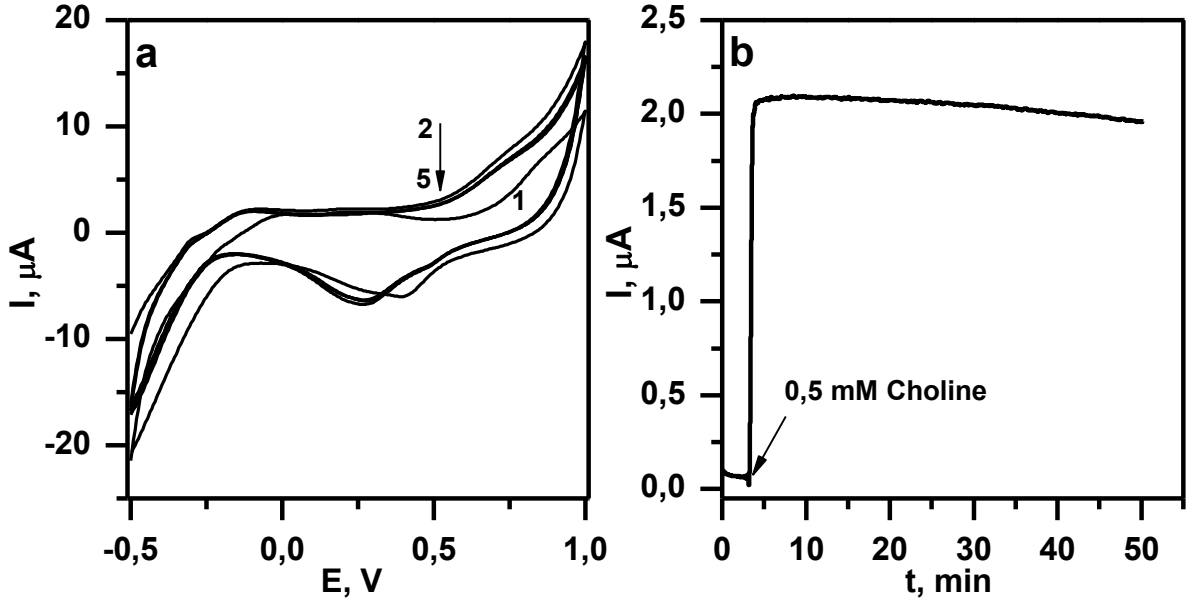

Fig. 3.14. (a) Cyclic voltammograms of AuSPE-SiO_2-ChOx (at optimum CTAB concentration) in the absence (1) and presence of 2 mM choline: 1st(2), 10th (3), 20th (4) and 30th (5) cycles of potential scan (50 mV/s); (b) Amperometric curve of AuSPE-SiO_2-ChOx in the presence of choline (0.5 mM). Applied potential +0.7 V. Supporting electrolyte: 0.025 M PBS (pH 7.5)

The constant response is also observed in amperometric mode. Catalytic oxidation current of hydrogen peroxide, which is formed by the enzymatic oxidation of choline after 50 minutes of continuous measurements while mixing decreases no more than at 6% (Fig. 3.14b).

Thus, these data indicate high operational stability of AuSPE-SiO_2-ChOx, which is achieved through the use of sol-gel encapsulation of enzymes and addition of surfactant CTAB. The resulting stability is quite sufficient for the application of developed modified electrode as a sensitive element of biosensor and its use in the analysis different objects.

Further, the optimum parameters were the EAD at potential -1.1 V for 20 s, and the presence of 12.2 mM CTAB in sol.

3.2.6. Dependence of the amperometric response of the gold screen-printed electrode modified with SiO_2-choline oxidase film from the choline concentration

Dependence of the amperometric response of AuSPE-SiO_2-ChOx on the concentration of choline resembles the saturation curve (Fig. 3.15a), which is typical for enzymatic Michaelis-Menten kinetics [247].

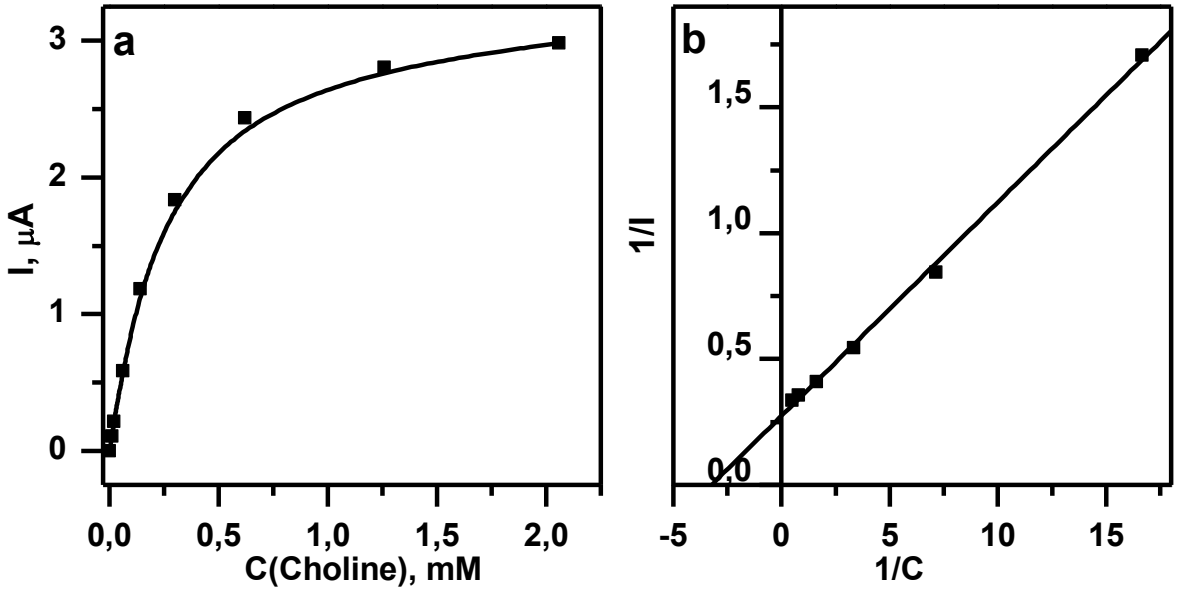

Fig. 3.15. (a) Dependence of the amperometric response of AuSPE-SiO_2-ChOx at potential +0.7 V on the choline concentration. Supporting electrolyte: 0.025 M PBS (pH 7.5); (b) Lineweaver-Burk plot for the determination of apparent Michaelis constant.

The apparent Michaelis constant calculated using the method Lineweaver-Burk was 0.27 mM (Fig. 3.15b). This value is lower than for ChOx, immobilized in a film PDDA (0.42 mM [263]), the glutaraldehyde-PVA film (0.78 mM [264]), and significantly lower than values for ChOx in solution (0.87 mM [265]). These data indicate a high activity ChOx, immobilized in a SiO_2-film and its high affinity for the substrate – choline.

The calibration graph for determination of choline was linear in the concentration range of 0.01 – 0.6 mM (Fig. 3.16).

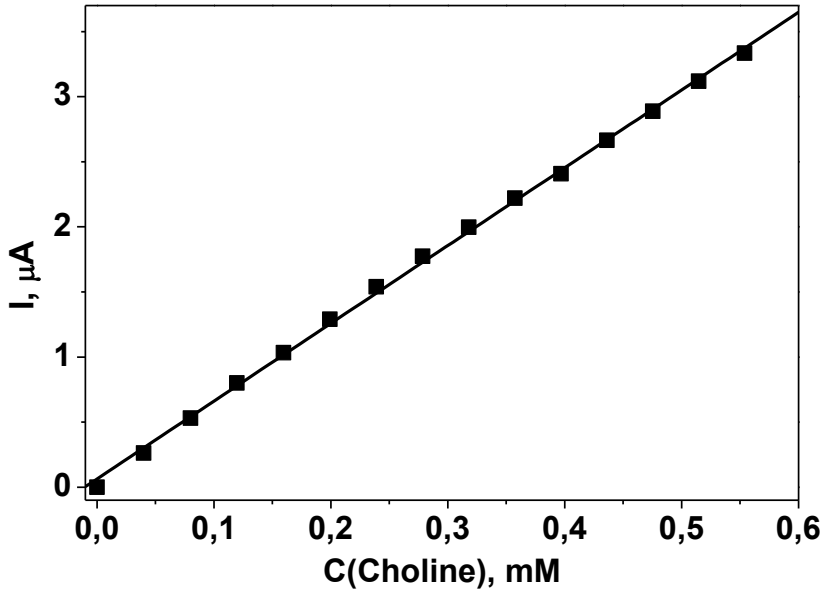

Fig. 3.16. Dependence of the amperometric response value of AuSPE-SiO_2-ChOx at potential +0.7 V on the choline concentration in the solution. Supporting electrolyte: 0.025 M PBS (pH 7.5).

The line equation has the form: I (μA) = (0.06 ± 0.01) + (5.97 ± 0.05) * C (mM) (R^2 = 0/998). The detection limit, calculated by 3S-criteria was 5 μM choline (0.7 mg/L). Thus, the sensitivity of the modified electrode is sufficient for the determination of choline in foods and biological fluids.

3.3. Conclusions to chapter 3

The oxidation current of hydrogen peroxide on the surface of platinum nanofibers is increases in about 10 times compared with bare platinum electrode, making the use of such nanofibers promising for the development of oxidase-based biosensors. At the same time platinum fibers coated with SiO_2-film do not have advantages over bare platinum electrode. The response of glucose oxidase immobilized in SiO_2-film on the surface of platinum nanofibers significantly depends on the thickness of biocomposite film.

Electrogeneration of platinum particles on the surface of the glassy carbon electrode increases the sensitivity of the latter to hydrogen peroxide. However, response of such modified electrode is unstable due to the gradual leaching of nanoparticles from the electrode surface, showing little promise of its application in the development of biosensors.

The use of gold screen-printed electrode is promising for the immobilization of choline oxidase in SiO_2-film. The application of simple one-step method of electrochemically-assisted deposition allows the immobilization of the enzyme on the surface of the gold electrode with preservation of its activity. The increase of the stability and sensitivity of the modified electrode to choline can be achieved by altering the deposition parameters and by introduction of the surfactants in the sol. The best performance of modified electrode was obtained using deposition at -1.1 V for 20 s and CTAB concentration in sol 12.2 mM. The developed sensitive element of the choline biosensor has a wide linear range and low detection limit.

CHAPTER 4. IMMOBILIZATION OF SORBITOL DEHYDROGENASE ON THE ELECTROPHORETICALLY-DEPOSITED CARBON NANOTUBES

The use of dehydrogenases in biosensors are usually less common than corresponding oxidases due to their low stability and difficulty of coenzyme NAD^+/NADH detection. For example, there are only a few works about the development of biosensors based on sorbitol dehydrogenase (DSDH) – enzyme that can be used to identify the substrate sorbitol. However, these works are limited to the definition of sorbitol in model solutions, data on the analysis of real objects are missing. Encapsulation in thin silica film can increase the stability of enzymes in the immobilized state, making appropriate the use of this method for the development of dehydrogenases-based biosensors. Given the lack of literature data on the application of EAD method to immobilize dehydrogenases, the point of interest is the development of methodological approaches of the EAD method application for the immobilization of DSDH into SiO_2-film, as well as the use of developed biosensor for sorbitol determination in the real objects.

The development of sensitive dehydrogenase-based biosensors requires the selective, sensitive and reliable detection of coenzyme NADH formed in the enzymatic reaction (see paragraph 1.5.2). As noted in the literature review, the metal electrodes (including platinum and gold) are unsuitable for such purposes because of the high potential of NADH oxidation and poisoning of the electrode surface by reaction products, leading to a sensitivity decrease. The better choice is electrodes based on allotropic modification of carbon. For example, carbon nanotubes (CNT) are promising for use as a matrix for such biosensors due to the low potential oxidation of NADH on them. However, their handling is difficult because of small size, negligible solubility in inorganic solvents and the tendency to aggregation. As previously stated in the literature review (paragraph 1.3.2), electrophoretic deposition method is able to solve these problems allowing controlled electrode modification with CNT from low-concentrated dispersions. CNT-coatings obtained therefore, have

not been used as a matrix for enzyme immobilization, but they have great potential and are promising for electrode modification including the sol-gel method. This chapter presents the results of study of CNT-layer, obtained by EPD on the surface of GCE, including the activity towards NADH oxidation. The prospects of its combination with EAD method for the immobilization of dehydrogenases are shown.

4.1. Characterization of the electrophoretically deposited carbon nanotubes layers

The electrophoretic deposition method allows the accumulation of charged particles from their suspension onto one of the two electrodes used in the device. For this reason, carbon nanotubes bearing a high content of negatively-charged carboxylic groups on their surface have been chosen to facilitate their dis-persion (as non-modified CNT of this sort are almost insoluble in the pure water) and to make them likely to move in the electric field in order to get fast deposition of high quality CNT layers. The rate of the precipitation of charged particles depends on the applied potential difference, surface area of electrodes, distance between them and the process duration [266]. Therefore, the quantity of deposited nanotubes can be finely controlled by varying the time of potential application while keeping other parameters constant. The optimal applied potential difference of 60 V was used throughout because it constitutes a good compromise between a high speed of deposition and limited decomposition of ultra- pure water (which would generate oxygen bubbles that may affect CNT assembly).

4.1.1. Morphological characteristics

A necessary condition for the efficiency of electrode modification with CNT is the formation of a homogeneous and reproducible coating. The application of EPD method allows obtaining of such coatings.

Scanning electron microscopy was first used to characterize CNT-layers obtained either at short (Fig. 4.1a) or longer (Fig. 4.1b) deposition times. As shown, short deposition times (e.g., 5 s for Fig. 4.1a) led to nanotubes arranged in a sparse interconnected network where single nanotubes can be easily distinguished. On the contrary, when potential was applied for longer times (e.g., 1 min for Fig. 4.1b), the deposits turned into thick films with dense packing and more or less parallel orientation of nanotubes to the surface, but still representing sufficiently porous structure likely to allow diffusion of reactants into the inner layers.

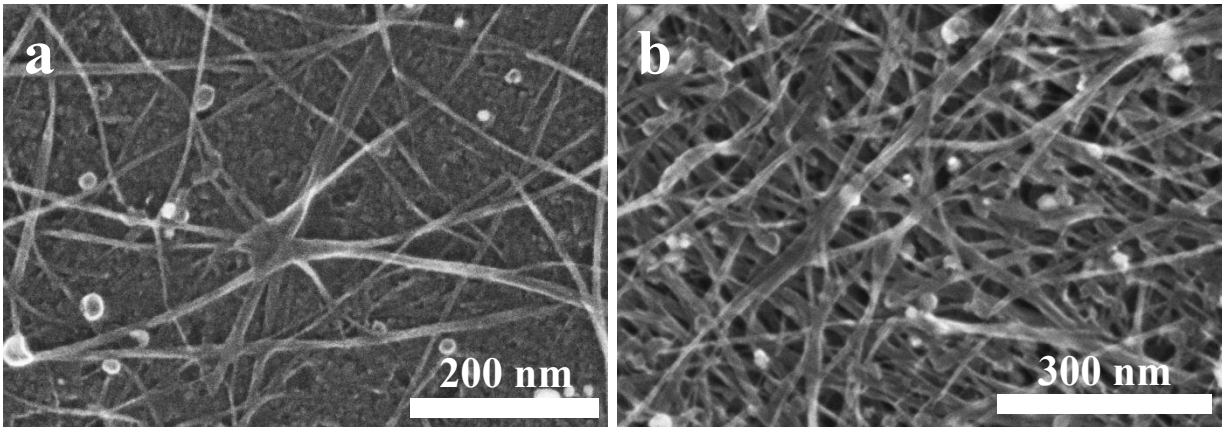

Fig. 4.1. SEM image of nanotubes deposit on the surface of GCE with (a) short time of potential applying (t = 5 s) and with (b) long time of potential applying (t = 60 s).

All images can clearly show the presence of distinct horizontally-oriented nanotubes, indicating the absence of aggregation, occuring, for example, when CNT dispersion is simply dropped on the electrode.

4.1.2. The influence of the duration of deposition on the CNT-layer thickness

The formation of CNT assemblies was also monitored by atomic force microscopy. In spite of the difficulties to recognize single nanotubes (for more detailed image see Appendix D), the overall thickness and uniformity of film can be

examined by analyzing AFM profiles sampled from images recorded at the border of the deposit comprising area (see Fig. 4.2 for a particular case).

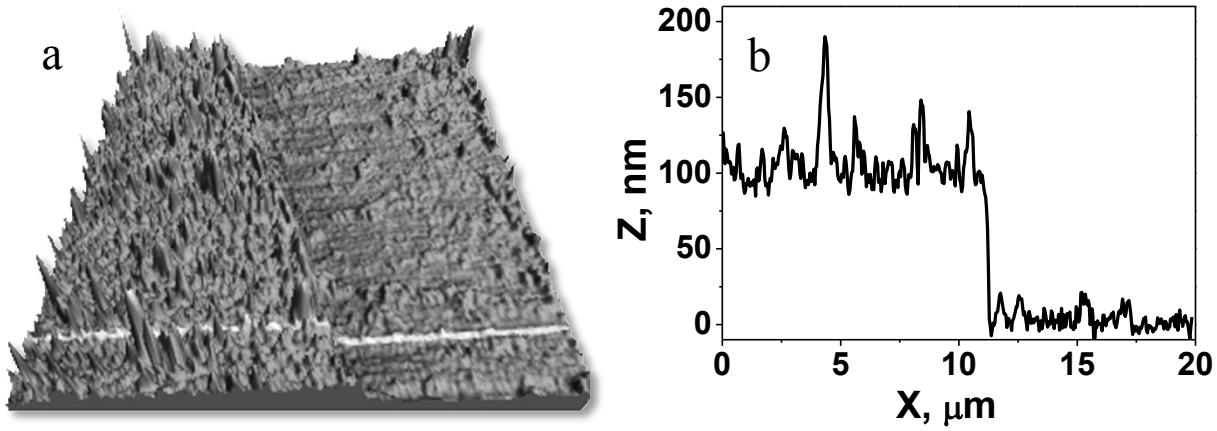

Fig. 4.2. (a) AFM image and (b) cross-section profile (along white line) of the CNT-layer with 30 s of deposition. Image size 20 x 20 μm.

The corresponding thickness data are depicted on Fig. 4.3, revealing a linear dependence of CNT layer thickness with the time of electrophoretic deposition, confirming the fact that the CNT deposit progressively grows when applying the electric field.

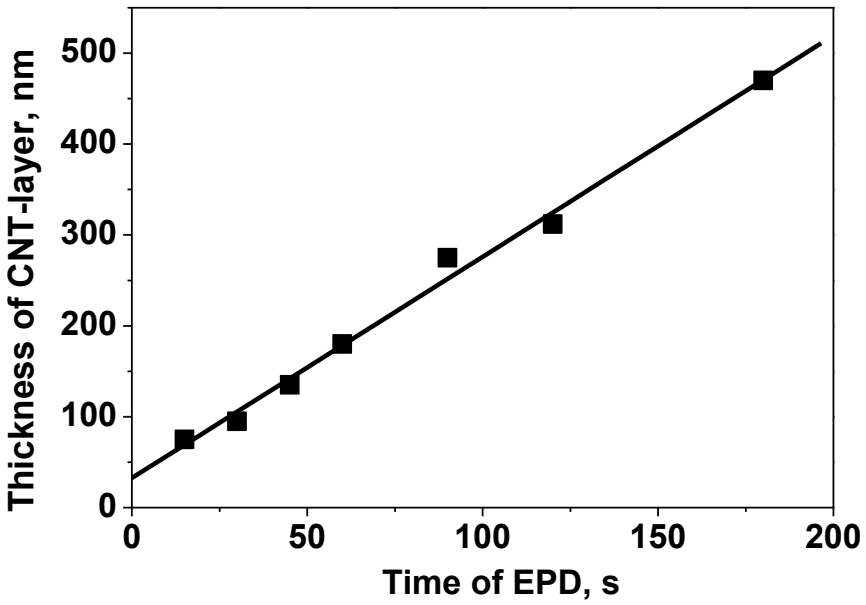

Fig. 4.3. Dependence of the thickness of carbon nanotubes layer measured by AFM from the time of electrophoretic deposition.

The equation of this dependence is following:

$$H = (32 \pm 9) + (2 \pm 0{,}1) \times t \quad (4.1)$$

wh. H – thickness of CNT-layer, nm;
t – duration of EPD, s.

That gives the possibility to control the quantity of deposited carbon nanotubes and, consequently, the film thickness by tuning the electrophoretic deposition time. Such variation could influence the electrochemical characteristics of modified electrode.

4.1.3. Measurement of the electroactive surface area of CNT-layer

Electroactive surface area is one of the most important parameters of the electrodes, whose increase usually leads to an increase in current density, and hence the sensitivity of such electrodes. To estimate the surface area of GCE-CNT electrodes, we have used the adsorption of the dye methylene green (MG). It is known that phenothiazine dyes can easily adsorb onto the surface of carbon nanotubes owing to the favorable electrostatic and π–π stacking interactions [233]. We have thus exploited the adsorption of methylene green, which is electrochemically active, to examine the modification of the electrode surface area in the course of electrophoretic deposition.

After being left in the dye solution overnight and washed, the resulting GC-CNT electrode still shows two pairs of peaks on the cyclic voltammograms recorded in PBS buffer (Fig. 4.4a). The first pair could be attributed to the presence of a small quantity of non-bound methylene blue, taking into account its potential [229]. The current heights of the second pair of peaks show a linear dependence on the potential scan rate (Fig. 4.4b), suggesting a non diffusion-controlled electron transfer process

and leading to the conclusion that these peaks originate from the methylene green adsorbed on the surface of carbon nanotubes [267].

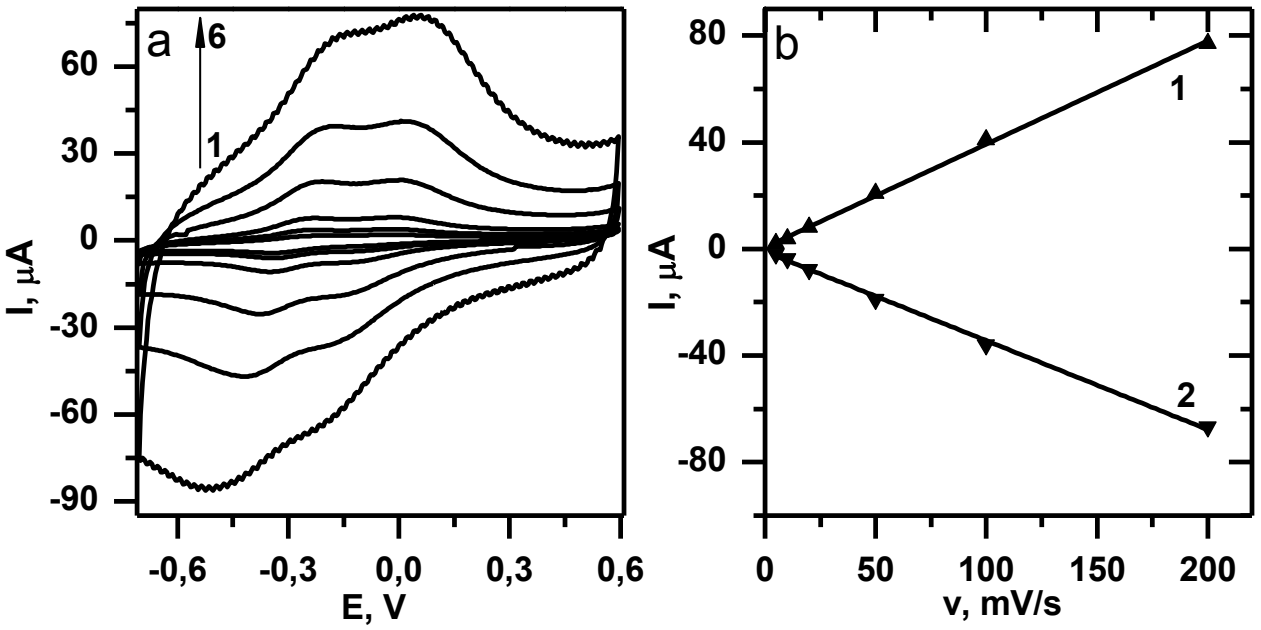

Fig. 4.4. (a) Cyclic voltammograms in the anaerobic conditions of GCE-CNT with adsorbed methylene green at different scan rates: (1) 5 mV/s, (2) 10 mV/s, (3) 20 mV/s, (4) 50 mV/s, (5) 100 mV/s, (6) 200 mV/s. (b) Oxidation (1) and reduction (2) peaks currents of methylene green versus scan rate.

Following the process of electrophoretic deposition, one can observe that the intensity of these peak currents evolved (Fig. 4.5a), starting from negligible values when clean glassy carbon is used (curve 1), then growing continuously as the deposition time increased (Fig. 4.5b). This behavior proves the porous structure of the so-formed CNT film since the dye molecules afford to diffuse inside the CNT layer to adsorb onto the walls of the underlying nanotubes.

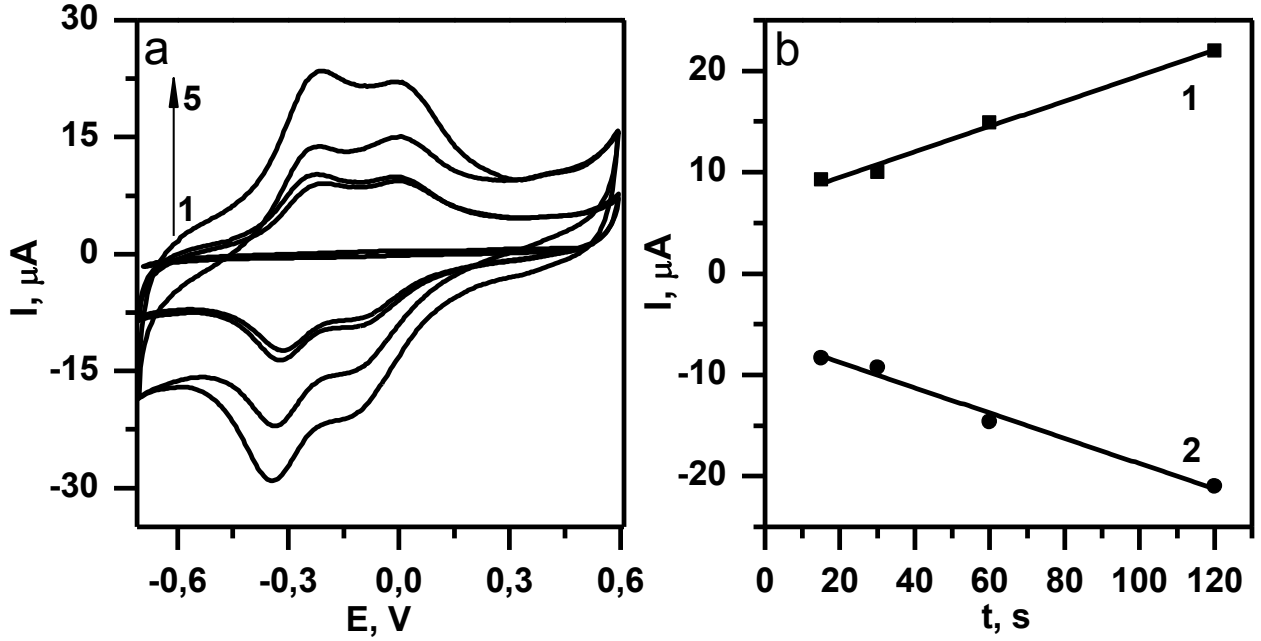

Fig. 4.5. (a) Cyclic voltammograms in the anaerobic conditions of the methylene green adsorbed on the GCE-CNT with different time of electrophoretic deposition of CNT: (1) 0 s, (2) 15 s, (3) 30 s, (4) 60 s, (5) 120 s. (b) Dependence of the methylene green cathodic (1) and anodic (2) peak heights from the time of CNT deposition. Supporting electrolyte 0.067 M PBS (pH 7.5), scan rate 20 mV/s.

Thus, the present electrophoretic method allows obtaining in a controlled way a porous conductive matrix with extended electroactive surface area, which might be of interest for the immobilization of a large quantity of enzyme.

According to the formula (2.3), by integrating the peak area of adsorbed MG one may calculate the approximate area of electroactive surface of electrode modified with CNT. For the electrode modified with CNT by EPD duration of 120 s (Fig. 4.5a, curve 5) electroactive surface area was 1033 mm^2, while the geometric area of the electrode of the same diameter (6 mm) is 28 mm^2 (according to the formula $S = \pi r^2$). Thus, modification of electrode with CNT by EPD method increases electroactive surface area of the electrode for almost 40 times, leading to the improvement of its sensitivity to electroactive substances.

4.2. Electrocatalytic properties of CNT assemblies towards NADH oxidation

To reveal the outlook for the application of hereby deposited carbon nanotubes film for the bioelectrode development, we examined its electrocatalytic effect toward the oxidation of NADH, an enzymatic cofactor mostly required for enzymes from dehydrogenases group.

4.2.1. Comparison of the voltammetric characteristics of NADH oxidation on the modified with CNT and non-modified glassy carbon electrods

Cyclic voltammograms depicting the electrochemical behavior of NADH on the different electrodes are presented in Fig. 4.6.

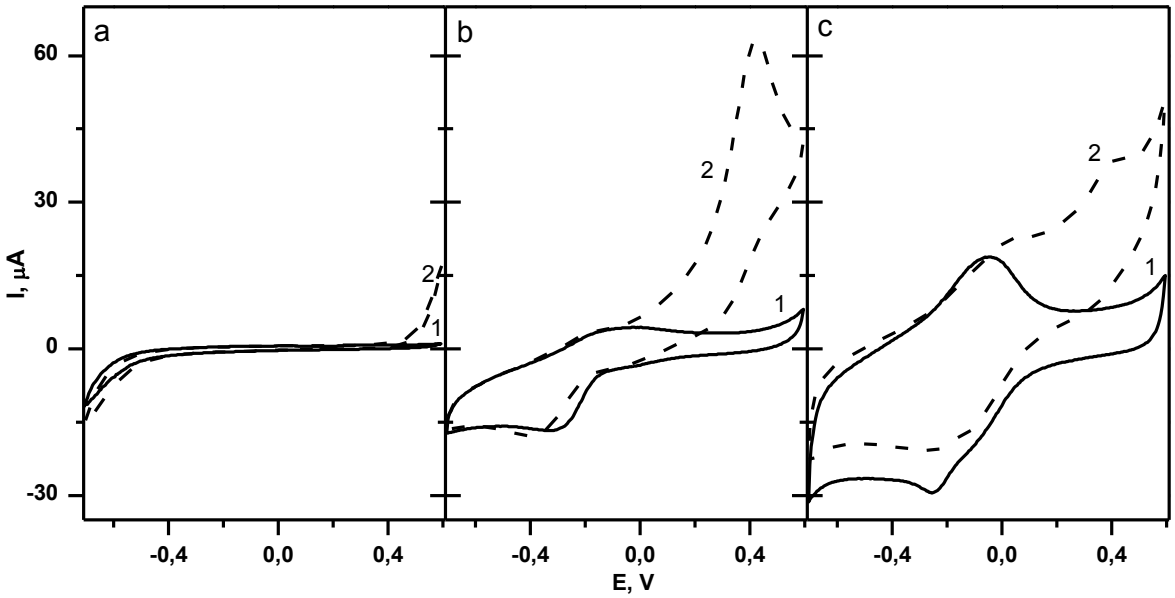

Fig. 4.6. Cyclic voltammograms of the (a) GCE, (b) GCE-CNT (prepared by EPD) and (c) GCE-CNT (drop-coated) in the 0.067 M PBS (pH 7.5) without (solid lines) and with (dashed lines) 5 mM NADH. Scan rate 20 mV/s.

Direct NADH oxidation (or NAD^+ regeneration) on bare glassy carbon electrode was reported to be unsatisfactory because of high overpotentials [213] and surface fouling with the reaction products [216]. This is confirmed here on Fig. 4.6a

showing no significant anodic current below 0.6 V (actually a peak (not shown on the figure) can be observed at ca. 0.8 V), in agreement with previous literature [89]). On the opposite, the cyclic voltammogram of NADH recorded using the GC-CNT electrode (Fig. 4.6b) revealed a well-defined peak located at 0.42 V. Hydrodynamic pseudo-voltammetry (Fig. 4.7) also supports this conclusion. The anodic current started to increase from 0.6 V and reached a plateau at 0.8 V when bare GCE used for NADH detection (Fig. 4.7, curve 1). Facilitated NADH oxidation on the GC-CNT electrode (Fig. 4.7, curve 2) occurred with a main wave around 0.5 V which was preceded by a pre-wave at ca. 0.1 V.

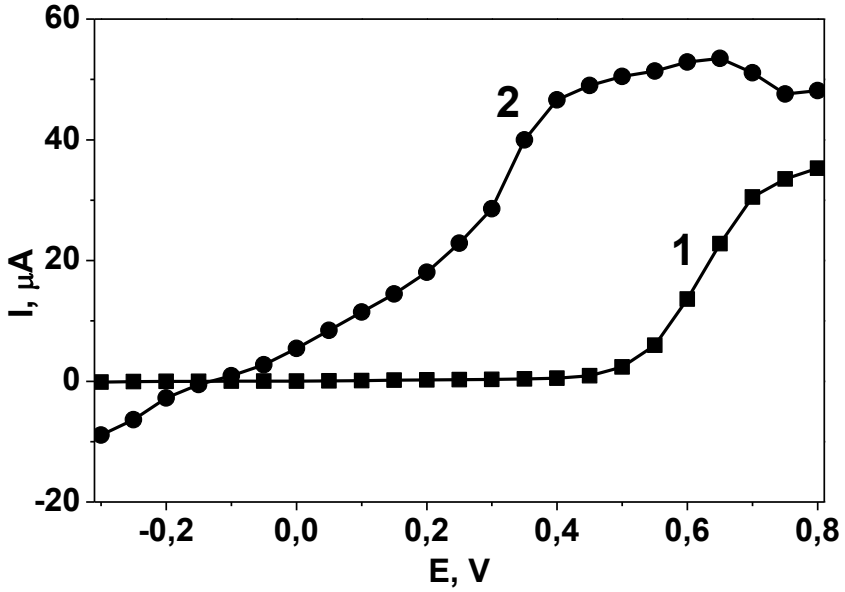

Fig. 4.7. Hydrodynamic voltammograms for 5 mM NADH in 67 mM PBS (pH 7.5) at (1) GCE and (2) GCE-CNT electrode.

Comparing parts a and b in Fig. 4.6 and curves 1 and 2 in Fig. 4.7 reveals significant decrease in overpotentials for NADH oxidation on carbon electrodes mainly due to the expected electrocatalytic action of CNT. These results are similar to those obtained in work [89]. The potential of NADH oxidation is not so low as ca. 0.0 V observed by some researchers on the nanotubes particularly treated to induce the formation of quinone-like functional groups [219, 220]. The absence of visible peaks in the low-potential range argues that here the high-voltage excitation during

the EPD does not produce quinone species and the catalytic effect of carbon nanotubes relies mostly on their edge plane sites exposed to the solution [217].

A comparison of the electrochemical behavior of CNT simply drop-coated on the electrode surface was also performed. One has to comment that it is not obvious to obtain a homogeneous film by drop-coating on the surface of the electrode because carbon nanotubes demonstrated a tendency to form aggregates during the drying-process. Here, we deposited the CNTs from aqueous solu tion, by dropping 10 μL of the same water suspension as for EPD (deposition has also been performed with DMF for the dispersion of the CNT with a similar result). The electrochemical behavior of the drop-coated film CNTs was then compared to the film deposited by EPD. On the voltammogram in PBS of GC-electrode with drop-coated CNTs (Fig. 4.6c) an anodic peak at potential about −0,05 V can be noticed that is absent in case of electrophoretically-deposited CNTs (Fig. 4.6b). This peak can be attributed to the presence of catalytic impurities or to some easily-oxidized groups on the surface of as-produced CNTs (e.g. quinone-like). One should notice also that the quantity of CNTs (indirectly compared from the magnitude of the background current) deposited in case of drop-coating was here several times higher than those deposited electrophoretically. But the current of NADH oxidation at 0.42 V was higher in case of electrophoretically-deposited CNTs, possibly because of the better distribution of the CNT in the porous structure obtained with EPD allowing a good access to the internal surface of the electrode.

4.2.2. Stability of the NADH voltammetric response

The stability of the signal is an important biosensors parameter. Oxidation of NADH at non-modified electrodes often leads to contamination of surface with reaction products and the decrease of response over time [89]. The stability of NADH oxidation peak at GCE and GCE-CNT have been investigated (Fig. 4.8).

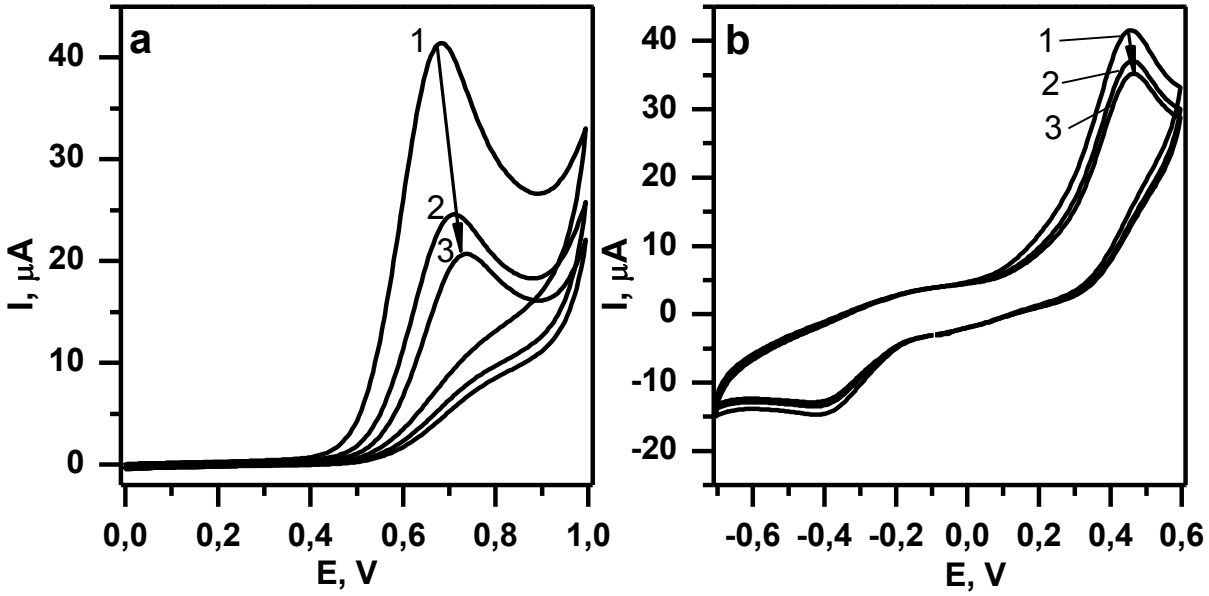

Fig. 4.8. Cyclic voltammograms of GCE (a) and GCE-CNT (b) in the presence of 5 mM NADH: 1-st (1), 2-nd (2) and 3-d (3) cycle. Supporting electrolyte: 0,067 M PBS (pH 7,5), scan rate 20 мV/s.

Thus, the NADH oxidation current on the unmodified GCE is significantly reduced after the second scan, and after the 3rd cycle the signal is only 50% of the original one (Fig. 4.8a). At the same time, current on the GCE-CNT decreases much more slowly, after the 3-d potential scan the current decrease is not more than 15% of the original response ((Fig. 4.8b). It should be noted that for the subsequent scans the current approaches to a constant value and remains constant over time.

Summing up the above, we can conclude that the modification of GCE with CNT by EPD method significantly improves its electrochemical characteristics toward NADH oxidation. In particular, the potential peak is shifted by 0.25 – 0.30 V toward negative values, that facilitates the process of coenzyme oxidation on electrode. In addition, the stability of the electrode response to NADH increases about 3 times due to the absence of surface electrode contamination with reaction products. It should be emphasized that the EPD method enables the obtaining of more homogeneous and porous coatings than conventional drop-coating method, which leads to increased in about two and a half times sensitivity of the electrode to NADH.

4.3. Electrochemically-assisted deposition of SiO_2-sorbitol dehydrogenase film on the CNT-modified electrode

To highlight the potential interest of such assemblies in designing bioelectrochemical devices, the electrophoretically-deposited CNT layer was used as a support for deposition of a sol–gel biocomposite comprising dehydrogenase enzymes (d-sorbitol dehydrogenase, DSDH). Due to the heterogeneous topography of the porous CNT layer, the evaporation-based sol–gel deposition approach is limited, at least as far as uniform film formation around CNT is expected, so that the EAD method (which already led to successful sol–gel film formation on non flat supports) was applied here.

One of the advantages of the method of sol–gel EAD is the possibility of partial modification of the required part of the electrode only. For instance, we showed earlier the feasibility of controlled modification by sol–gel biocomposite of platinum nanofibers lying on a glass substrate (see paragraph 3.1). The situation of the GC-CNT electrode is more complex as the glassy carbon used as a substrate is conductive and the formation of silica film could be triggered not only by the carbon nanotubes but also by the underlying support. Therefore, the linear sweep voltammograms were recorded at the different types of electrodes dipped in the silica sol in order to examine the activity of the reactions responsible for the generation of the catalyst for the silica condensation (i.e., water and/or oxygen reduction (1.1)). Comparing the curves obtained for bare GC and GC-CNT electrodes (see curve 1 and 2 on Fig. 4.9), clearly indicates much higher reduction rates on the carbon nanotubes than on the bare electrode (e.g., more than one order of magnitude at −1.3 V). The reason for this has to be found in the much larger electroactive surface area for GC-CNT as well as catalytic effect of carbon nanotubes leading to faster reaction rate. Thus, by applying the negative potential of −1.3 V to the GC-CNT electrode, one would be able to induce the formation of hydroxyl-ions mainly in the vicinity of the nanotubes walls and not so much onto the glassy carbon support, which should lead

to preferable CNT covering with DSDH-doped silica as it was demonstrated before for the localized sol–gel deposition on Pt nanoparticles lying on a glassy carbon surface [64].

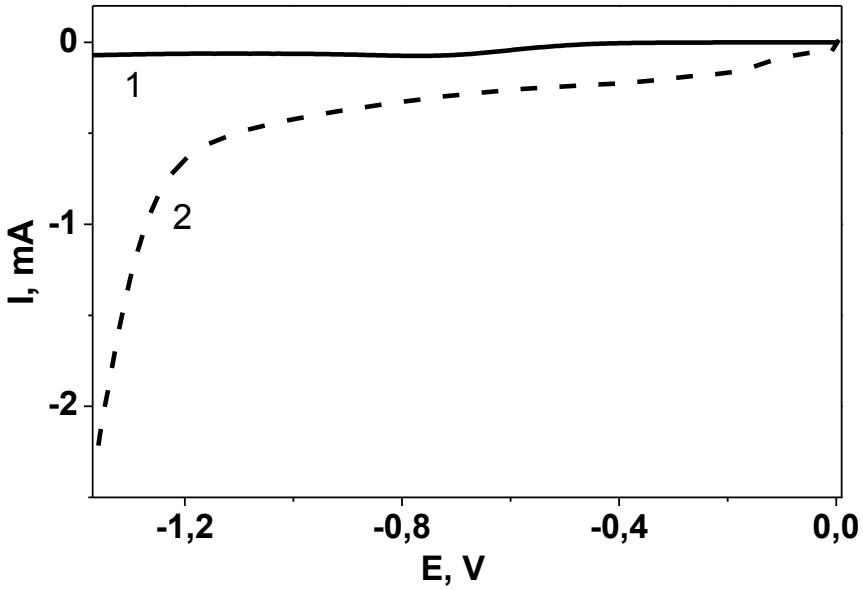

Fig. 4.9. Linear sweep voltammograms of GC electrode (1) and GC-CNT electrode (2) in the sol–gel solution. Scan rate 100 mV/s.

Fig. 4.10 exhibits the voltammetric responses obtained for 5 mM d-sorbitol using either bare GC or the GC-CNT electrode covered with a silica film containing DSDH generated by the method of EAD. Note that to make the data comparable, it was necessary to apply a more cathodic potential to the bare GC electrode (i.e., −1.8 V, with respect to −1.3 V for GC-CNT) to ensure the generation of the same electrolysis current and thus the same amount of so-produced hydroxyl ions catalysts [268] (which would lead to similar quantities of deposited biocomposite on both electrodes).

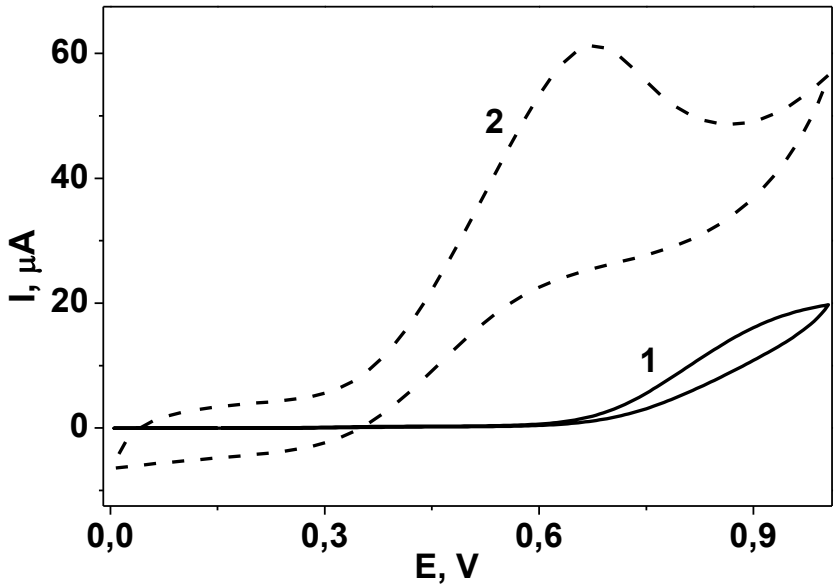

Fig. 4.10. Cyclic voltammograms of GCE (1) and GCE-CNT electrode (2) modified with thin film SiO_2-DSDH by sol–gel EAD in the 0.1 M Tris–HCl buffer (pH 9.0) containing 5 mM D-sorbitol and 1 mM NAD^+. Scan rate 20 mV/s. The conditions of sol–gel EAD were: −1.8 V, 16 s for GCE and −1.3 V, 16 s for GCE-CNT electrode.

The results indicate well-defined voltammetric signals located respectively at 0.67 V for the GC-CNT electrode (see curve 2 on Fig. 4.10) and 0.95 V for the bare GC electrode (see curve 1 on Fig. 4.10). They correspond to the oxidation of the NADH generated in the issue of the fermentative reaction:

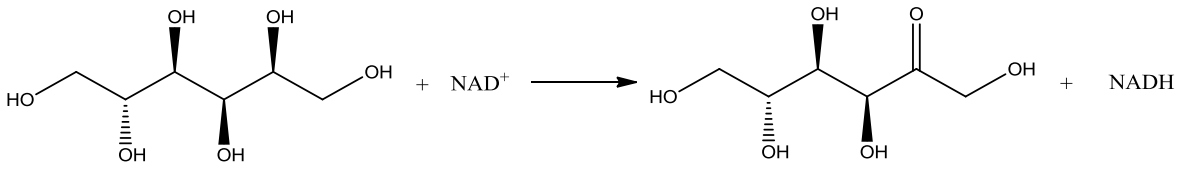

(4.2)

Thus NADH oxidation was facilitated when performed using the GC-CNT electrode (by ca. 0.3 V). Also, significantly larger bioelectrocatalytic currents were obtained in the presence of CNT. Assuming a same amount of deposited materials in both cases (as discussed above) and thus a same quantity of enzyme in the film, the smaller current observed with bare GC can be explained by some diffusional restrictions for the analyte to reach the active enzymatic centers through the silica

layer, whereas the porous structure of the carbon nanotube assemblies resembles more to a large surface area 3D-electrode ensuring fast diffusion of reactants to the proximal electrode surface. Thereby, the biocomposite modified electrode constructed on the basis of electrophoretically deposited carbon nanotubes offers the advantages of lower potential of detection and larger current due to its porous structure associated to the intrinsic electrocatalytic properties of nanotubes.

4.3.1. Optimization of the parameters of the biocomposite film

In order to receive the best response of the immobilized enzyme and to study the influence of the main parameters affecting the characteristics of either the silica-based biocomposite layer or the underlying carbon nanotube assemblies, the two-step optimization of the deposition parameters was performed. First, we examined the effect of the electrodeposition time (in the range 5–25 s), which directly affects the quantity of deposited biocomposite, while keeping the same parameters of carbon nanotubes layer (time of electrophoretic deposition 60 s). The naked-eyes appearance of the electrode was not changed while the potential was applied for 5 s, nevertheless a clearly visible silica layer could be remarked for 25 s deposition. Analyzing the amperometric response of such electrodes to the d-sorbitol analyte (Fig. 4.11a) revealed a very strong impact of the deposition time on the bioelectrode sensitivity. The highest responses only appear in a narrow time window, i.e., between 12 and 20 s, with a maximum reached at 16 s (Fig. 4.11b). Such great influence of the EAD process duration relies on the catalytic nature of this sol–gel deposition process. As previously assessed using AFM and EQCM techniques [269], the sol–gel deposition can be basically divided in two successive regimes, the first one being characterized by a slow rate of deposition and the second one by the fast deposition of much larger quantities of sol–gel material. As a consequence, the particular shape of the variation depicted in Fig. 4.11b can be rationalized as follows: short biocomposite deposition time resulted in low amounts of incorporated enzyme and thus to low bioelectrochemical response, whereas long deposition times led to thick deposits

preventing fast mass transport into the biocomposite films resulting thereby in sensitivity loss as it was described before for the sol–gel deposition on the Pt-Nfbs (see paragraph 3.1) and macroporous gold electrode [56]. The optimal situation arises thus from the best compromise of sufficiently high amount of incorporated enzyme while maintaining a porous structure open enough to ensure fast diffusion of reactants.

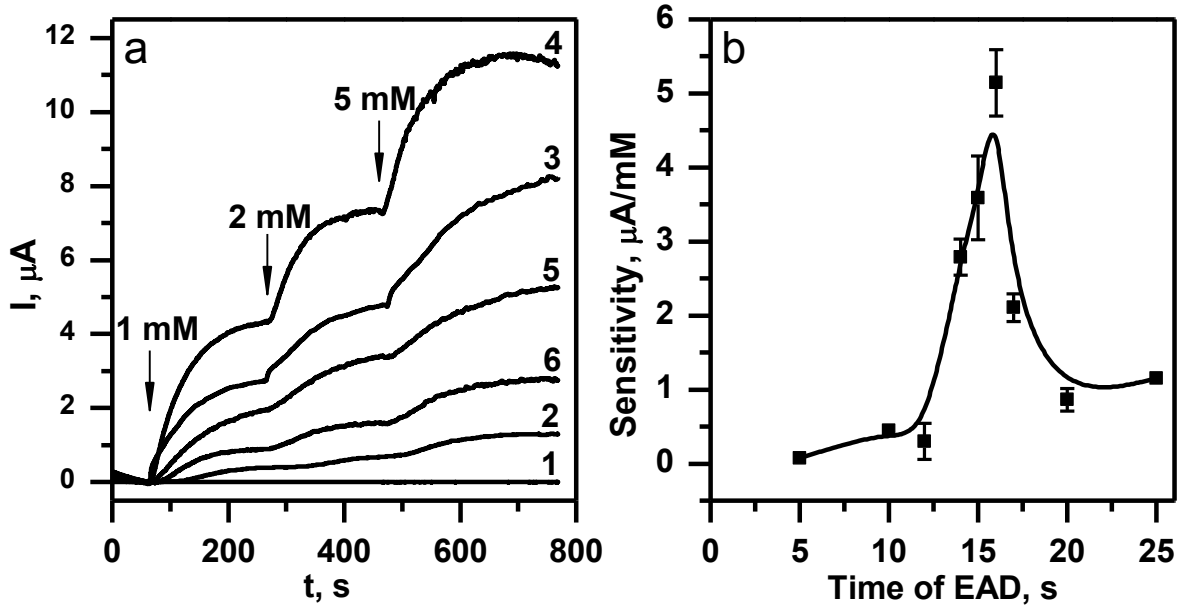

Fig. 4.11. (a) Amperometric response of the GCE-CNT electrode modified by SiO_2-DSDH film with different time of EAD to the additions of D-sorbitol: (a) 0 s, (b) 10 s, (c) 14 s, (d) 16 s, (e) 17 s, (f) 25 s. E = +0.5 V. (b) Sensitivity of the GCE-CNT electrode modified with SiO_2-DSDH film to the D-sorbitol at +0.5 V as a function of the time used for the sol–gel EAD. Supporting electrolyte 0.1 M Tris–HCl buffer (pH 9.0) contains 1 mM NAD^+. The time of electrophoretic deposition of carbon nanotubes was 60 s for all samples.

A second important point to be investigated is the impact of the carbon nanotubes film thickness on the electrochemically assisted bioencapsulation. Fig. 4.12 shows the dependence of the bioelectrode sensitivity on the time of electrophoretic deposition of the CNT assemblies while keeping constant the parameters of sol–gel deposition (−1.3 V, for 16 s). The relation has also a sharpened

shape with better sensitivities in the range from 20 to 60 s electrophoretic deposition. According to the equation (4.1) this corresponds to a layer thickness of CNT from 100 to 150 nm.

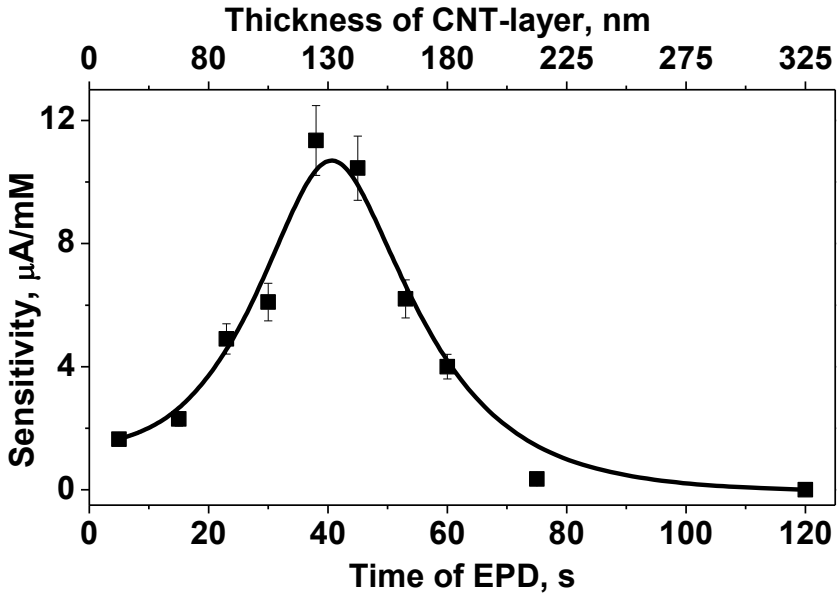

Fig. 4.12. Electrochemical response of the GCE-CNT electrode modified by SiO_2-DSDH with optimal parameters (−1.3 V, 16 s) to the D-sorbitol at +0.5 V as a function of the electrophoretic deposition time and corresponding layer thickness (from equation (4.1)) of carbon nanotubes. Supporting electrolyte 0.1 M Tris–HCl buffer (pH 9.0) contains 1 mM NAD^+.

In fact, not only the time of sol–gel electrodeposition but also the quantity of carbon nanotubes on the glassy carbon electrode affect the quantity of sol–gel materials deposited because sol electrolysis is facilitated on carbon nanotubes (see Fig. 4.9). A higher quantity of carbon nanotubes on the electrode surface leads to faster sol–gel deposition. A great care has thus to be taken when optimizing the sol–gel electrodeposition on porous and catalytically active materials. At the same time, the results are reproducible, while maintaining constant parameters.

4.3.2. Analytical performance of the modified electrode

The d-sorbitol dehydrogenase immobilized into silica film on the surface of carbon nanotubes showed typical Michaelis–Menten kinetics and the gradual saturation of response after concentration of d-sorbitol 5 mM (Fig. 4.13a). The apparent Michaelis–Menten constant (K_m) was calculated from the Lineweaver–Burk plot and its value was found to be 4.1 mM which is very similar to one measured in the solution [270] indicating a good activity of DSDH entrapped in the electrogenerated silica film and rapid mass transfer of reagents.

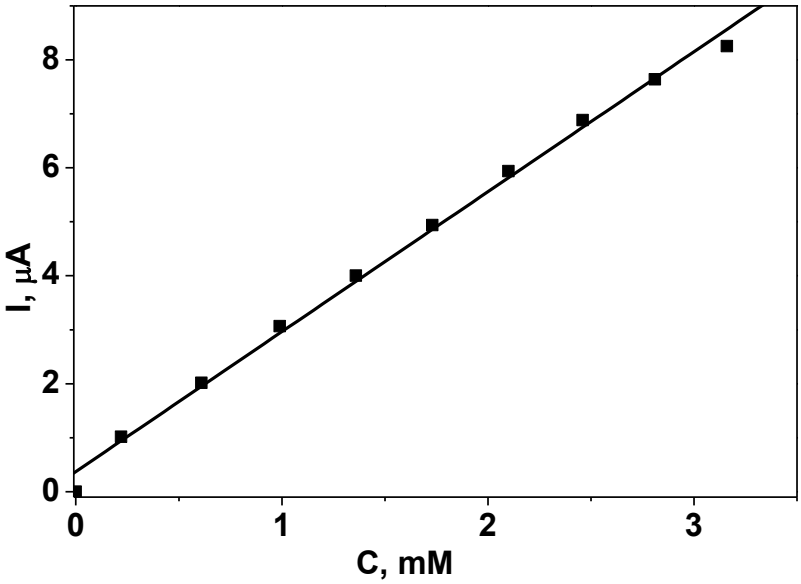

Fig. 4.13. (a) Dependence of the amperometric response of GCE-CNT-SiO_2-DSDH from the D-sorbitol concentration at potential +0,5 V. Supporting electrolyte: 0,1 M Tris-HCl (pH 9,0) and 1 mM NAD^+.

Finally, the analytical characteristics of the bioelectrode have been determined by recording its amperometric response at the applied potential of +0.5 V, as a function of the d-sorbitol concentration. Using the optimal thickness of carbon nanotubes layer and the best parameters of sol–gel EAD, the calibration plot for the oxidation of d-sorbitol was obtained and found to be linear in the range from 0.5 mM to 3.5 mM. The linear regression equation was $I(\Delta A) = (-0.09 \pm 0.15) + (2.77 \pm 0.07) \times C$ (mM) with the correlation coefficient 0.995. The detection limit by 3S criteria

was found to be 0.16 mM. The modification method can be reproduced on the different electrodes and on different days with a precision of 9% (n = 3). The bioelectrode demonstrated sufficient stability for the measurements during one month as it was shown before for the film with same composition [241], the signal drop after 20 consecutive measurements did not exceed 10%.

4.4. Electrophoretic deposition of macroporous CNT-assemblies for electrochemical applications

The application of macroporous electrodes is a promising approach to increase the sensitivity of electrochemical analysis [271]. They can be used in particular for the immobilization of biomolecules [56, 272–274]. Due to the porous structure, the electrode has higher electroactive surface area and the pore size is large enough to allow the quick and unobscured diffusion of reagents from solution to the electrode. In particular, macroporous gold electrode was used to immobilize the enzyme with coenzyme that was possible thanks to the large pore volume [275].

The application of carbon nanotubes as nanoscale building blocks for the construction of analogous macroporous electrodes appears as a promising way to combine the advantages belonging to the macroporous structure [276] and the electrocatalytic properties of individual nanotube [86]. This notwithstanding, there are only a few examples dealing with three-dimensional 3D carbon nanotube ensembles with engineered and controlled macroporosity. The method of direct synthesis allows creation of 3D CNT-ensembles with long tube-to-tube distance [277, 278] but it gives rather insufficient possibility of porosity control. Interesting results can be obtained by the method of ice-segregation induced self-assembly (ISISA) that was applied for the fabrication of self-supported porous CNT monoliths [279]. Another widespread method is a template approach that consists in mixing single-walled carbon nanotubes with sacrificial particles, formation of a composite and further removal of the particles [280]. A two-dimensional network can also be

obtained by using patterning methods from the solution [281]. To date, the above mentioned ensembles have not been applied in the area of electrochemical biosensors.

The method of vacuum filtration allows obtaining rather thick porous CNT films [282], but it can lead to the segregation of particle and nanotube layers during the filtration process [283] and does not permit to get the films on the solid support. A possible way to overcome these limitations could be the resort to an electrophoretic deposition method for the fabrication of macroporous CNT-electrode. One drawback of such CNT-assemblies can be the uncontrolled packing of the material that hinders the access to the CNT at the bottom of the film, especially for biosensors applications. In this chapter the formation of 3D-macroporous CNT-assemblies in the form of thin films on electrode surfaces by means of electrophoretic deposition is described. With a view to evaluate the prospects of such kind of films for possible application in biosensing, their electrochemical response to hydrogen peroxide and nicotinamide adenine dinucleotide have been investigated and the first example of enzyme immobilization using electrophoretically deposited 3D macroporous CNT-electrode have been shown.

4.4.1. Fabrication of macroporous CNT-layers on the electrode surface

The method of the electrophoretic deposition basically allows the formation of deposits from suspensions of charged particles. The carbon nanotubes are negatively charged in a broad pH range due to the presence of carboxylic groups on their surface. On the other hand, the polystyrene beads are also negatively charged owing to the presence of sulfonate groups on their surface [284] (potassium persulfate was used as initiator of the polymerization in their synthesis) and can be electrophoretically deposited as well. However, we did not succeed in fabricating a uniform 3D-film consisting of PS beads only as they tended to form a monolayer with big gaps between the deposited beads (see Appendix A). This likely occurs because of the weak adhesion between the polystyrene and glassy carbon together

with unfavorable interaction originated from their spherical shape and the electrostatic repulsion between particles. Considering the above observations, the deposition of a mixture of carbon nanotubes and PS beads could contribute to overcome the lacks of each individual component by bringing a volume from polymeric particles while nanotubes contribute to the reinforcement of the composite.

Fig. 4.14A and B show edge-views of a typical CNT-PS film obtained by electrophoretic deposition on the surface of a glassy carbon electrode. The PS beads and carbon nanotubes are homogeneously mixed together forming a uniform deposit with thickness of about 4.5 μm. The apparent small amount of carbon nanotubes in the interspace of beads is a visual artifact that can be explained by low contrast of the image. The real quantity of nanotubes is much bigger as proved on the images of the film after template removal (see part C and D in Fig. 4.14). After calcination of the PS beads, the film structure is maintained, forming a cellular 3D network with pore sizes corresponding to those of the removed beads (≈ 500 nm). These pores are separated by a 40–60 nm thick CNT layer. The thickness of the template-free macroporous-CNT film (Fig. 4.14C) was only slightly smaller than the one of CNT-PS film (Fig. 4.14A).

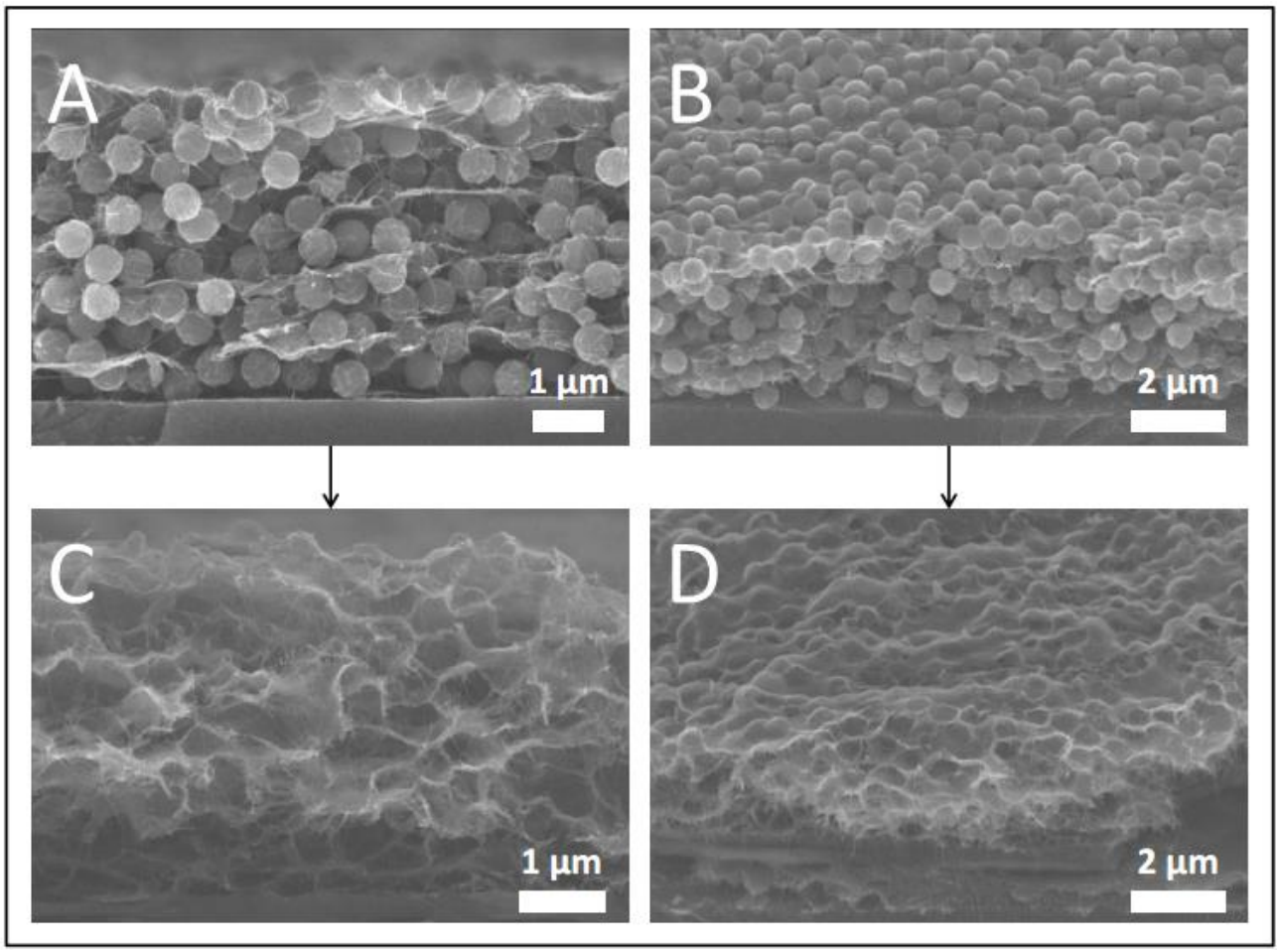

Fig. 4.14. SEM-images on the edge (left column) and under the angle of 35° (right column) of a CNT-PS composite film deposited in the presence of PS-beads at 0.2 mg/mL, before (A, B) and after (C, D) template removal. Time of electrophoretic deposition was 135 s.

A straightforward expectation is that increasing the beads quantity would contribute to increase the deposit thickness, but could also lead to film collapsing after template removal. Otherwise, decreasing the PS beads content would result in thinner and less porous film. Supporting these suggestions, Fig. 4.15 depicts the structures (after template removal) of the deposits with lower (Fig. 4.15A and B) and higher (Fig. 4.15C and D) contents of PS beads in the initial dispersion. The structure of the film formed from more diluted PS beads media (Fig. 4.15A and B) is rather

similar to that described above, but the thick- ness is about two times smaller, owing to less amount of volume-forming polymeric particles.

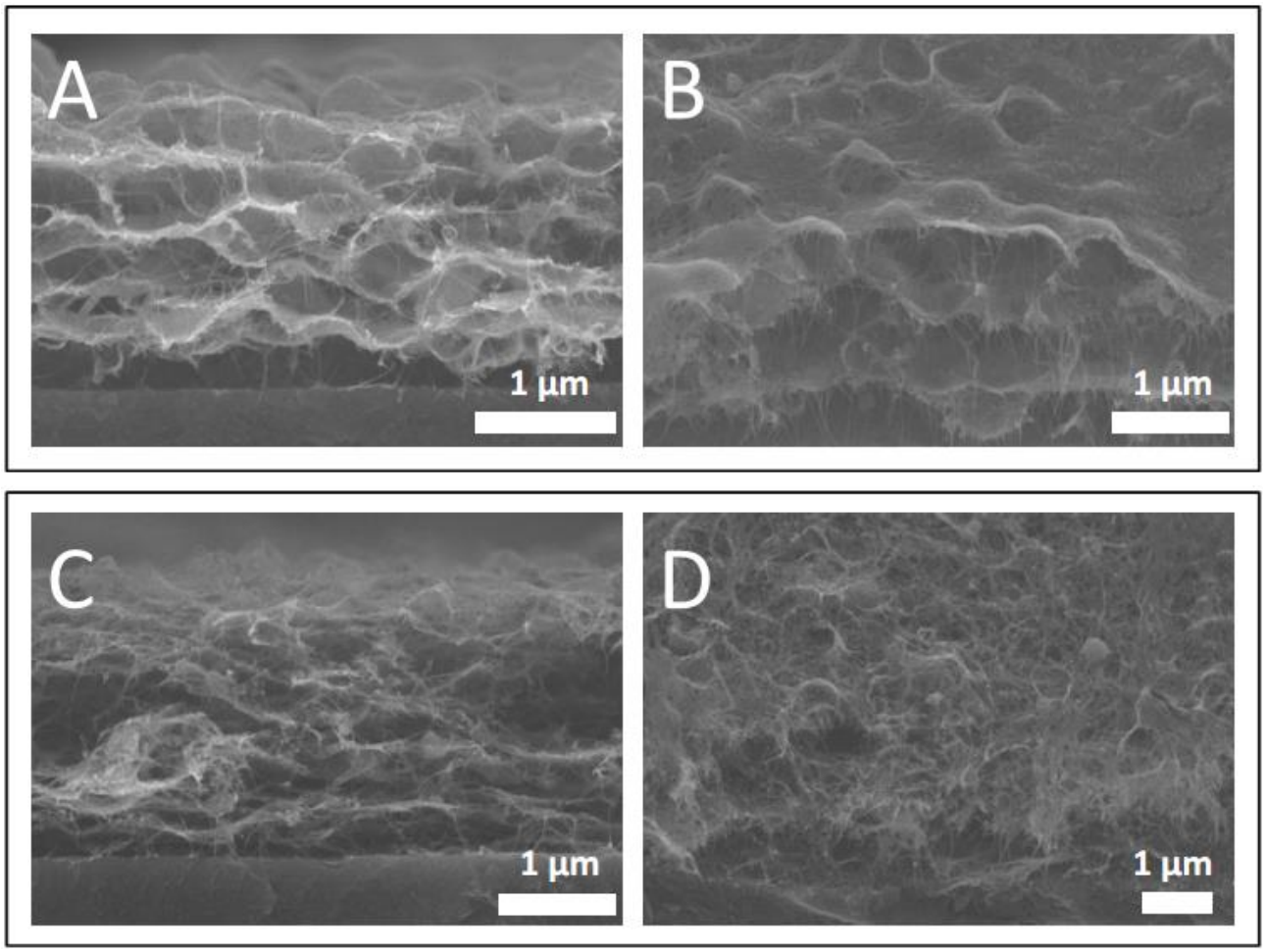

Fig. 4.15. SEM-images on the edge (left column) and under the angle of 35° (right column) of CNT-PS composite films deposited in the presence of various contents of PS-beads (A, B) 0.1 mg/mL and (C, D) 0.5 mg/mL. Time of electrophoretic deposition was 135 s.

In contrast, the appearance of the film formed in the presence of larger amounts of PS beads is different, demonstrating the absence of well-defined 500 nm-macropores but showing rather a disordered sparse packing of nanotubes (Fig. 4.15C and D), suggesting the collapsing of such thick macroporous film.

4.4.1.1. Optimization of PS-beads concentration in the suspension

To investigate the optimal concentration of PS beads leading to thick and highly porous CNT films, we analyzed different samples obtained with the same 135 s deposition time and PS beads contents varying from 0.05 and 0.5 mg/mL. The dependence of the deposit thickness on the PS beads concentration represents a linear correlation with quite big slope since higher amounts of PS beads increase significantly the volume of deposit (Fig. 4.16a). At the same time, when the PS template is removed, this dependence has a dramatically different shape (compare curves 1 and 2 in Fig. 4.16a) and can be basically divided into three parts. At the initial part of the plot the thickness of the template-free macroporous CNT deposit is close to the CNT-PS one (yet lower), demonstrating that burning of the template does not have significant influence on the macrostructure of deposit due to a small quantity of beads. For the same reason, such films suffer from rather small thicknesses and low pore volumes. At the second part, the rate of the thickness increasing slows down and reaches the maximum at a PS beads concentration of 0.2 mg/mL. At higher concentrations the thickness suddenly drops lower than 1 μm and does not change significantly in the third part of the plot. This demonstrates that too large concentrations of polystyrene have to be avoided as they lead to pore collapse during the calcination. In conclusion, the maximal thickness of the macroporous film can be obtained at a concentration of PS beads of about 0.2 mg/mL, defining a maximal PS beads / CNT ratio above which collapsing of macropores starts to occur.

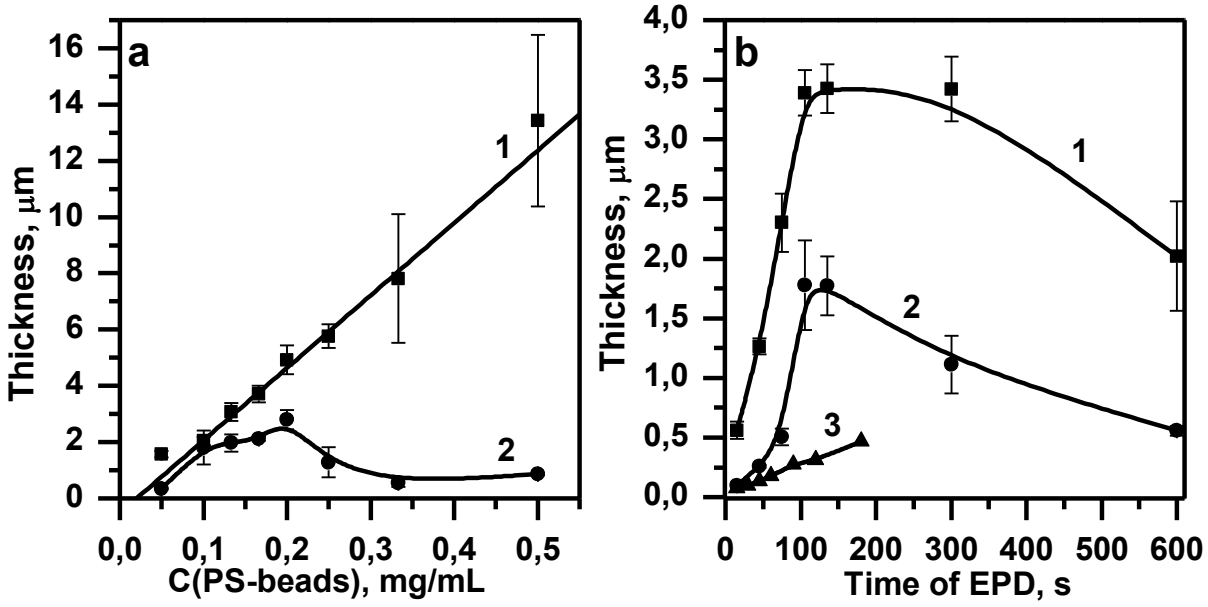

Fig. 4.16. (a) Variation of the CNT-PS layer thickness (135 s deposition) as a function of the concentration of PS-beads in the initial dispersion before (1) and after (2) template removal. (b) Variation of the CNT-PS (0.2 mg/mL) deposit thickness as a function of the electrophoretic deposition time, as measured with AFM or profilometry, before (1) and after template removal (2), as well as for the samples deposited without PS beads (3).

As a rule, the quantity of the electrophoretically deposited material depends strongly on the deposition time [266]. We verified thereby this approach and its impact on the feasibility of the macroporous film formation. Fig. 4.16b shows a dependence of the film thickness on the time of electrophoretic deposition. This dependence has linear type when only carbon nanotubes (no PS beads) are present in the dispersion (see curve 3 in Fig. 4.16b). In the same manner, but with much bigger slope, grows the deposit thickness when the PS beads have been introduced in the mixture (Fig. 4.16, curve 1). But this increase occurs until 100 s of deposition, and then tends to level off and could even decrease at much longer deposition times. We suppose that the rate of the PS beads deposition significantly decreases above 100 s because of a significant depletion of the particles concentrations consumed during the deposition. The loss in thickness at longer time is more difficult to explain but it

might be due to the film destruction by oxygen bubbles formed on a larger time window during the deposition (they were clearly observed at the naked eye).

In agreement with the observation made in Fig. 4.16a for a PS-beads content of 0.2 mg/mL, the thickness of the deposit decreases by ca. a factor 2 after template removal (Fig. 4.16b, curve 2) but still remains much bigger than that of the deposit fabricated without PS beads (Fig. 4.16b, curve 3). At low deposition time (i.e., less than 75 s), the thickness of the macroporous CNT film is below 500 nm, which is likely to correspond to a sparse thin film similar to the one that can be obtained by the patterning from solution. After 75 s of deposition, the thickness of the deposit considerably increases, up to 2 lm, indicating a formation of true macroporous film with cellular structure.

4.4.1.2. Methylene green adsorption and electrochemical characterization

The strong adsorption on the CNT-surface and the electroactive nature of MG was exploited to compare the surface area of the different films prepared here. Fig. 4.17a shows the cyclic voltammograms of MG adsorbed on the macroporous CNT-film obtained at various deposition time after template removal. The height of both oxidation and reduction peaks grows with increasing of the deposition time (Fig. 4.17b, curves 2 and 2') in accordance with the expectation of extended surface area while larger quantity of carbon nanotubes is deposited. But this growing is much bigger as compared with the nonporous CNT film obtained in the absence of template (Fig. 4.17b, curves 1 and 1'), exhibiting much more important adsorption of MG, notably in the area of higher deposition times (Fig. 4.17b, curves 2 and 2'). This agrees well with the results discussed above indicating the formation of truly three-dimensional macroporous network starting from the 75 s of deposition time. Hence, such porous network demonstrates much higher (8x) electroactive surface area than that obtained by non-templated deposition.

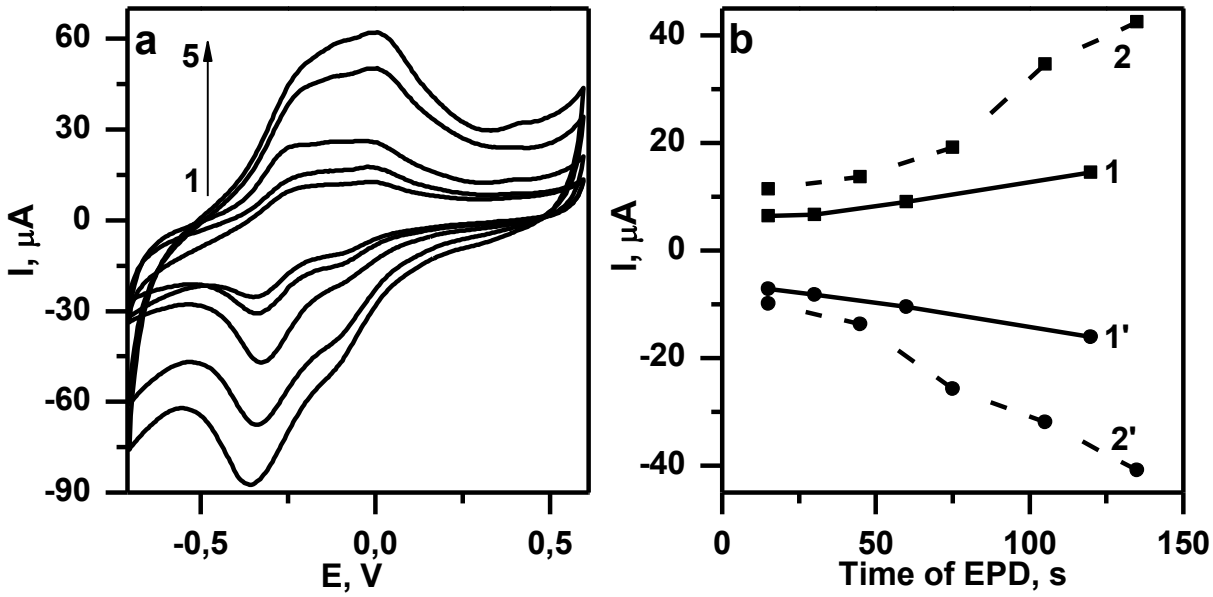

Fig. 4.17. (a) Cyclic voltammograms of MG adsorbed on the macroporous CNT layers ([PS-beads] = 0.1 mg/mL) with different duration of electrophoretic deposition: (1) 15 s, (2) 45 s, (3) 75 s, (4) 105 s, (5) 135 s. Supporting electrolyte: 0,067 M PBS (pH 7,5), scan rate 20 mV/s. (b) Peak current of MG as a function of electrophoretic deposition time of non-macroporous CNT layers (1,1') and macroporous CNT layers ([PS beads] = 0.1 mg/mL) (2,2').

4.4.2. Functionalization of the macroporous CNT electrode for (bio)sensing applications

For analytical purposes we examined the performance of the macroporous carbon nanotube film for the detection of nicotinamide adenine dinucleotide (NAD^+/NADH) and hydrogen peroxide (H_2O_2) systems, two substances that are involved in enzymatic reactions of dehydrogenases and oxidases, respectively.

4.4.2.1. CNT assembly modification with Pt-nanoparticles for the detection of H_2O_2

The detection of hydrogen peroxide is very important for the biosensors based on the immobilized oxidases as H_2O_2 is a usual product of such enzymatic reactions. Moreover, as H_2O_2 is characterized by slow electron transfer kinetics, it constitutes a

good model probe to evaluate the potentialities of such macroporous carbon nanotube electrode in electroanalysis. Owing to a high overpotential for hydrogen peroxide oxidation at the raw nanotubes of present type (more than 1 V, see Appendix F), we used the electrodeposition of platinum nanoparticles on the walls of the macroporous CNT assemblies to show the possible advantages of the macroporous structure over the non-macroporous one towards H_2O_2 detection. Fig. 4.18 shows a SEM image of carbon nanotube layer with electrochemically-deposited platinum nanoparticles.

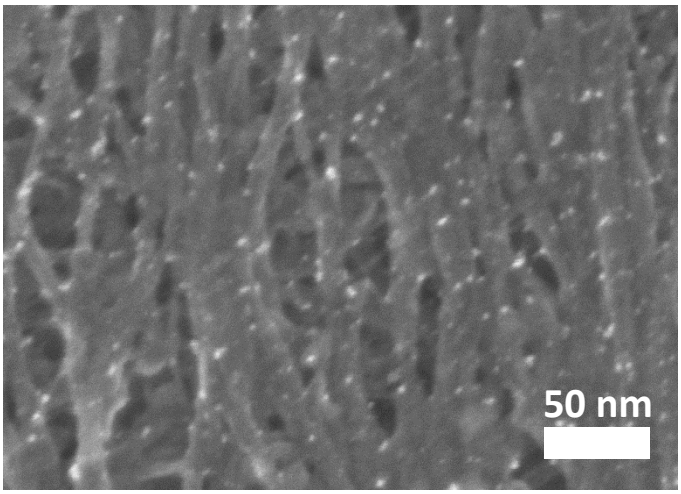

Fig. 4.18. SEM image of Pt-NPs modified non-macroporous CNT-layer (t = 135 s).

The size of the particles is smaller than 5 nm and they are evenly distributed over the surface being formed probably on the wall defects of nanotubes. The amount of so-generated Pt-Nps was expected to be proportional to the amount of deposited CNT. However, such increase in the Pt-Nps amount per geometric area of the electrode resulted in almost no change in the height of neither oxidation nor reduction peak of hydrogen peroxide reactions on the nanoparticles-modified non-macroporous CNT film (see curves 1 in Fig. 4.19 and curves 1,1’ in Fig. 4.20). Such behavior argues that diffusion layers of nanoparticles are completely overlapped in this case because of the closed structure of the film and the solution in- side the film quickly becomes depleted of hydrogen peroxide. Under these conditions, the current is

determined by the planar diffusion of the electroactive species from the outward solution and does not change with varying the film thickness.

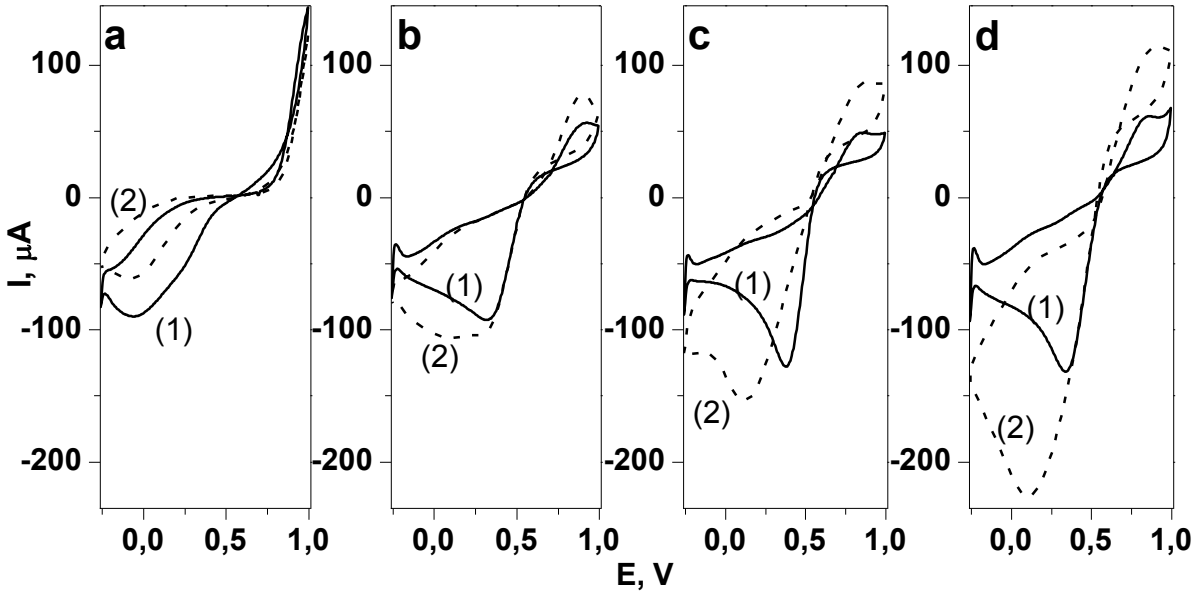

Fig. 4.19. Response of Pt-NPs modified non-macroporous CNT layers (1) and macroporous CNT layers ([PS beads] = 0.2 mg/mL) (2) to 10 mM H_2O_2. Time of electrophoretic deposition: (a) 15 s, (b) 45 s, (c) 75 s, (d) 105 s; supporting electrolyte: 0.1M H_2SO_4; scan rate: 10 mV/s.

The situation is different when the Pt-Nps are deposited on the macroporous carbon nanotube assemblies obtained for different deposition times (see curves 2 in Fig. 4.19 and curves 2,2' in Fig. 4.20). In this case both the oxidation and reduction peaks of hydrogen peroxide demonstrate strong correlation with the deposition time and thus respectively the thickness of carbon nanotube film. Such growth in the peak currents while increasing the film thickness can be attributed to the open structure of the macroporous CNT-Pt-Nps film. Owing to the presence of microcavities within the deposit, the electroactive species are allowed to diffuse not only from the outward solution but also from the inner pores volume. In this case the flux of the electroactive species becomes also significant in the internal porous volume of the deposit, which leads to the increase in current while increasing deposition time. Therefore, the macroporous CNT film can be promising matrix for the

immobilization of enzymes from oxidase group and the development of efficient biosensors.

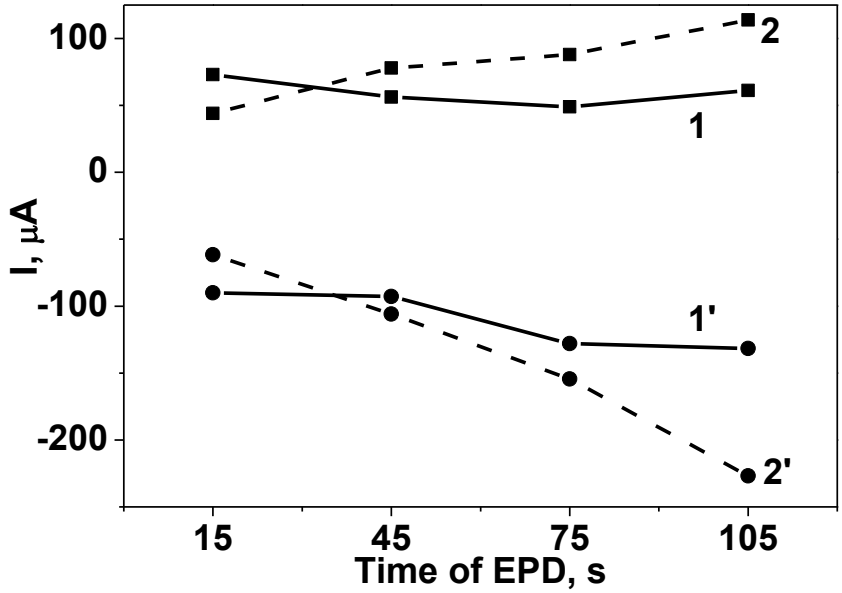

Fig. 4.20. Variation of the oxidation and reduction peak currents of H_2O_2 for Pt-NPs modified non-macroporous CNT layer (1,1') and macroporous CNT layer (2,2') as a function of the of electrophoretic deposition time.

4.4.2.2. Electrochemical response of NADH on the macroporous CNT-assembly

Operating with carbon nanotubes can significantly reduce the overpotential of NADH oxidation, by themselves [100], or by using additional the mediators from the class of phenothiazine dyes [235]. Actually, MG adsorbed on the CNT layer can act as such mediator decreasing the oxidation potential of NADH. This is shown in the voltammograms recorded with a macroporous carbon nanotube layer with adsorbed MG in the presence of NADH, where one can notice a sharp increase in the current of the anodic peak located at 0.05 V, owing to the electrocatalytic oxidation of NADH (Fig. 4.21c).

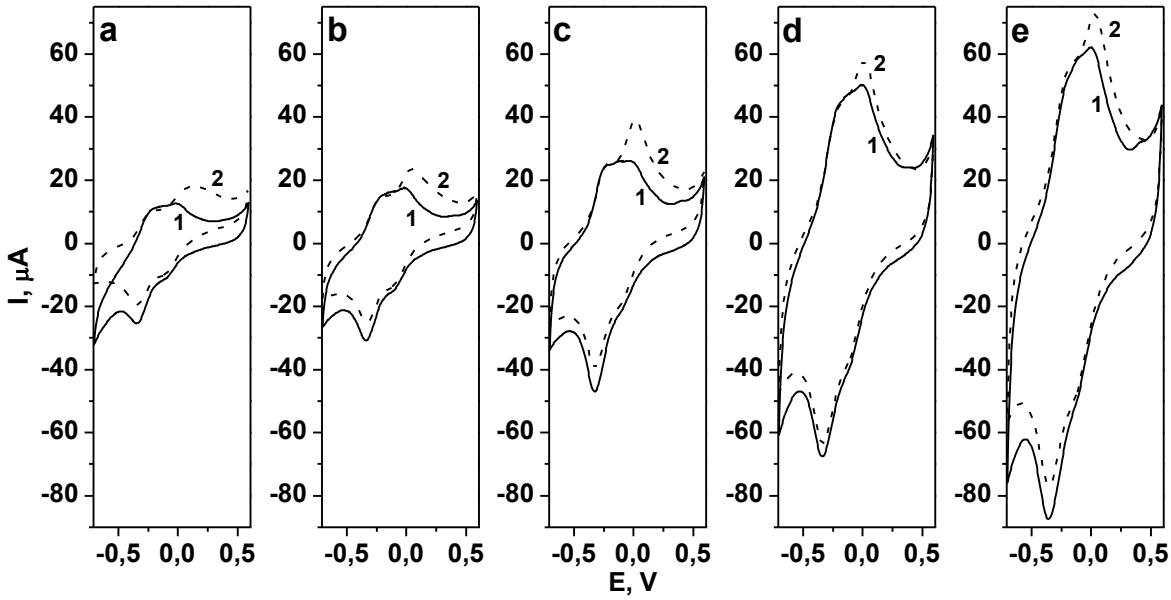

Fig. 4.21. Cyclic voltammograms of GCE-CNT-PS-MG, obtained with EPD time 15 s (a), 45 s (b), 75 s (c), 105 s (d) and 135 s (e) in the absence (1) and in the presence (2) of 1 mM NADH. Supporting elecrolyte: 0,067 M PBS (pH 7,5), scan rate 20 mV/s.

Nevertheless we were not able to find any correlation between the response of the macroporous CNT-MG electrode to NADH and the thickness of CNT layer, as the electrocatalytic current remained nearly constant for all samples (see Fig. 4.21 and almost the same step current values in the presence of NADH in Fig. 4.22). This can be explained by the rather large heterogeneous electron transfer constant associated to NADH oxidation at the MG-modified carbon nanotubes, thus it reacts completely at the outermost layer before the species are able to diffuse into the film [274]. For the same reason, we did not find correlation between the response of NADH and the effect of porosity while comparing macroporous and non-macroporous CNT layers.

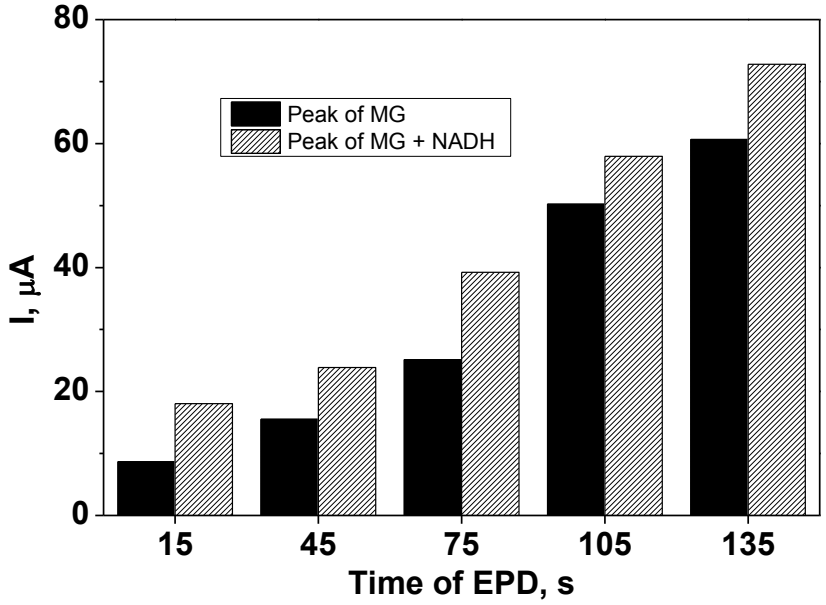

Fig. 4.22. Anodic peak current values corresponding to the adsorbed MG alone or in the presence of 1mM NADH, as a function of the electrophoretic deposition time applied to prepare the macroporous CNT electrodes.

4.5. Co-immobilization of sorbitol dehydrogenase and coenzyme on the macroporous CNT-assembly

Though the macroporous structure does not provide true direct advantage for the direct detection of NADH in the solution, it still could be useful for the development of biosensors based on the NAD-dependent enzymes. In that case, the enhancement can be achieved by immobilization of both the enzyme and the cofactor inside the porous film. The larger inner surface area together with the bigger pore volume would lead to increasing of the number of active sites where the enzymatic reaction is allowed to take place.

We used here a recently described protocol for the immobilization of NAD+ inside a silica sol–gel film [203], together with an enzyme DSDH, onto the surface of a the CNT films with adsorbed MG. The biological activity of DSDH co-immobilized with co-factor into the silica film on both the macroporous and non-macroporous CNT electrodes is indeed preserved upon immobilization, as shown by the current

increase measured at 0.4 V in the presence of 2 mM D-sorbitol (Fig. 4.23), this signal being attributed to the mediated oxidation by adsorbed MG of the enzymatically produced NADH. When the CNT film was deposited in the absence of template, no marked differences can be noticed between the cyclic voltammograms obtained on the electrodes with thin (15 s EPD) and thick (135 s EPD) CNT layers (see parts a and b in Fig. 4.23).

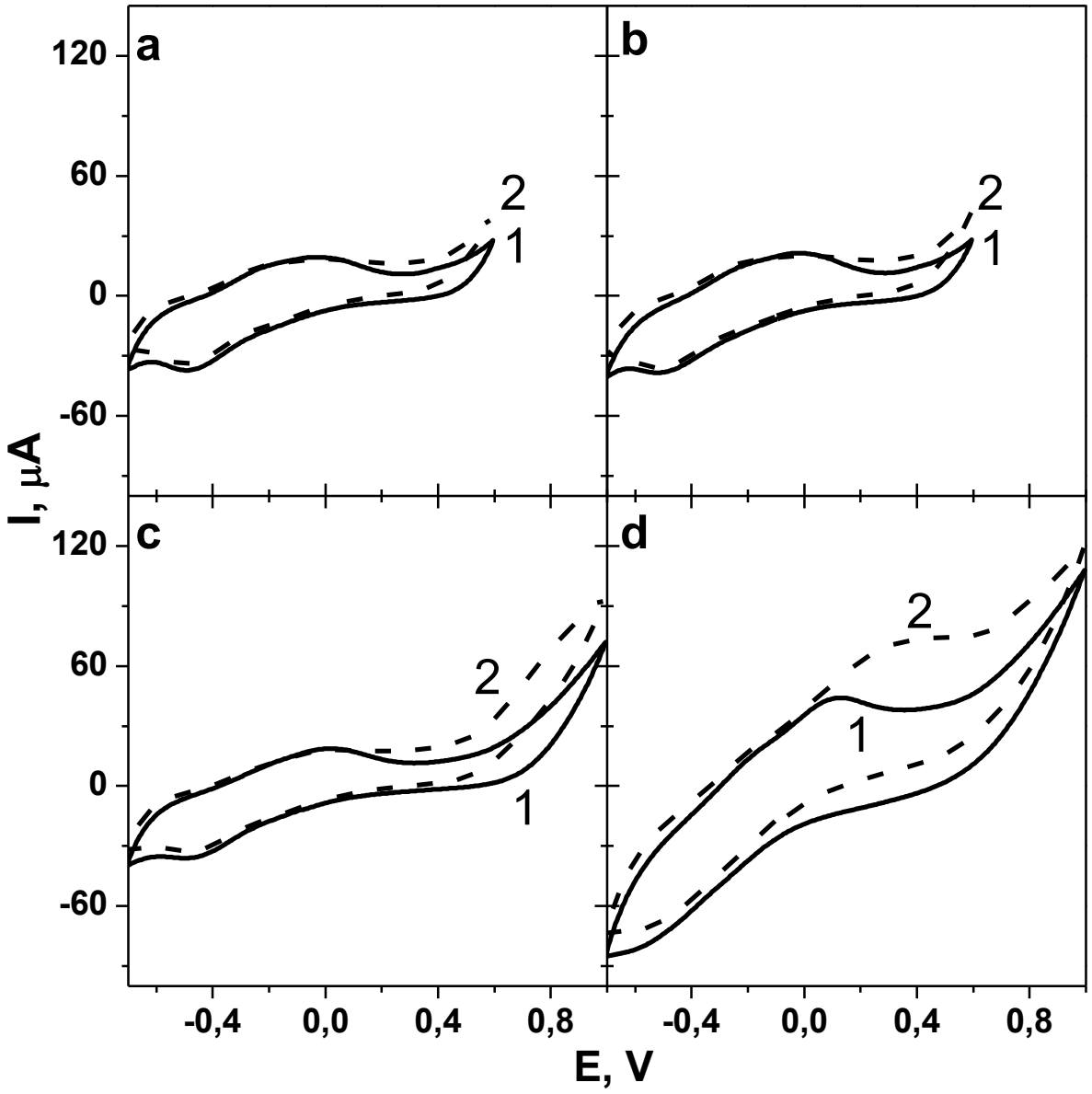

Fig. 4.23. Cyclic voltammograms of (a, b) non-macroporous and (c, d) macroporous CNT film ([PS beads] = 0.2 mg/mL) prepared by electrophoretic deposition for (a, c) 15 s and (b, d) 135 s and modified with adsorbed MG and SiO_2-

PEI-NAD^+-DSDH film for characterization in Tris–HCl buffer in the absence (1) and in the presence of 2 mM D-sorbitol (2). Scan rate: 20 mV/s.

On the contrary, the macroporous CNT film prepared with long deposition time (Fig. 4.23d) demonstrates obvious current increase in the range 0.1–0.5 V in comparison with the same film prepared with low deposition time (Fig. 4.23c). The increase of the film thickness in this case leads to the increase of the inner pores volume where the NAD^+ and DSDH can be successfully immobilized, while maintaining a good accessibility to the diffusion of the reagents from the solution. Thus, the porous structure of the macroporous CNT film provides higher sensitivity for the detection of D-sorbitol when the NAD^+ and DSDH are immobilized together into the silica film and this could be further exploited for the construction of advanced dehydrogenase-based biosensors.

4.6. Conclusions to chapter 4

Modification of glassy carbon electrode with carbon nanotubes by electrophoretic deposition method significantly improves the efficiency of the latter when detecting coenzyme NADH. The presence of carbon nanotubes shifts NADH oxidation potential at 0.25-0.30 V in negative potentials direction, and significantly increases the stability of the response.

Electrochemically-assisted deposition method allows immobilization of dehydrogenases in SiO_2-film with preservation of enzymatic activity, which was illustrated by sorbitol dehydrogenase example. The electrode modified with this enzyme, shows stable and reproducible response to changes in the concentration of sorbitol in solution.

The electrode modified with carbon nanotubes and sorbitol dehydrogenase demonstrates significant advantages in comparison with the electrode without carbon nanotubes. In particular, the sensitivity and selectivity of sorbitol detection are

increased thanks to the use of low working potential 0.5 V. The response of the modified electrode depends on the thickness of carbon nanotubes layer and SiO_2-film deposition parameters. Best analytical characteristics were obtained when using carbon nanotube layer thickness of 100 – 150 nm and electrochemically-assisted deposition parameters -1.3 V, 16 s.

Macroporous layer of carbon nanotubes obtained by the method of electrophoretic deposition is a promising matrix for developing biosensors based on oxidases and dehydrogenases. In particular, it allows to improve the sensitivity and selectivity of the electrode modified with film SiO_2-dehydrogenase when combined with adsorbed methylene green dye and immobilized coenzyme.

CHAPTER 5. APPLICATION OF MODIFIED ELECTRODES AS SENSITIVE ELEMENTS OF BIOSENSORS FOR THE DETERMINATION OF SORBITOL AND CHOLINE

Selective determination of biologically-active organic substances is an important task of modern analytical chemistry. Such substances are often used in food production, resulting in their significant intake with food. However, excess or deficiency of such substances in the human body can cause serious physiological disorders.

Currently, analytical determination of these substances is a complex task due to the similarity of the chemical properties of individual substances in homologous series (e.g., polyhydric alcohols, monosaccharides, polysaccharides have OH^- groups). In fact, the only method that allows sensitive and selective analysis of organic substances is chromatography. However, it had disadvantages, such as considerable length analysis, complex sample preparation, high cost and complexity of the equipment, the need of pure reagents. All this makes impossible screening of organic substances. However, the sensitivity at the level of 10^{-5}-10^{-4} M is usually quite sufficient for analysis of substances, particularly in foods [285]. Examples of substances that require determination in the food are sorbitol and choline, important members of metabolism in the human body.

Electrochemical biosensors are promising alternative for the determination of organic compounds in complex objects with minimal sample preparation. They are characterized by sufficient sensitivity, speed of analysis, and that is the most important, high selectivity of determination thanks to the use of enzymes as recognition elements. Price of one analysis is rather low due to the possibility of multiple use, a small amount of enzyme and cheapness of electrodes (e.g. screen-printed electrodes).

This section describes the results of the application of developed modified electrodes for the determination of choline and sorbitol. The determination of sorbitol

was carried out using the glassy carbon electrode modified with non-porous CNT-layer and biocomposite film SiO_2-DSDH with optimal parameters (as described in chapter 4, paragraph 4.3). The choline analysis was conducted using gold screen-printed electrode modified with biocomposite film SiO_2-ChOx with optimal parameters (as described in chapter 3, paragraph 3.2). The deposition of silica-biocomposite in both cases was performed by electrochemically-assisted deposition method.

5.1. Determination of sorbitol using glassy carbon electrode modified with CNT and SiO_2-sorbitol dehydrogenase film

Sorbitol is an alcohol contained in fruits that has a sweet flavor. It is widely used in the food industry (food additive E 420) as a sweetener and [286] as well as in the cosmetic and pharmaceutical industries. Very often it is used along with fructose as a sweetener in diabetic foods for people with diabetes.

In human body, sorbitol is formed from glucose and is converted to fructose with DSDH. Its abundance in the tissues leads to the swelling that occurs in diabetes [287]. It also fermented by the bacteria of large intestine to acetate and H_2, which leads to diarrhea, severe disorders of the gastrointestinal tract and weight loss when its excessive consumption [288]. These symptoms have been reported for the abuse of sorbitol in amounts of more than 10 g/day.

Thus, monitoring of sorbitol in the food is an important analytical task. In addition, it is important to determine the concentration of sorbitol in biological fluids and tissues, to prevent the development of complications of diabetes [287, 289]. As standard techniques of sorbitol the chromatographic and enzymatic methods are mainly used, however, they have several disadvantages, which are discussed below in paragraph 5.1.4.

5.1.1. Procedure of the amperometric determination of sorbitol using the glassy carbon electrode modified with CNT and SiO_2-sorbitol dehydrogenase film.

Determination of sorbitol using modified GCE-CNT-SiO_2-DSDH electrode was performed by the amperometric method of additions in the range of linearity of the calibration graph (P 97, Fig. 4.13).

For determination of sorbitol the modified GCE-CNT-SiO_2-DSDH electrode, silver-chlorine reference electrode and platinum auxiliary electrode were immersed in the electrochemical cell containing 2.54 mL of Tris-HCl and 1 mM NAD^+. The magnetic stirrer was turned on and the potential 0.5 V was applied, waiting if necessary (up to 200 s) until the current value stabilizes. This value was considered as background and subtracted from all further received values. Next, 20 μL of standard 50 mM sorbitol solution was added to the cell using micropipette, and the resulting current increase was recorded (Fig. 5.1). Then, 20 μL of a solution of unknown sorbitol concentration was added to the cell and the current increase was measured. The last addition was 20 μL of standard 50 mM sorbitol solution to compare with the first one and ensure the absence of changes in electrode sensitivity [290].

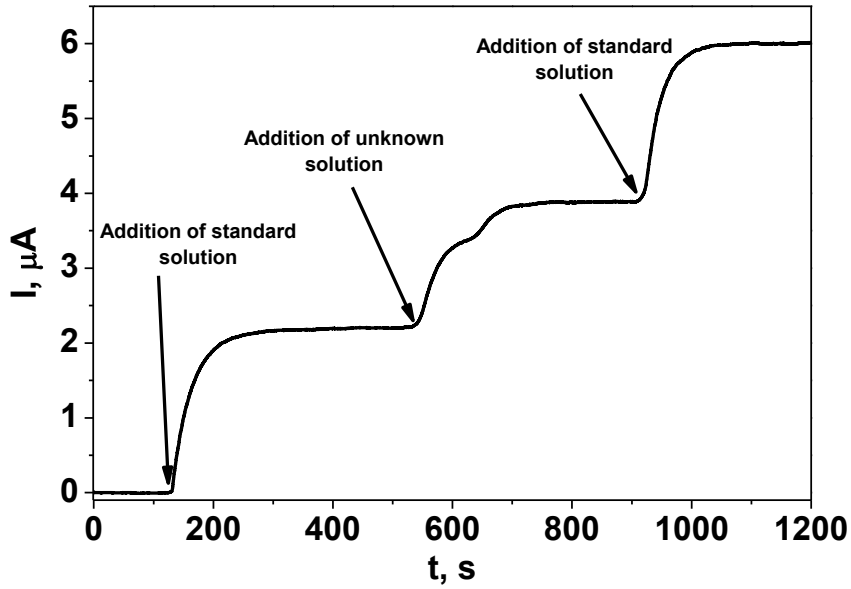

Fig. 5.1. Typical amperogram obtained during D-sorbitol determination with GCE-CNT-SiO_2-DSDH using method of standard addition. Applied potential +0,5 V.

The concentration of sorbitol in the test solution was calculated by the modified formula for the method of standard additions, taking into account the increase of volume of the solution during the introduction of additions:

$$C_x = \frac{V_{st} \times C_{st} \times \left((V_s + V_{st} + V_x) \times I_x - (V_s + V_{st}) \times I_{st}\right)}{I_{st} \times V_x \times (V_s + V_{st})} \quad (5.1)$$

wh. V_s – initial volume of solution in the electrochemical cell, mL;

V_{st}, C_{st} – volume and concentration of the standard solution addition, mL, mM;

V_x, C_x – volume and concentration of the studied solution addition, mL, mM;

I_{st} – current value after the standard solution addition, μA;

I_x – current value after the studied solution addition, μA;.

For the verification, the method of "added – found" was used. Results of the determination of sorbitol additions in buffer solution are presented in Table 5.1.

Table 5.1

Results of the determination of sorbitol additions in the buffer solution using GCE-CNT-SiO_2-DSDH. n = 3, P = 0,95

Sorbitol concentration, mM		
Added	Found	S_r
0.40	0.41 ± 0.04	0.04
0.60	0.60 ± 0.05	0.03
0.90	0.90 ± 0.04	0.02

5.1.2. Interference of some substances on the determination of sorbitol

As objects of study we selected products of the food and cosmetic industries that may contain sorbitol. These products are dietary sweets, chewing gum, and

toothpaste. The effect of the components contained in these objects that can have interfering influence on the results of determination of sorbitol by GCE-CNT-SiO_2-DSDH was studied. The concentration of sweeteners was equimolar to sorbitol and the concentration of glycerol and sodium lauryl sulfate was average for the cosmetic products [291]. Selected sorbitol concentration (1 mM) correlates with its average content in the solution after sample preparation. The results are shown in Table 5.2.

Table 5.2

Interfering influence of some substances on the results of amperometric determination of sorbitol with GCE-CNT-SiO_2-DSDH. C_{sorb} = 1 mM.

Substance (X)	Approximate molar ratio in studied samples, (C_{sorb} :C_x)	Molar ratio that does not interfere (C_{sorb} :C_x)
Sucrose	1 : 1	1 : 5
Fructose	1 : 1	1 : 5
Glucose	1 : 1	1 : 1
Mannitol	1 : 1	1 : 5
Xylitol	1 : 1	1 : 5
Glycerol	1 : 1	1 : 1
Ascorbic acid	1 : 0,1	1 : 0,02
Fe(III), Fe(II)	-	1 : 5
Ascorbic acid : Fe(III) = 1:5 (mol.)	-	1 : 0,1
Sodium lauryl sulfate*	1 : 0,5	1 : 0,5

* at time of analysis less than 10 minutes

Carbohydrates and polyhydric alcohols do not interfere with determination of 1 mM sorbitol, including mannitol, which is a stereoisomer of sorbitol, indicating the high selectivity of the modified electrode.

Ascorbic acid does quite significant interfering influence due to the nonenzymatic oxidation on the electrode at operating potential 0.5 V. But lower working potential (0.5 V) enables an approach for its masking – the introduction of Fe (III). It was investigated that even fivefold excess of Fe(III) does not interfere with determination of sorbitol (Table 5.2). Given the fact that the objects of study contain sorbitol in significantly higher amounts than ascorbic acid, 3 mM of $Fe(NO_3)_3$ will be sufficient for the masking and will not interfere with the determination of sorbitol. According to the literature data [292, 293], the masking effect Fe(III) can be explained by two factors: the formation of the transition complex of Fe(III) with ascorbic acid and subsequent oxidation of ascorbic acid by ferric iron in the complex forming Fe (II) and dehydroascorbic acid .

The presence of anionic surfactant leads to a gradual decrease in signal with time during the time of contact of the electrode with the solution more than 10 minutes, probably due to leaching of the enzyme from the film [36]. Consequently, when analyzing cosmetic products containing surfactants one should avoid prolonged (over 10 minutes) contact of modified electrode with test solutions.

Thus, given the absence of interfering effects of most of the investigated compounds and the ability to mask ascorbic acid the developed modified electrode can be used for determination of sorbitol in the food and cosmetic samples.

5.1.3. Determination of sorbitol in the food and cosmetic samples

As objects of study we used toothpaste for children «Oral B Stages berry bubble» (manufacturer «Procter & Gamble Co.», Germany), chewing gum «Orbit» (manufacturer LLC «Wrigley», Russia), biscuits "Diabetic" (producer PJSC "Kharkiv biscuit Factory", Ukraine), shower gel "White honey" (produced by "Yaka", Ukraine). The composition of the objects is given in Appendix G.

Sample preparation was performed in accordance with State Standard [294]. The samples of objects was weighed on an analytical balance so that in the final volume the concentration of sorbitol was between 20-50 mM. Sample was manually crushed in a porcelain mortar, quantitatively transferred into a 100 mL beaker and 40 mL of heated to 60 - 70 C bidistilled water was added and stirred for one hour on a heated magnetic mixer. The additions of standard 50 mM solution of sorbitol were injected in some samples. The resulting suspension was filtered through a paper filter in a 50 mL flask and adjusted to the mark on the flask. Further determination of sorbitol in the resulting solution was performed by the method of standard additions, as described in paragraph 5.1.1.

Results of sorbitol determination in the objects of food and cosmetic industries are shown in Table 5.3. The obtained data are characterized by satisfactory accuracy and reproducibility. The found sorbitol content in the object "Shower gel" is perhaps somewhat underestated due to the presence of anionic surfactants, which lead to a decrease in the signal.

Table 5.3

Results of sorbitol determination in the food and cosmetics samples. n = 3, P = 0,95

Sample	Sorbitol content, мг/г		
	Added	Found	S_r
Toothpaste for children «Oral B Stages berry bubble»	0	117 ± 20	0,06
	296	411 ± 33	0,04
Chewing gum «Orbit»	0	549 ± 46	0,03
	694	1251 ± 122	0,04

Biscuits "Diabetic"	0	321 ± 29	0,04
	664	985 ± 29	0,01
Shower gel "White honey"	0	15 ± 3	0,07
	230	243 ± 20	0,03

5.1.4. Comparison of the standard methods of sorbitol determination with the developed technique

For determination of sorbitol the electrochemical, titrimetric, polarimetric, chromatographic and enzymatic methods are used.

The titrimetric method of sorbitol analysis, which is used in the pharmacopoeia is based on the formation of its complex with copper, the concentration of which is determined by iodometric titration [295]. There is also a method of reverse iodometric titration of periodate excess that remains after sorbitol oxidation in sulfuric acid medium [296]. However, these methods are not sensitive and selective - in fact they determine the total content of polyols and glucose.

One of the methods is direct electrochemical detection of sorbitol on platinum [297, 298] and copper electrodes [299], but the potentials used (above 0.7 V vs Ag/AgCl [299]) are too large, resulting in interfering effects of many reductants, which greatly reduces the selectivity analysis. A significant drawback of this method is the need for electrode regeneration after each measurement.

Polarimetric methods are broadly applied for sorbitol determination in foodstuffs. Under State Standard 25268-82 [294], the determination of sorbitol is carried out using polarimetry and difference in optical activity before and after the addition of ammonium molybdate.

Among the chromatographic methods for the determination of sorbitol, which are the most sensitive and selective, one may note ion chromatography with

polarization photometric detector [300], high-performance liquid chromatography with amperometric [289] and UV detector [287], capillary electrophoresis with UV detector [301] and capillary isotachophoresis with conductometric detection [302]. Although chromatographic methods of analysis provide selective and sensitive determination of sorbitol in many objects, their common drawback is an expensive equipment, complex sample preparation and significant duration of analysis, as well as the need for special training and high requirements for reagents purity.

In enzymatic methods of analysis DSDH is most often used with diaphorase which catalyzes reduction of iodonitrotetrazolium chloride to iodonitrotetrazolium formazan (Fig. 5.2), while measuring the value of the absorption of the latter at λ = 492 nm photometrically [303]. There are also ready test kits for sorbitol and xylitol determination by this method in food [304, 305].

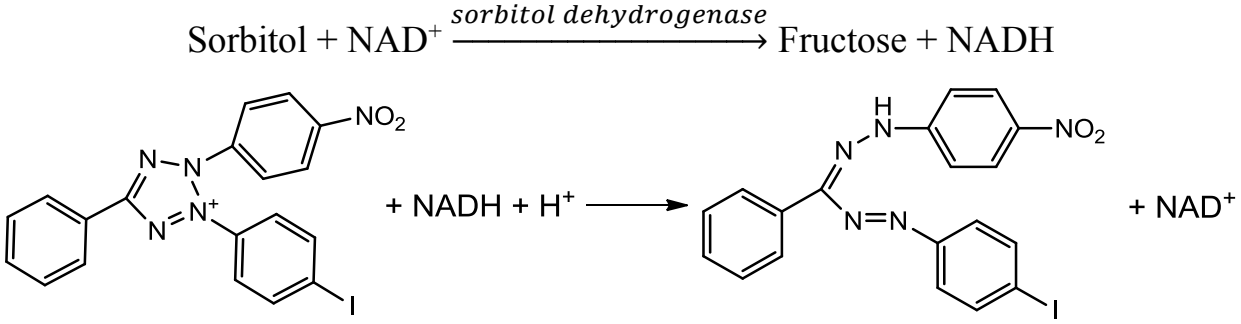

Fig. 5.2. Schemes of reactions of enzymatic determination of sorbitol

This method is very selective and sensitive, but the significant consumption of enzymes and cofactors, including their high cost (especially diaphorase), makes it not viable from an economic point of view. In addition, this method is not express, and the error of determination increases because of the use of complex two-enzyme system.

The advantages of the developed method for the sorbitol determination using modified GCE-CNT-SiO_2-DSDH electrode compared with titrimetric, polarimetric and electrochemical methods are the high selectivity of determination in the presence of other polyhydric alcohols and carbohydrates, as well as the lower limit of

detection. Compared with chromatographic methods, the technique requires minimal sample preparation, characterized by expressivity and the possibility of using by unqualified personnel. The sensitivity of this method is sufficient to determine the sorbitol in the majority of objects. The method can be applied for screening sorbitol content in the objects of food and cosmetics industries, as well as for the analysis of biological fluids if sensitivity increased.

To date there are only a few examples of the development of amperometric biosensors based on DSDH to determine sorbitol (Table 5.4). However, in most cases, these sensors were used only for the analysis of model solutions, not real objects. Compared with them the developed GCE-CNT-SiO_2-DSDH electrode has high stability and reproducibility of results, limit of detection is sufficient to determine sorbitol in most objects. The advantage is also a simple modification and the absence of mediator.

Table 5.4

Comparative characteristics of known amperometric biosensors based on DSDH

Electrode	Modifier	Response time, s	Linear range, mM	Limit of detection, μM	Potential of detection, mV	Stability*	RSD, %	Real object analysis	Link
Carbon fiber	Covalent binding to «Immunodin» membrane	300	0,0065 – 0,2	6,5	150	-	-	-	[199]

GCE-CNT	Nafion-Hyaluronic acid	53	0,5 – 1,0	18	400	95% / 22 h.		-	[201]
Gold	Polyethyleneimine-Mercaptopropionic acid-Toluidine		1,0 – 5,0	100	400	50% / 14 d.	7,1	-	[200]
Carbon paste	Polyphenylethylenediamine	120	0,02 – 0,8	40	0	60% / 3 d.	6,1	+	[198]
GCE-CNT	**SiO_2-PDDA**	**100**	**0,5 – 3,5**	**160**	**500**	**85% / 30 d.**	**6**	**+**	**This work**

* The stability of the electrode is expressed in the format X% / Y, where X - the percentage of response (from the original) that persists after use of the electrode during the time interval Y.

5.2. Determination of choline using gold screen-printed electrode modified with film SiO_2-choline oxidase

Choline – a quaternary ammonium base, which belongs to the vitamin B (B_4) group, although the human body is able to synthesize it. However, it should be necessarily present in the diet of humans; its recommended dose is 425 and 550 mg per day for women and men respectively [306]. In the body choline participates in the synthesis of important neurotransmitter acetylcholine, it also participates in the regulation of insulin levels, in the transport of fat in the liver (as the part of some phospholipids) and in the formation of cell membranes. The deficiency of choline in the body leads to serious violations: lipopexia and liver damage, kidney damage, bleeding. However, excessive consumptionof choline leads to the so-called "fish odor syndrome", sweating, excessive salivation, reduced pressure [129].

Foods rich in choline are veal liver, egg yolks, milk, spinach and cauliflower. In addition, choline is artificially added to some specialized food such as baby food, vitamin formula, sports drinks. Control of choline content in these foods is an important analytical task. For example, infant vitamin mixture is almost the only source of choline for infants, and its lack in food can lead to severe developmental disorders [129]. It is also important to determine choline in biological fluids, where it is acts as a marker of cholinergic activity in the tissues of the brain and is used for the diagnosis of severe neurodegenerative disorders such as Parkinson's disease and Alzheimer's disease [307, 308].

5.2.1. Procedure of amperometric determination of choline using gold screen-printed electrode modified with film SiO_2-choline oxidase

Amperometric determination of choline with AuSPE-SiO_2-ChOx was performed by standard additions method, similar to the determination of sorbitol in paragraph 5.1.1. Modified AuSPE-SiO_2-ChOx electrode was placed in the electrochemical cell containing 5 ml of 0.025 M PBS (pH 7.5), and the potential 0.7 V was applied together with stirring. When the current constant value established 10 µl of standard 50 mM choline solution was added to the cell using micropipette. Then 0.2 ml of the studied solution with an unknown concentration of choline was added to the cell using micropipette. The last addition was 10 µl of standard solution of choline in order to ensure the stability of the response. Choline concentration in the studied solution was calculated using the obtained amperogram (Fig. 5.3), according to the formula (5.1) in section 5.1.1.

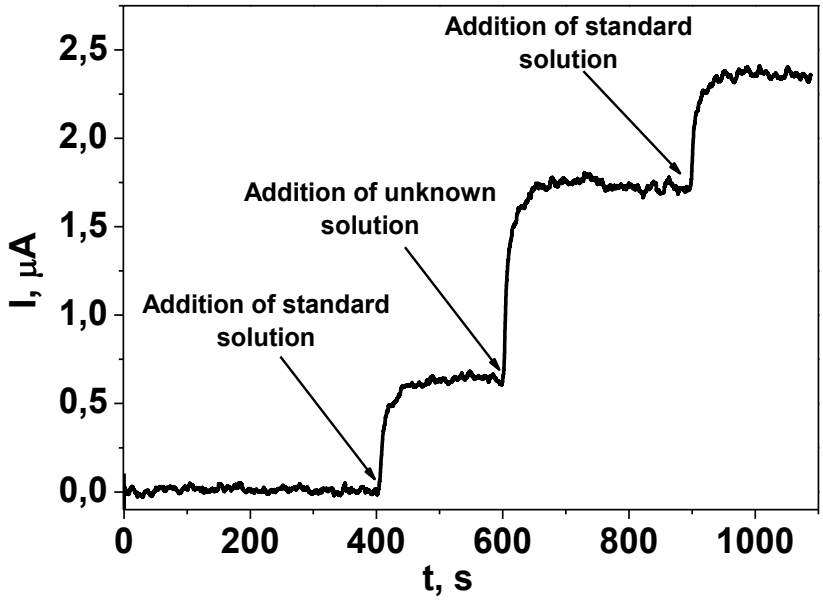

Fig. 5.3. Typical amperogram obtained during choline determination with AuSPE-SiO_2-ChOx using method of standard addition. Applied potential +0,7 V.

Results of choline additions determination in phosphate buffer solution are presented in Table 5.5. They are characterized by satisfactory accuracy and reproducibility.

Table 5.5

Results of choline additions determination in phosphate buffer solution using AuSPE-SiO_2-ChOx. n = 3, P = 0,95

Choline concentration, мМ		
Added	Found	S_r
0.50	0.51 ± 0.06	0.05
1.30	1.28 ± 0.08	0.03

5.2.2. Interference of some substances on the determination of choline

The influence of the substances contained in the food and able to interfere with the determination of choline by the modified electrode was studied. The effect of substances at their average concentrations in the corresponding objects was investigated (Appendix G). Since urea and uric acid are lacking in food, their

concentration was chosen according to their content in blood plasma. The chosen concentration of choline (1 mM) corresponding to its maximum content in the solution after sample preparation. Results of the study are presented in Table 5.6.

Table 5.6

Interfering influence of some substances on the results of amperometric determination of choline with AuSPE-SiO_2-ChOx. C_{ch} = 1 mM.

Substance (X)	Approximate molar molar ratio according in studied samples, (C_{ch} :C_x)	Molar ratio that does not interfere (C_{ch} :C_x)
Glucose	1 : 10	1 : 10
Sucrose	1 : 10	1 : 10
Lactose	1 : 50	1 : 100
Fructose	1 : 10	1 : 10
Uric acid*	1 : 10	1 : 10
Urea*	1 : 50	1 : 100
Ascorbic acid	1 : 1	1 : 0.02
Ethanol	-	1 : 100
Pb^{2+}	-	1 : 0.1
Zn^{2+}	1 : 0.1	1 : 0.5
Cu^{2+}	1 : 0.01	1 : 0.2
Mn^{2+}	1 : 0.01	1 : 5
Fe^{3+}	1 : 0.1	1 : 0.5

* blood plasma content

As seen from the results, the main macrocomponents do not interfere with the determination of choline. One should note the absence of interfering effects of ethanol in relatively high concentrations. The presence of equimolar amounts of Cu(II) leads to the signal decrease, it is known from the literature that copper cations inhibit ChOx [309], but the presence of copper in such high concentrations in the studied objects is ruled out. Ascorbic acid significantly interferes with the determination of choline due to its nonenzymatic oxidation on the electrode at 0.7 V.

5.2.2.1. Elimination of interfering influence of ascorbic acid

Given the fact that ascorbic acid is a common interfering component in the development of biosensors, the literature offers several ways to eliminate its impact. In particular, the most common way is the use of semipermeable membranes that limit the access of interfering substances to the electrode due to the size or charge of their molecules [310, 311]. However, this approach often leads to a decrease in the sensitivity of the biosensor to analyte [176]. Therefore, another promising approach is the eliminatation of the reductants effect by their prior oxidation on the membrane-oxidants [175]. The composition of such membranes can vary, but one of the best oxidants that can be used for this purpose is the oxide of manganese (IV) [173, 174]. The disadvantage of such membranes is the low reproducibility of the signal and slow response time. Therefore, to simplify the procedure of the modified electrode fabrication, we decided to add MnO_2 powder directly into the solution of the analyte so that he could oxidize ascorbic acid before determination.

The dry powder of MnO_2 was added (10 mg per 10 ml of solution) to the solution that was stirred with a magnetic stirrer for 30 min. Then the sample was filtered through a paper filter and used for the determination of choline as described in paragraph 5.2.1.

Fig. 5.4 shows that the current increase on the AuSPE after addition of ascorbic acid solution after contact with MnO_2 is very small (Fig. 5.4a). For comparison, the

addition of ascorbic acid solution of the same concentration but without treatment with MnO_2 (Fig. 5.4b) leads to a significant amperometric response.

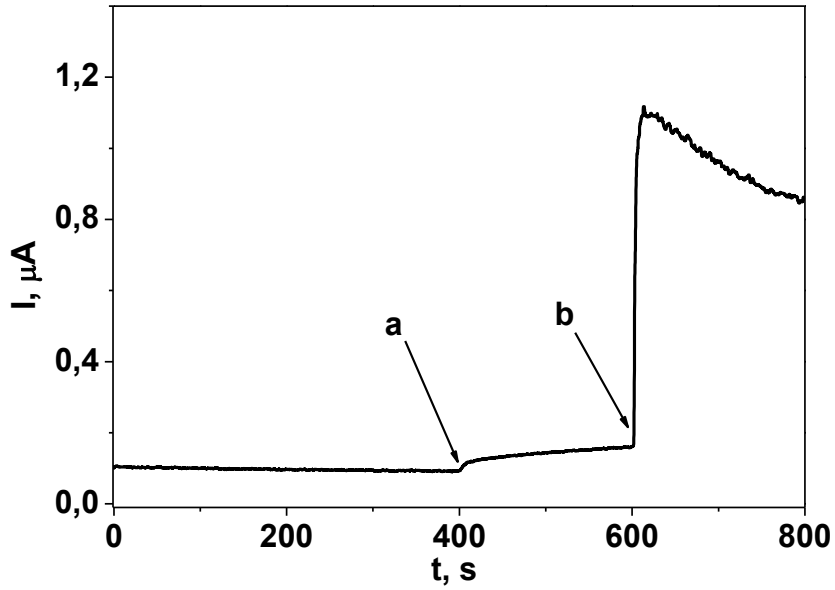

Fig. 5.4. Amperogram of AuSPE in PBS: (a) addition of ascorbic acid solution (0,1 mM) after contact with MnO_2, and (b) initial ascorbic acid solution (0,1 mM). Applied potential +0.7 V.

To test the impact of MnO_2 on choline signal its determination was conducted using AuSPE-SiO2-ChOx in a series of model solutions (Table 5.7). From the obtained data it can be concluded that MnO_2 does not interact with choline because found choline amount remains constant before and after treatment with MnO_2 (solutions 1, 2, Table 5.7). At the same time, the presence of ascorbic acid leads to an overestimation of the expected results of choline determination (solution 3, Table 5.7). However, after the treatment of this solution with MnO_2 (solution 4, Table 5.7), the found amount of choline correlates with added.

Table 5.7

Influence of MnO_2 on the results of 0.8 mM choline determination using AuSPE-SiO_2-ChOx

№	Solution content	Choline found, mM
1	Choline	0.81 ± 0.06
2	Choline + 10 mg MnO_2	0.81 ± 0.06
3	Choline + 0.1 mM ascorbic acid	0.91 ± 0.09
4	Choline + 0.1 mM ascorbic acid + 10 mg MnO_2	0.81 ± 0.07

Thus, treatment of 0.1 mM ascorbic acid solution with MnO_2 leads to the elimination of its interfering impact in choline determination using AuSPE-SiO_2-ChOx. According to the stoichiometry of the reaction [312], the amount of MnO_2 1 mg/ml is sufficient to eliminate the interfering effects of ascorbic acid up to its concentration in a solution 10 mM. The ascorbic acid content should not exceed 5 mM after sample preparation, so such quantity of MnO_2 is enough to mask its influence.

5.2.3. Determination of choline in food products

The infant formula «Bebi» was chosen as an object of study, its composition is listed in Appendix G.

Sample preparation was carried out according to the [313]. The sample was weighed on analytical balance, transferred to a beaker and 30 ml of 1 M HCl was added. The beaker was covered with a glass and heated at 60 - 70 C in a water bath for 4 hours, stirring occasionally. Heating with acid promotes separation of milk proteins and hydrolysis of bound in the form of esters of choline to the free form. After cooling, the mixture was filtered through filter paper in 50 ml flask. The pH of

the solution was adjusted to 3.0 - 4.0 with 10 M NaOH. Treatment with 50 mg of MnO_2 was performed as indicated in section 5.2.2.1, the volume of the solution was adjusted to the mark with water. The resulting solution was stored in a refrigerator at 4 C up to one week.

Determination of choline in the resulting solution was performed by the method of standard additions as described in paragraph 5.2.1. Results of determination are given in Table 5.8. The data obtained are characterized by satisfactory accuracy and reproducibility and correlated with the content of choline, declared by the manufacturer (Appendix G).

However, attempts to determine choline in food mixture using a standard photometric method with Reinecke salt [314] were unsuccessful due to the low sensitivity and reproducibility of the method, and chromatographic technique requires the use of special columns.

Table 5.8

Results of choline determination in model solution and food products.

n = 3, P = 0,95

sample	Choline content, mM		
	Added	Found, $x \pm \Delta x$	S_r
Model solution*	0.30	0.34 ± 0.04	0.05
	1.00	1.09 ± 0.12	0.05
	Choline content, mg/g		
Infant formula «Bebi»	0	0.95 ± 0.14	0.06
	1.12	1.99 ± 0.19	0.04

5.2.4. Comparison of the standard methods of choline determination with the developed technique

For determination of choline in foods the spectrophotometric, chromatographic and enzymatic methods of analysis are used. Its analysis is complicated because it can be either in free form or in the ester derivatives of phosphoric acid, so its preliminary hydrolysis is necessary before determining total choline [129].

Historically, the first photometric method for choline determination is based on formation of insoluble colored compound with Reinecke salt, whose absorption is detected in methanolic solution at 520 nm [314]. The gravimetric variant of this method is also possible [315]. Despite its simplicity, this method is time-consuming, low-sensitive (the loss of choline during washing is possible), requires the use of toxic reagents. In addition, this method is not selective, determination of choline is prevented by most other amines.

Chromatographic determination of choline is possible using liquid [316–318], gas [318, 319], ion chromatography [320] and capillary electrophoresis [321]. The mass detector [316, 317], ion exchange membrane detector [320] and indirect UV detection [321] can be applied. The general drawbacks of chromatographic techniques are long and complex sample preparation, high cost and the inability of analysis in the field.

NMR spectroscopy can be also used for determination of choline [322]. The method allows to determine choline content with great accuracy in various forms, but is unsuitable for most laboratories because of the high cost of equipment and low linearity and sensitivity.

Enzymatic methods for choline determination are based on its oxidation with ChOx (after preliminary hydrolysis of esters by phospholipase) with the release of H_2O_2. The hydrogen peroxide reacts with phenol and 4- aminoantypyrine contained in the mixture in the presence of peroxidase, giving a colored reaction product, which is detected photometrically at a wavelength of 505 nm [313, 323]. There are also modifications of this method with other dyes [324] [324]. This method of choline

determination is quite expensive, given the high cost of the enzyme, with a significant error of determination by photometric method of signal detection. In addition, the determination of choline by this method is influenced by many reductants that can react with hydrogen peroxide. Their influence can be removed by using activated carbon [325].

The developed method of choline determination with AuSPE-SiO_2-ChOx has significant advantages over existing methods. In particular, the use of planar technology, relatively cheap reagents and small quantities of enzyme allow producing large number of electrodes with little cost. Sensitivity and selectivity of the modified electrode is sufficient to determine choline in foods and biological fluids with minimal sample preparation. Small time of analysis and its simplicity allows the use of the developed technique by unskilled personal.

Compared with other known biosensors based on ChOx, the developed modified electrode is characterized by fast response and low detection limit, which can be explained by the porous structure of SiO_2-film that facilitates the diffusion of reactants inside (Table 5.9). Modification procedure is simple and, unlike most other biosensors, does not use mediator, which could worsen the analytical characteristics and reproducibility of biosensors. The sensitivity developed electrode slightly lower than in some works [168, 307, 326], but it is quite sufficient to determine choline in foods that has been shown in the analysis of real objects.

Table 5.9

Comparative characteristics of known amperometric biosensors based on ChOx

Electrode	Modifier	Response time, s	$K_м$, mM	Linear range, mM	Limit of detection, μM	Potential of detection, mV	Stability*	RSD, %	Real object analysis	Link
Pt	Diaminobenzen-Prussian blue	30	1.2	0.05 ÷ 2	50	0	85% / 2 m.	8	-	[327]
Pt	Polyvinylferrocene chlorate	70	2.32	0.004 ÷ 1.2	4	750	-	4,6	-	[328]
Carbon paste	Prussian blue	30	2	0.02 ÷ 2	20	50	1 m.	14	-	[329]
Pt	Au-Nps-PVA-Glutaraldehyde	20	0.78	0.02 ÷ 0.4	10	400	80% / 14 d.	7,4	-	[264]
GCE	PDDA-$FePO_4$-Prussian blue	2	0.47	0.002 ÷ 3.2	0.4	0	95% / 14 d.	3,2	-	[307]
Pt	SiO_2-CNT	15	-	0.005 ÷ 0.1	0.1	160	75% / 1 m.	4,8	+	[168]
Pt-CNT	PDDA-poly(allylamine)-poly(vinyl sulfate)	8	-	0.005 ÷ 0.1	0.2	600	90% / 1 m.	5,4	-	[326]
Au	**SiO_2-CTAB**	**15**	**0.27**	**0.01 ÷ 0.6**	**5**	**700**	**52% / 14 d.**	**5**	+	**This work**

* The stability of the electrode is expressed in the format X% / Y, where X - the percentage of response (from the original) that persists after use of the electrode during the time interval Y.

It should be noted that immobilized on the electrode surface ChOx is characterized by low apparent Michaelis constant (Table 5.9), indicating the preservation of its native structure due to biocompatibility of SiO_2-materials. In addition, immobilization into SiO_2-film increases the stability of the ChOx structure, for example, large amounts of ethanol do not lead to its deactivation. The developed electrode is stable and can be used repeatedly (as was shown in section 3.2.5), which is particularly important for biosensors.

5.3. Conclusions to chapter 5.

The prospects of the developed modified electrodes application as amperometric biosensors for the analysis of real objects were shown.

The technique of amperometric determination of sorbitol using glassy carbon electrode modified with biocomposite film SiO_2-sorbitol dehydrogenase was developped. The calibration graph was linear in the range of concentrations of $5 \cdot 10^{-4}$ – $3{,}5 \cdot 10^{-5}$ M, the detection limit was $1{,}6 \cdot 10^{-4}$ M. The equimolar amounts of sucrose, glucose, urea, mannitol, and glycerol do not interfere with the determination of sorbitol. Interfering effect of ascorbic acid can be eliminated by the introduction of trivalent iron. Results of sorbitol determination by the developed technique in the food and cosmetic products are characterized by satisfactory accuracy and reproducibility.

The technique of amperometric determination of choline using gold screen-printed electrode modified with film SiO_2-choline oxidase was proposed. The calibration graph was linear in the concentration range of $1 \cdot 10^{-5}$ – $6 \cdot 10^{-4}$ M, the

detection limit was $5 \cdot 10^{-6}$ M. The 10-fold excess of sucrose, lactose, urea and heavy metals except Cu (II) do not interfere with the choline determination. Interfering effect of ascorbic acid may be eliminated by prior mixing with MnO_2. Results of choline determination in the food using developed technique are characterized by satisfactory accuracy and reproducibility.

The advantages of the developed techniques in comparison with known methods of sorbitol and choline determination are simple sample preparation, higher selectivity and expressivity of analysis, and low cost of a single determination.

CONCLUSIONS

- The simple one-step procedure for immobilization of oxidases and dehydrogenases in SiO_2-film on the surface of different types of electrodes by electrodeposition method was unified. The examples of choline oxidase and sorbitol dehydrogenase showed that immobilized enzymes more actively bind to the substrate and retain their activity longer than in solution.
- Electrodes modified with platinum nanomaterials are more sensitive to hydrogen peroxide than platinum macroelectrodes. At the same time, these electrodes coated with biocomposite SiO_2-enzyme film exhibit analytical characteristics similar to platinum macroelectrodes.
- Modification of glassy carbon electrode with carbon nanotubes (CNT) by electrophoretic deposition method increases the sensitivity and stability of the amperometric response of coenzyme NADH, which is promising for the development of dehydrogenase-based biosensors. The use of CNT shifts NADH oxidation potential at 0.25-0.3 V towards negative values, increasing thereby the selectivity of its detection.
- The use of gold screen-printed electrode is promising for the immobilization of choline oxidase in SiO_2-film. The increase of modified electrode sensitivity to choline is achieved by optimization of the parameters of electrochemically-assisted deposition, the maximum response was obtained during the deposition for 20 s at potential of -1.1 V.
- Electrode modified with CNT and sorbitol dehydrogenase, shows significant advantages in terms of sensitivity and selectivity of sorbitol detection compared with electrode containing no CNT. Analytical signal of modified electrode depends on the parameters of electrodeposition and thickness of CNT-layer. Best characteristics were obtained using -1.3 V, 16 s of electrochemically-assisted deposition and CNT-layer thickness from 100 to 150 nm.

• The laboratory models of sensors and express techniques of amperometric determination of sorbitol and choline in foods and cosmetics using electrodes modified with CNT and/or biocomposite SiO_2-enzyme film were developed. The advantages of the application of electrodes modified with biocomposite film SiO_2-enzyme as sensitive elements amperometric biosensors for the determination of sorbitol and choline were shown.

APPENDICES

Appendix A

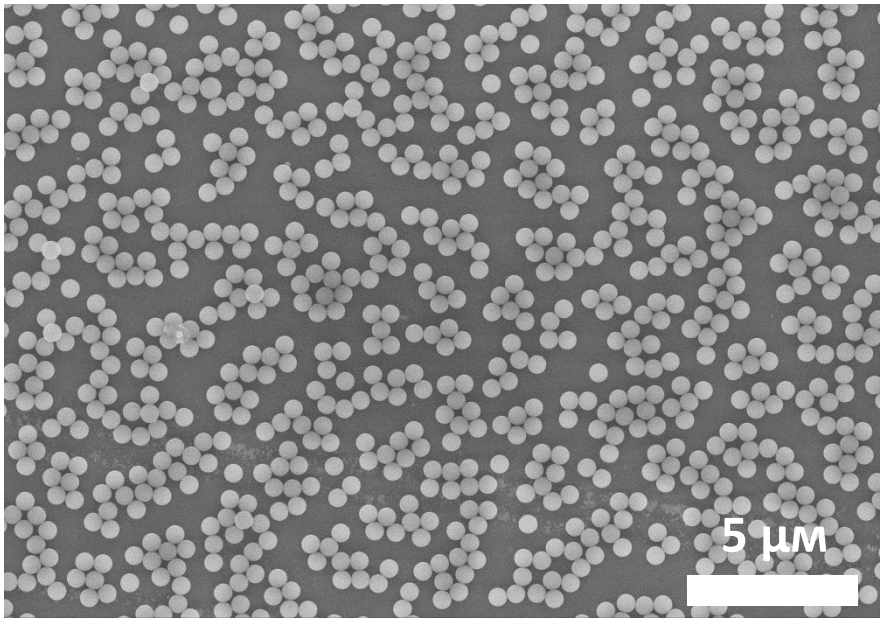

Fig. A.1. SEM-image obtained after deposition of PS-beads on GCE by means of EPD (60 V, 120 s)

Appendix B

Randles-Sevcik equation:

$$i_p = 2{,}68 \times 10^5 n^{3/2} A D^{1/2} C v^{1/2} \text{ (at 298 K)}$$

wh. A – electroactive surface area;

D – diffusion coefficient;

n – number of electrons;

C – concentration of electrochemically-active substance;

v – potential scan rate.

Cottrell equation:

$$i = \frac{nFAD^{1/2}C}{\delta} \tag{5.2}$$

wh. A – electroactive surface area;

D – diffusion coefficient;

n – number of electrons;

C – concentration of electrochemically-active substance;

F – Faraday constant;

δ – constant of the electric double-layer

Appendix C

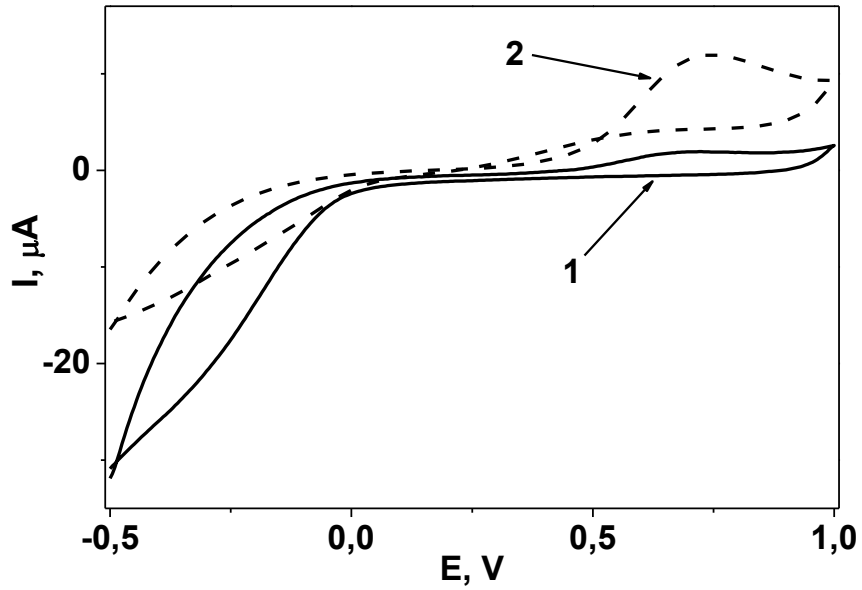

Fig. C.1. Cyclic voltammograms of AuSPE, modified with Pt-Nps and SiO_2-ChOx film in the absence (1) and presence (2) of 1 mM choline. Supporting electrolyte: 0.025 M PBS (pH 7.5), potential scan rate 50 mV/s.

Appendix D

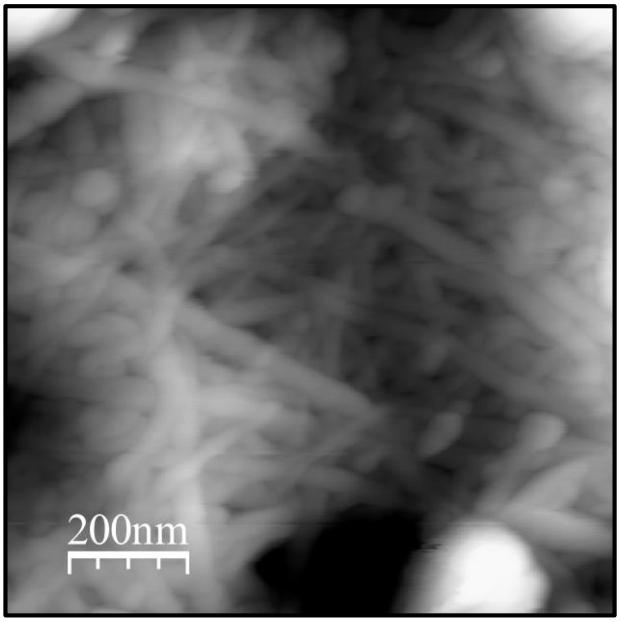

Fig. D.1. AFM-image of the surface of GCE, modified with CNT by EPD.

Appendix E

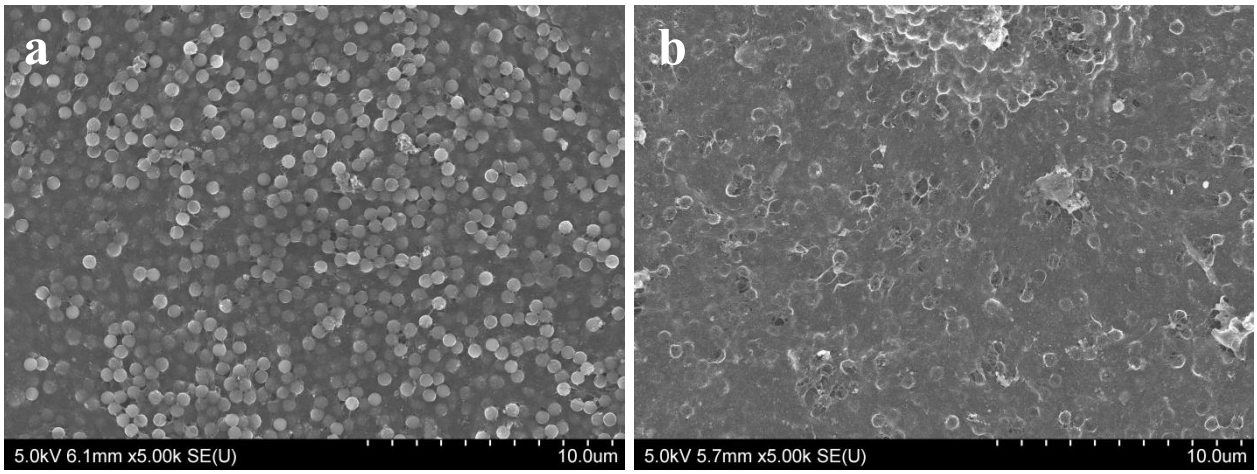

Fig. E.1. SEM-image (top view) of the GCE surface modified with CNT-PS composite by EPD before (a) and after (b) template removal. Concentration of PS-beads 0.1 mg/mL; EPD time – 135 s.

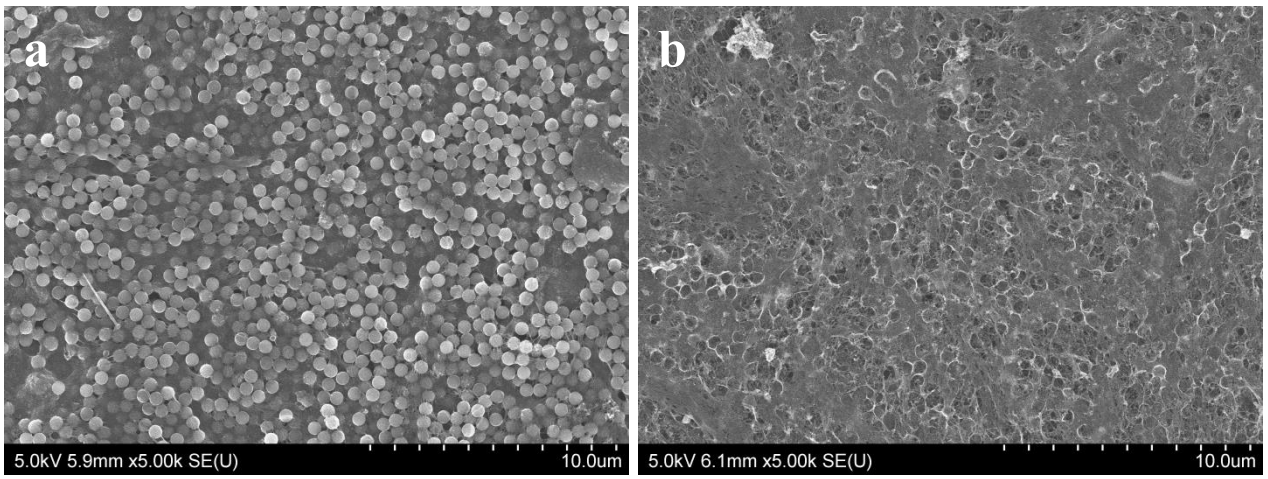

Fig. E.2. SEM-image (top view) of the GCE surface modified with CNT-PS composite by EPD before (a) and after (b) template removal. Concentration of PS-beads 0.2 mg/mL; EPD time – 135 s.

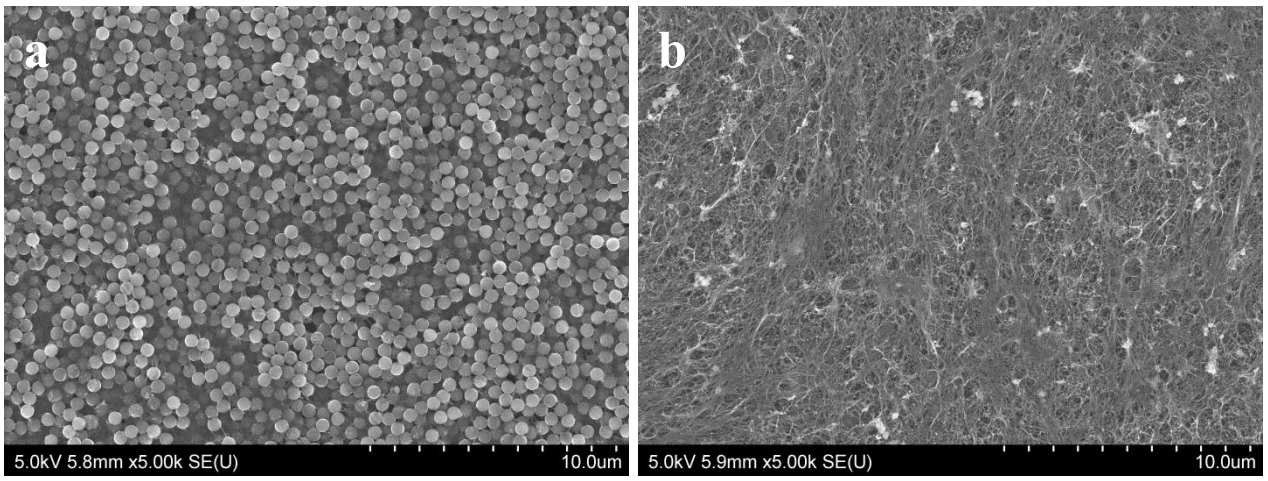

Fig. E.3. SEM-image (top view) of the GCE surface modified with CNT-PS composite by EPD before (a) and after (b) template removal. Concentration of PS-beads 0.5 mg/mL; EPD time – 135 s.

Appendix F

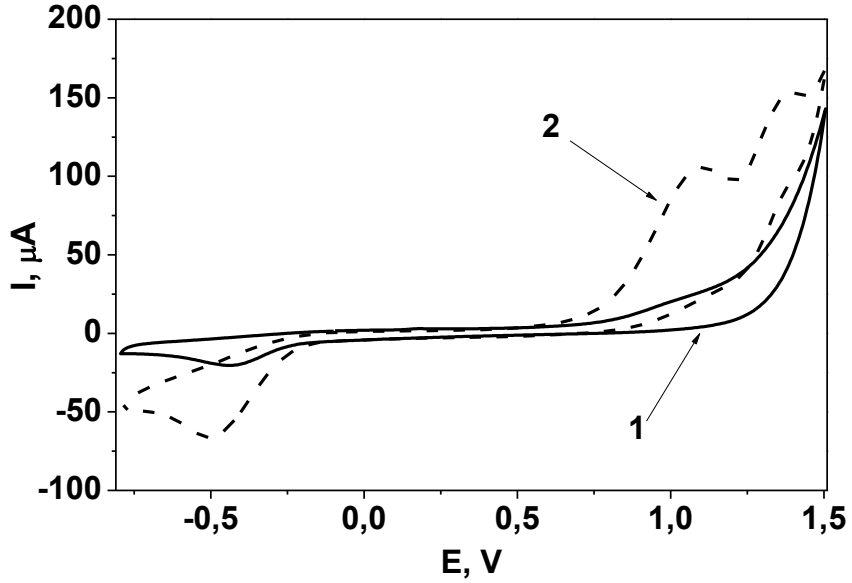

Fig. F.1. Cyclic voltammogram of GCE-CNT in the absence (1) and presence (2) of 2 mM H_2O_2. Supporting electrolyte: 0.025 M PBS (pH 7.5), potential scan rate 20 mV/s.

Appendix G

Composition of objects of study

Shower Gel "White honey":

Water, soap root decoction, decoction of leaves of mint, violet root decoction, ammonium lauryl sulfate, sodium glutamate, coco betaine, sodium chloride, extracts of herbs and flowers, sorbitol (0 – 10 % [291]), panthenol, citric acid, natural flavor, velsan.

Toothpaste «Oral B Stages berry bubble»:

Sodium fluoride, sorbitol (10 -30 % [330]), water, hydrated silica, glycerin, sodium lauryl sulfate, flavor, xanthan, saccharin sodium, carbomer, sodium hydroxide, dye FD & C Blue 1.

Cookies "Diabetic":

Wheat flour, margarine, flour, oatmeal, sorbitol (15 – 40 % [331]), baking soda, salt, cinnamon, vanilla.

Chewing gum «Orbit»:
Sorbitol (40 – 80 % [332]), rubber base, stabilizer, mannitol, natural flavorings and artificial flavors, soy lecithin, malic acid, citric acid, fumaroles acid, aspartame, acesulfame, flavor enhancers, antioxidant.

Infant formula «Bebi» (content per 100 g of the mixture):
Linoleic acid (4.4 g), casein (4.8 g), whey protein (7.2 g), lactose (55 g), vitamins (retinol acetate (570 mg), cholecalciferol (7.8 mg) α-tocopherol acetate (6 mg) fitomenadion (42 mg), ascorbic acid (90 mg), thiamine hydrochloride (0.75 mg), riboflavin (1 mg), niacinamide (4.2 mg), calcium pantothenate (4, 1 mg), pyridoxine HCl (0.5 mg), biotin (18 μg), folic acid (117 μg), cyanocobalamin (1.5 mg)), minerals (Mn^{2+} (42 mg), Cu^{2+} (300 μg), K^{+} (520 mg), Fe^{3+} (4,2 mg), Na^{2+} (150 mg), PO_4^{3-} (210 mg), Mg^{2+} (40 mg), Zn^{2+} (4 mg), I^{-}(95 mg), Cl^{-}(350 mg), Se (13 μg)), taurin (30 mg), choline (100 mg), inositol (35 mg), L-carnitine (9.4 mg).

REFERENCES

1. Zhang Xueji. Electrochemical Sensors, Biosensors and their Biomedical Applications / X. Zhang, H. Ju, J. Wang. – Academic Press, 2007. – P. 593.

2. Viswanathan Subramanian. Electrochemical biosensors for food analysis / S. Viswanathan, H. Radecka, J. Radecki // Monatshefte Für Chemie - Chemical Monthly. – 2009. – V. 140, № 8. – P. 891–899.

3. Mutlu Mehmet. Biosensors In Food Processing, Safety, And Quality Control / M. Mutlu. – CRC Press, 2012. – P. 358.

4. Rogers K R. Recent advances in biosensor techniques for environmental monitoring. / K. R. Rogers // Analytica Chimica Acta. – 2006. – V. 568, № 1-2. – P. 222–231.

5. Monošík Rastislav. Application of Electrochemical Biosensors in Clinical Diagnosis / R. Monošík, M. Stred'anský, E. Šturdík // Journal of Clinical Laboratory Analysis. – 2012. – V. 26, № 1. – P. 22–34.

6. Otto M. Modern methods in analytical chemistry. V. II. / M. Otto. – M. : Tehnosfera, 2004. – P. 288.

7. Harvey David. Modern Analytical Chemistry / D. Harvey. – McGraw-Hill, 2000. – P. 798.

8. Analytical Chemistry: A Modern Approach to Analytical Science. V I. / R. Kellner, J.-M. Mermet, M. Otto, H. M.. Widmer. – M. : Mir, 2004. – P. 608.

9. Evans Alun. Potentiometry and Ion Selective Electrodes / A. Evans. – John Wiley & Sons, 1987. – P. 324.

10. Wang Joseph. Analytical Electrochemistry / J. Wang. – John Wiley & Sons, 2000. – P. 236.

11. Eggins Brian R. Chemical Sensors and Biosensors / B. R. Eggins. – M. : Tehnosfera, 2005. – P. 336.

12. Continuous recording of blood oxygen tensions by polarography. / L. C. Clark, R. Wolf, D. Granger, Z. Taylor // Journal of Applied Physiology. – 1953. – V. 6, № 3. – P. 189–193.

13. Updike S. J. The enzyme electrode / S. J. Updike, G. P. Hicks // Nature. – 1967. – V. 214, № 5092. – P. 986–988.

14. Dzyadevych S. V. Amperometric enzyme biosensors / S. V. Dzyadevych // Biotehnologiya. – 2008. – V. 1, № 1. – P. 46–60.

15. Direct Electron Transfer : An Approach for Electrochemical Biosensors with Higher Selectivity and Sensitivity / R. S. Freire, C. A. Pessoa, L. D. Mello, L. T. Kubota // Journal of the Brazilian Chemical Society. – 2003. – V. 14, № 2. – P. 230–243.

16. Budnikov G. K. Fundamentals of modern electrochemical analysis / G. K. Budnikov, V. N. Maistrenko, V. R. Vyaselev. – M. : Mir, 2003. – P. 592.

17. Filippovich U. B. Fundamentals of biochemistry / U. B. Filippovich. – M. : Agar, 1999. – P. 512.

18. Enzyme Nomenclature: Recommendations of the NCIUBMB on the Nomenclature and Classification of Enzymes / E. C. Webb, ed. – Academic Press, 1992. – P. 862.

19. Chaniotakis Nikolas A. Enzyme stabilization strategies based on electrolytes and polyelectrolytes for biosensor applications. / N. A. Chaniotakis // Analytical and Bioanalytical Chemistry. – 2004. – V. 378, № 1. – P. 89–95.

20. Gill Iqbal. Bioencapsulation within synthetic polymers (Part 1): sol-gel encapsulated biologicals. / I. Gill, A. Ballesteros // Trends in Biotechnology. – 2000. – V. 18, № 7. – P. 282–296.

21. Sassolas Audrey. Immobilization strategies to develop enzymatic biosensors. / A. Sassolas, L. J. Blum, B. D. Leca-Bouvier // Biotechnology Advances. – 2012. – V. 30, № 3. – P. 489–511.

22. Tischer Wilhelm. Immobilized enzymes: methods and applications, in: Biocatalysis-from Discovery to Application, Berlin : Springer, 1999. pp. 95–126.

23. Krajewska B. Application of chitin- and chitosan-based materials for enzyme immobilizations: a review / B. Krajewska // Enzyme and Microbial Technology. – 2004. – V. 35, № 2-3. – P. 126–139.

24. Cao Linqiu. Immobilised enzymes: science or art? / L. Cao // Current Opinion in Chemical Biology. – 2005. – V. 9, № 2. – P. 217–226.

25. Gupta R. Entrapment of biomolecules in sol-gel matrix for applications in biosensors: problems and future prospects. / R. Gupta, N. K. Chaudhury // Biosensors and Bioelectronics. – 2007. – V. 22, № 11. – P. 2387–2399.

26. Exciting new directions in the intersection of functionalized sol–gel materials with electrochemistry / A. Walcarius, D. Mandler, J. A. Cox [et al.] // Journal of Materials Chemistry. – 2005. – V. 15, № 35-36. – P. 3663–3689.

27. Walcarius Alain. Electroanalysis with Pure, Chemically Modified and Sol-Gel-Derived Silica-Based Materials / A. Walcarius // Electroanalysis. – 2001. – V. 13, № 8-9. – P. 701–718.

28. Walcarius Alain. Electrochemical Applications of Silica-Based Organic−Inorganic Hybrid Materials / A. Walcarius // Chemistry of Materials. – 2001. – V. 13, № 10. – P. 3351–3372.

29. Biochemically active sol-gel glasses: the trapping of enzymes / S. Braun, S. Rappoport, R. Zusman [et al.] // Materials Letters. – 1990. – V. 10, № 1-2. – P. 1–5.

30. Sol-gel encapsulation methods for biosensors / B. C. Dave, B. Dunn, J. S. Valentine, J. I. Zink // Analytical Chemistry. – 1994. – V. 66, № 22. – P. 1120A–1127A.

31. Organically modified sol-gel sensors / O. Lev, M. Tsionsky, L. Rabinovich [et al.] // Analytical Chemistry. – 1995. – V. 67, № 1. – P. 22–30.

32. Enzymes and Other Proteins Entrapped in Sol-Gel Materials / D. Avnir, S. Braun, O. Lev, M. Ottolenghi // Chemistry of Materials. – 1994. – V. 6, № 10. – P. 1605–1614.

33. Kandimalla Vivek. Immobilization of Biomolecules in Sol–Gels: Biological and Analytical Applications / V. Kandimalla, V. Tripathi, H. Ju // Critical Reviews in Analytical Chemistry. – 2006. – V. 36, № 2. – P. 73–106.

34. Heme proteins sequestered in silica sol–gels using surfactants feature direct electron transfer and peroxidase activity / O. Y. Nadzhafova, V. N. Zaitsev, M. V Drozdova [et al.] // Electrochemistry Communications. – 2004. – V. 6, № 2. – P. 205–209.

35. Surfactant-Induced Modification of Dopants Reactivity in Sol−Gel Matrixes / C. Rottman, G. Grader, Y. De Hazan [et al.] // Journal of the American Chemical Society. – 1999. – V. 121, № 37. – P. 8533–8543.

36. Electroanalytical properties of haemoglobin in silica-nanocomposite films electrogenerated on pyrolitic graphite electrode / T. Rozhanchuk, O. Tananaiko, I. Mazurenko [et al.] // Journal of Electroanalytical Chemistry. – 2009. – V. 625, № 1. – P. 33–39.

37. Brinker C. Jeffrey. Sol-Gel Science: the physics and chemistry of sol-gel processing / C. J. Brinker, G. W. Scherer. – San Diego : Academic Press, 1990. – P. 912.

38. Wang Joseph. Sol-gel materials for electrochemical biosensors / J. Wang // Analytica Chimica Acta. – 1999. – V. 399, № 1-2. – P. 21–27.

39. Flora Kulwinder K. Characterization of the Microenvironments of PRODAN Entrapped in Tetraethyl Orthosilicate Derived Glasses / K. K. Flora, J. D. Brennan // The Journal of Physical Chemistry B. – 2001. – V. 105, № 48. – P. 12003–12010.

40. Pankratov I. Sol-gel derived renewable-surface biosensors / I. Pankratov, O. Lev // Journal of Electroanalytical Chemistry. – 1995. – V. 393, № 1-2. – P. 35–41.

41. Gun J. Sol-gel derived, ferrocenyl-modified silicate-graphite electrode: Wiring of glucose oxidase / J. Gun, O. Lev // Analytica Chimica Acta. – 1996. – V. 336. – P. 95–106.

42. Gold nanoparticles-mesoporous silica composite used as an enzyme immobilization matrix for amperometric glucose biosensor construction / Y. Bai, H.

Yang, W. Yang [et al.] // Sensors and Actuators B: Chemical. – 2007. – V. 124, № 1. – P. 179–186.

43. Covalent immobilization of an enzyme (glucose oxidase) onto a carbon sol–gel silicate composite surface as a biosensing platform / X. Yang, L. Hua, H. Gong, S. N. Tan // Analytica Chimica Acta. – 2003. – V. 478, № 1. – P. 67–75.

44. Lin Cheng-Li. Amperometric L-lactate sensor based on sol-gel processing of an enzyme-linked silicon alkoxide. / C.-L. Lin, C.-L. Shih, L.-K. Chau // Analytical Chemistry. – 2007. – V. 79, № 10. – P. 3757–3763.

45. Glucose Biosensor Based on a Sol-Gel-Derived Platform / U. Narang, P. N. Prasad, F. V. Bright [et al.] // Analytical Chemistry. – 1994. – V. 66, № 19. – P. 3139–3144.

46. Immobilization and Characterization of Lactate Dehydrogenase on TEOS Derived Sol-Gel Films / K. Ramanathan, M. Kamalasanan, B. Malhotra [et al.] // Journal of Sol-Gel Science and Technology. – 1997. – V. 10, № 3. – P. 309–316.

47. Immobilization of lactate dehydrogenase on tetraethylorthosilicate-derived sol-gel films for application to lactate biosensor. / A. Chaubey, M. Gerard, V. S. Singh, B. D. Malhotra // Applied Biochemistry and Biotechnology. – 2001. – V. 96, № 1-3. – P. 293–301.

48. Sol-gel based amperometric biosensor incorporating an osmium redox polymer as mediator for detection of L-lactate. / T. M. Park, E. I. Iwuoha, M. R. Smyth [et al.] // Talanta. – 1997. – V. 44, № 6. – P. 973–978.

49. Kane Stephen A. Development of a sol–gel based amperometric biosensor for the determination of phenolics† / S. A. Kane, E. I. Iwuoha, M. R. Smyth // The Analyst. – 1998. – V. 123, № 10. – P. 2001–2006.

50. Park Tae-Myung. Development of a sol-gel enzyme inhibition-based amperometric biosensor for cyanide / T.-M. Park, E. I. Iwuoha, M. R. Smyth // Electroanalysis. – 1997. – V. 9, № 14. – P. 1120–1123.

51. Review of sol-gel thin film formation / C. J. Brinker, A. J. Hurd, P. R. Schunk [et al.] // Journal of Non-Crystalline Solids. – 1992. – V. 147-148. – P. 424–436.

52. Shacham Ronen. Electrodeposition of Methylated Sol-Gel Films on Conducting Surfaces / R. Shacham, D. Avnir, D. Mandler // Advanced Materials. – 1999. – V. 11, № 5. – P. 384–388.

53. Shacham Ronen. Pattern recognition in oxides thin-film electrodeposition: Printed circuits / R. Shacham, D. Mandler, D. Avnir // Comptes Rendus Chimie. – 2010. – V. 13, № 1-2. – P. 237–241.

54. Electrodeposition of Porous Silicate Films from Ludox Colloidal Silica / M. M. Collinson, N. Moore, P. N. Deepa, M. Kanungo // Langmuir : the ACS Journal of Surfaces and Colloids. – 2003. – V. 19, № 18. – P. 7669–7672.

55. Electrochemically deposited sol-gel-derived silicate films as a viable alternative in thin-film design. / P. N. Deepa, M. Kanungo, G. Claycomb [et al.] // Analytical Chemistry. – 2003. – V. 75, № 20. – P. 5399–5405.

56. Electrogeneration of ultra-thin silica films for the functionalization of macroporous electrodes / F. Qu, R. Nasraoui, M. Etienne [et al.] // Electrochemistry Communications. – 2011. – V. 13, № 2. – P. 138–142.

57. Electrochemically assisted self-assembly of mesoporous silica thin films. / A. Walcarius, E. Sibottier, M. Etienne, J. Ghanbaja // Nature Materials. – 2007. – V. 6, № 8. – P. 602–608.

58. A glucose biosensor based on chitosan-glucose oxidase-gold nanoparticles biocomposite formed by one-step electrodeposition. / X.-L. Luo, J.-J. Xu, Y. Du, H.-Y. Chen // Analytical Biochemistry. – 2004. – V. 334, № 2. – P. 284–289.

59. One-Step Immobilization of Glucose Oxidase in a Silica Matrix on a Pt Electrode by an Electrochemically Induced Sol− Gel Process / W.-Z. Jia, K. Wang, Z.-J. Zhu [et al.] // Langmuir : the ACS Journal of Surfaces and Colloids. – 2007. – V. 23, № 23. – P. 11896–11900.

60. Nadzhafova Oksana. Direct electrochemistry of hemoglobin and glucose oxidase in electrodeposited sol–gel silica thin films on glassy carbon / O. Nadzhafova, M. Etienne, A. Walcarius // Electrochemistry Communications. – 2007. – V. 9, № 5. – P. 1189–1195.

61. Simple approach for efficient encapsulation of enzyme in silica matrix with retained bioactivity. / S. Yang, W. Jia, Q.-Y. Qian [et al.] // Analytical Chemistry. – 2009. – V. 81, № 9. – P. 3478–3484.

62. Wilson R. Glucose oxidase: an ideal enzyme / R. Wilson, A. P. F. Turner // Biosensors and Bioelectronics. – 1992. – V. 7, № 3. – P. 165–185.

63. Kanungo Mandakini. Quantitative Control over Electrodeposition of Silica Films onto Single-Walled Carbon Nanotube Surfaces / M. Kanungo, H. S. Isaacs, S. S. Wong // The Journal of Physical Chemistry C. – 2007. – V. 111, № 48. – P. 17730–17742.

64. Schwamborn Stefanie. Local electrocatalytic induction of sol–gel deposition at Pt nanoparticles / S. Schwamborn, M. Etienne, W. Schuhmann // Electrochemistry Communications. – 2011. – V. 13, № 8. – P. 759–762.

65. Pandey Pratibha. Prospects of Nanomaterials in Biosensors / P. Pandey, M. Datta, B. D. Malhotra // Analytical Letters. – 2008. – V. 41, № 2. – P. 159–209.

66. Asefa Tewodros. Recent advances in nanostructured chemosensors and biosensors. / T. Asefa, C. T. Duncan, K. K. Sharma // The Analyst. – 2009. – V. 134, № 10. – P. 1980–1990.

67. Wang Joseph. Nanomaterial-based electrochemical biosensors / J. Wang // The Analyst. – 2005. – V. 130, № 4. – P. 421.

68. Electrochemical nanobiosensors / M. Pumera, S. Sánchez, I. Ichinose, J. Tang // Sensors and Actuators B: Chemical. – 2007. – V. 123, № 2. – P. 1195–1205.

69. Valentini F. Nanomaterials and Analytical Chemistry / F. Valentini, G. Palleschi // Analytical Letters. – 2008. – V. 41, № 4. – P. 479–520.

70. Functional One-Dimensional Nanomaterials: Applications in Nanoscale Biosensors / N. Chopra, V. G. Gavalas, L. G. Bachas, B. J. Hinds // Analytical Letters. – 2007. – V. 40, № 11. – P. 2067–2096.

71. Electric field effect in atomically thin carbon films. / K. S. Novoselov, A. K. Geim, S. V Morozov [et al.] // Science (New York, N.Y.). – 2004. – V. 306, № 5696. – P. 666–669.

72. Graphene for electrochemical sensing and biosensing / M. Pumera, A. Ambrosi, A. Bonanni [et al.] // TrAC Trends in Analytical Chemistry. – 2010. – V. 29, № 9. – P. 954–965.

73. Katz Eugenii. Electroanalytical and Bioelectroanalytical Systems Based on Metal and Semiconductor Nanoparticles / E. Katz, I. Willner, J. Wang // Electroanalysis. – 2004. – V. 16, № 12. – P. 19–44.

74. Wang Fang. Electrochemical sensors based on metal and semiconductor nanoparticles / F. Wang, S. Hu // Microchimica Acta. – 2009. – V. 165, № 1-2. – P. 1–22.

75. Cheng Wenlong. Colloid chemical approach to nanoelectrode ensembles with highly controllable active area fraction. / W. Cheng, S. Dong, E. Wang // Analytical Chemistry. – 2002. – V. 74, № 15. – P. 3599–3604.

76. Pingarrón José M. Gold nanoparticle-based electrochemical biosensors / J. M. Pingarrón, P. Yáñez-Sedeño, A. González-Cortés // Electrochimica Acta. – 2008. – V. 53, № 19. – P. 5848–5866.

77. Guo Shaojun. Synthesis and electrochemical applications of gold nanoparticles. / S. Guo, E. Wang // Analytica Chimica Acta. – 2007. – V. 598, № 2. – P. 181–192.

78. Amperometric glucose biosensor based on integration of glucose oxidase with platinum nanoparticles/ordered mesoporous carbon nanocomposite / X. Jiang, Y. Wu, X. Mao [et al.] // Sensors and Actuators B: Chemical. – 2010. – V. 153, № 1. – P. 158–163.

79. Electrochemical biosensing platforms using platinum nanoparticles and carbon nanotubes. / S. Hrapovic, Y. Liu, K. B. Male, J. H. T. Luong // Analytical Chemistry. – 2004. – V. 76, № 4. – P. 1083–1088.

80. Shao Minhua. Electrocatalysis on platinum nanoparticles: particle size effect on oxygen reduction reaction activity. / M. Shao, A. Peles, K. Shoemaker // Nano Letters. – 2011. – V. 11, № 9. – P. 3714–3719.

81. Patolsky Fernando. Nanowire-Based Biosensors / F. Patolsky, G. Zheng, C. M. Lieber // Analytical Chemistry. – 2006. – V. 78, № 13. – P. 4260–4269.

82. Platinum nanowire nanoelectrode array for the fabrication of biosensors. / M. Yang, F. Qu, Y. Lu [et al.] // Biomaterials. – 2006. – V. 27, № 35. – P. 5944–5950.

83. Electrochemical biosensing utilizing synergic action of carbon nanotubes and platinum nanowires prepared by template synthesis. / F. Qu, M. Yang, G. Shen, R. Yu // Biosensors and Bioelectronics. – 2007. – V. 22, № 8. – P. 1749–1755.

84. Iijima Sumio. Helical microtubules of graphitic carbon / S. Iijima // Nature. – 1991. – V. 354, № 6348. – P. 56–58.

85. New materials for electrochemical sensing VI: Carbon nanotubes / A. Merkoci, M. Pumera, X. Llopis [et al.] // TrAC Trends in Analytical Chemistry. – 2005. – V. 24, № 9. – P. 826–838.

86. Agüí Lourdes. Role of carbon nanotubes in electroanalytical chemistry: a review. / L. Agüí, P. Yáñez-Sedeño, J. M. Pingarrón // Analytica Chimica Acta. – 2008. – V. 622, № 1-2. – P. 11–47.

87. Wang Joseph. Carbon-Nanotube Based Electrochemical Biosensors: A Review / J. Wang // Electroanalysis. – 2005. – V. 17, № 1. – P. 7–14.

88. Wang Joseph. Carbon-nanotube-modified glassy carbon electrodes for amplified label-free electrochemical detection of DNA hybridization / J. Wang, A.-N. Kawde, M. Musameh // The Analyst. – 2003. – V. 128, № 7. – P. 912–916.

89. Low-potential stable NADH detection at carbon-nanotube-modified glassy carbon electrodes / M. Musameh, J. Wang, A. Merkoci, Y. Lin // Electrochemistry Communications. – 2002. – V. 4, № 10. – P. 743–746.

90. Protein electrochemistry using aligned carbon nanotube arrays. / J. J. Gooding, R. Wibowo, J. Liu [et al.] // Journal of the American Chemical Society. – 2003. – V. 125, № 30. – P. 9006–9007.

91. Patolsky Fernando. Long-range electrical contacting of redox enzymes by SWCNT connectors. / F. Patolsky, Y. Weizmann, I. Willner // Angewandte Chemie (International Ed. in English). – 2004. – V. 43, № 16. – P. 2113–2117.

92. Vertically Aligned Carbon Nanotube Electrodes Directly Grown on a Glassy Carbon Electrode. / S. Park, P. Dong-Won, C.-S. Yang [et al.] // ACS Nano. – 2011. – № 9. – P. 7061–7068.

93. Carbon nanotube purification: preparation and characterization of carbon nanotube paste electrodes. / F. Valentini, A. Amine, S. Orlanducci [et al.] // Analytical Chemistry. – 2003. – V. 75, № 20. – P. 5413–5421.

94. Rubianes María D. Enzymatic Biosensors Based on Carbon Nanotubes Paste Electrodes / M. D. Rubianes, G. A. Rivas // Electroanalysis. – 2005. – V. 17, № 1. – P. 73–78.

95. Wang Joseph. Carbon nanotube/teflon composite electrochemical sensors and biosensors. / J. Wang, M. Musameh // Analytical Chemistry. – 2003. – V. 75, № 9. – P. 2075–2079.

96. Carbon nanotube–polymer composites: Chemistry, processing, mechanical and electrical properties / Z. Spitalsky, D. Tasis, K. Papagelis, C. Galiotis // Progress in Polymer Science. – 2010. – V. 35, № 3. – P. 357–401.

97. Habibi Biuck. Simultaneous determination of acetaminophen and dopamine using SWCNT modified carbon–ceramic electrode by differential pulse voltammetry / B. Habibi, M. Jahanbakhshi, M. H. Pournaghi-Azar // Electrochimica Acta. – 2011. – V. 56, № 7. – P. 2888–2894.

98. Carbon nanotubes for electrochemical biosensing. / G. A. Rivas, M. D. Rubianes, M. C. Rodríguez [et al.] // Talanta. – 2007. – V. 74, № 3. – P. 291–307.

99. Advances in carbon nanotube based electrochemical sensors for bioanalytical applications. / S. K. Vashist, D. Zheng, K. Al-Rubeaan [et al.] // Biotechnology Advances. – 2011. – V. 29, № 2. – P. 169–188.

100. Lin Yuehe. Carbon nanotubes (CNTs) for the development of electrochemical biosensors / Y. Lin, W. Yantasee, J. Wang // Frontiers in Bioscience. – 2005. – V. 10, № 1-3. – P. 492–505.

101. Gooding John Justin. Nanostructuring electrodes with carbon nanotubes: A review on electrochemistry and applications for sensing / J. J. Gooding // Electrochimica Acta. – 2005. – V. 50, № 15. – P. 3049–3060.

102. Fernández-Abedul M Teresa. Carbon nanotubes (CNTs)-based electroanalysis. / M. T. Fernández-Abedul, A. Costa-García // Analytical and Bioanalytical Chemistry. – 2008. – V. 390, № 1. – P. 293–298.

103. Boccaccini Aldo R. Application of electrophoretic and electrolytic deposition techniques in ceramics processing / A. R. Boccaccini, I. Zhitomirsky // Current Opinion in Solid State and Materials Science. – 2002. – V. 6, № 3. – P. 251–260.

104. Electrophoretic deposition of biomaterials. / A. R. Boccaccini, S. Keim, R. Ma [et al.] // Journal of the Royal Society, Interface / the Royal Society. – 2010. – № May.

105. Du Chunsheng. Preparation and preliminary property study of carbon nanotubes films by electrophoretic deposition / C. Du, D. Heldbrant, N. Pan // Materials Letters. – 2002. – V. 57, № 2. – P. 434–438.

106. Characterisation of carbon nanotube films deposited by electrophoretic deposition / J. Cho, K. Konopka, K. Rozniatowski [et al.] // Carbon. – 2009. – V. 47, № 1. – P. 58–67.

107. Electrophoretic deposition of carbon nanotubes / A. R. Boccaccini, J. Cho, J. Roether [et al.] // Carbon. – 2006. – V. 44, № 15. – P. 3149–3160.

108. Cho Johann. Ceramic matrix composites containing carbon nanotubes / J. Cho, A. R. Boccaccini, M. S. P. Shaffer // Journal of Materials Science. – 2009. – V. 44, № 8. – P. 1934–1951.

109. Qin Yuxiang. Field emission properties of electrophoretic deposition carbon nanotubes film / Y. Qin, M. Hu // Applied Surface Science. – 2009. – V. 255, № 17. – P. 7618–7622.

110. Jung S. Horizontally aligned carbon nanotube field emitters fabricated on ITO glass substrates / S. Jung, H. Jung, J. Suh // Carbon. – 2008. – V. 46, № 14. – P. 1973–1977.

111. Bakhoum Ezzat G. Electrophoretic coating of carbon nanotubes for high energy-density capacitor applications / E. G. Bakhoum, M. H. M. Cheng // Journal of Applied Physics. – 2009. – V. 105, № 10. – P. 104314.

112. Wang Yaohui. Electrophoretic deposition of manganese dioxide-multiwalled carbon nanotube composites for electrochemical supercapacitors. / Y. Wang, I. Zhitomirsky // Langmuir : the ACS Journal of Surfaces and Colloids. – 2009. – V. 25, № 17. – P. 9684–9689.

113. Single-wall carbon nanotube-based proton exchange membrane assembly for hydrogen fuel cells. / G. Girishkumar, M. Rettker, R. Underhile [et al.] // Langmuir : the ACS Journal of Surfaces and Colloids. – 2005. – V. 21, № 18. – P. 8487–8494.

114. Girishkumar G. Carbon Nanostructures in Portable Fuel Cells: Single-Walled Carbon Nanotube Electrodes for Methanol Oxidation and Oxygen Reduction / G. Girishkumar, K. Vinodgopal, P. V. Kamat // The Journal of Physical Chemistry B. – 2004. – V. 108, № 52. – P. 19960–19966.

115. Membrane-less and mediator-free enzymatic biofuel cell using carbon nanotube/porous silicon electrodes / S. Wang, F. Yang, M. Silva [et al.] // Electrochemistry Communications. – 2009. – V. 11, № 1. – P. 34–37.

116. Carbon Nanotube Coatings on Bioglass-Based Tissue Engineering Scaffolds / A. R. Boccaccini, F. Chicatun, J. Cho [et al.] // Advanced Functional Materials. – 2007. – V. 17, № 15. – P. 2815–2822.

117. Electrophoretic deposition of carbon nanotubes and bioactive glass particles for bioactive composite coatings / M. Charlotte Schausten, D. Meng, R. Telle, A. R. Boccaccini // Ceramics International. – 2010. – V. 36, № 1. – P. 307–312.

118. Minnikanti Saugandhika. Electrochemical characterization of multi-walled carbon nanotube coated electrodes for biological applications / S. Minnikanti, P. Skeath, N. Peixoto // Carbon. – 2009. – V. 47, № 3. – P. 884–893.

119. Polyaniline-carbon nanotube composite film for cholesterol biosensor. / C. Dhand, S. K. Arya, M. Datta, B. D. Malhotra // Analytical Biochemistry. – 2008. – V. 383, № 2. – P. 194–199.

120. Polyaniline/Single-Walled Carbon Nanotubes Composite Based Triglyceride Biosensor / C. Dhand, P. R. Solanki, M. Datta, B. D. Malhotra // Electroanalysis. – 2010. – V. 22, № 22. – P. 2683–2693.

121. Clark Leland C. Electrode systems for continuous monitoring in cardiovascular surgery / L. C. Clark, C. Lyons // Annals of the New York Academy of Sciences. – 1962. – V. 102, № 1. – P. 29–45.

122. Wang Joseph. Glucose Biosensors: 40 Years of Advances and Challenges / J. Wang // Electroanalysis. – 2001. – V. 13, № 12. – P. 983–988.

123. Amperometric Biosensors, in: Bioelectrochemistry, John Wiley & Sons, 2012. p. 411.

124. Assessment of the lactate biosensor methodology / B. Detry, W. Nullens, M. L. Cao [et al.] // European Respiratory Journal. – 1998. – V. 11, № 1. – P. 183–187.

125. Design and characterization of a lactate biosensor based on immobilized lactate oxidase onto gold surfaces / A. Parra, E. Casero, L. Vázquez [et al.] // Analytica Chimica Acta. – 2006. – V. 555, № 2. – P. 308–315.

126. Sol-gel immobilization of lactate oxidase from organic solvent: toward the advanced lactate biosensor. / E. I. Yashina, A. V Borisova, E. E. Karyakina [et al.] // Analytical Chemistry. – 2010. – V. 82, № 5. – P. 1601–1604.

127. Development of long life lactate sensor using thermostable mutant lactate oxidase / H. Minagawa, N. Nakayama, T. Matsumoto, N. Ito // Biosensors and Bioelectronics. – 1998. – V. 13, № 3-4. – P. 313–318.

128. Investigation into immobilisation of lactate oxidase to improve stability / B. Lillis, C. Grogan, H. Berney, W. . Lane // Sensors and Actuators B: Chemical. – 2000. – V. 68, № 1-3. – P. 109–114.

129. Phillips Melissa M. Analytical approaches to determination of total choline in foods and dietary supplements. / M. M. Phillips // Analytical and Bioanalytical Chemistry. – 2012. – V. 403, № 8. – P. 2103–2112.

130. Amperometric determination of choline released from rat submandibular gland acinar cells using a choline oxidase biosensor. / S. S. Razola, S. Pochet, K. Grosfils,

J. M. Kauffmann // Biosensors & Bioelectronics. – 2003. – V. 18, № 2-3. – P. 185–191.

131. Mitchell Kim M. Acetylcholine and choline amperometric enzyme sensors characterized in vitro and in vivo. / K. M. Mitchell // Analytical Chemistry. – 2004. – V. 76, № 4. – P. 1098–1106.

132. Fennouh Souad. Increased paraoxon detection with solvents using acetylcholinesterase inactivation measured with a choline oxidase biosensor / S. Fennouh, V. Casimiri, C. Burstein // Biosensors and Bioelectronics. – 1997. – V. 12, № 2. – P. 97–104.

133. Kok Fatma N. Determination of binary pesticide mixtures by an acetylcholinesterase–choline oxidase biosensor / F. N. Kok, V. Hasirci // Biosensors and Bioelectronics. – 2004. – V. 19, № 7. – P. 661–665.

134. Applications of laccases and tyrosinases (phenoloxidases) immobilized on different supports: a review / N. Durán, M. A Rosa, A. D'Annibale, L. Gianfreda // Enzyme and Microbial Technology. – 2002. – V. 31, № 7. – P. 907–931.

135. Tyrosinase/laccase bienzyme biosensor for amperometric determination of phenolic compounds / J. Kochana, P. Nowak, A. Jarosz-Wilkolazka, M // Microchemical Journal. – 2008. – V. 89, № 2. – P. 171–174.

136. Development of a tyrosinase biosensor based on gold nanoparticles-modified glassy carbon electrodes Application to the measurement of a bioelectrochemical polyphenols index in wines / V. Carralero Sanz, M. L. Mena, A. Gonzalez-Cortes [et al.] // Analytica Chimica Acta. – 2005. – V. 528, № 1. – P. 1–8.

137. A comparative study of immobilization methods of a tyrosinase enzyme on electrodes and their application to the detection of dichlorvos organophosphorus insecticide. / J. C. Vidal, S. Esteban, J. Gil, J. R. Castillo // Talanta. – 2006. – V. 68, № 3. – P. 791–799.

138. Cholesterol oxidase: sources, physical properties and analytical applications. / J. MacLachlan, A T. Wotherspoon, R. O. Ansell, C. J. Brooks // The Journal of Steroid Biochemistry and Molecular Biology. – 2000. – V. 72, № 5. – P. 169–195.

139. An amperometric cholesterol biosensor based on multiwalled carbon nanotubes and organically modified sol-gel/chitosan hybrid composite film. / X. Tan, M. Li, P. Cai [et al.] // Analytical Biochemistry. – 2005. – V. 337, № 1. – P. 111–120.

140. Fabrication of novel chitosan nanofiber/gold nanoparticles composite towards improved performance for a cholesterol sensor / P. Gomathi, D. Ragupathy, J. H. Choi [et al.] // Sensors and Actuators B: Chemical. – 2011. – V. 153, № 1. – P. 44–49.

141. Multi-walled carbon nanotubes/sol–gel-derived silica/chitosan nanobiocomposite for total cholesterol sensor / P. R. Solanki, A. Kaushik, A. A. Ansari [et al.] // Sensors and Actuators B: Chemical. – 2009. – V. 137, № 2. – P. 727–735.

142. Tombelli S. Electrochemical biosensors for biogenic amines: a comparison between different approaches / S. Tombelli, M. Mascini // Analytica Chimica Acta. – 1998. – V. 358, № 3. – P. 277–284.

143. Amine Oxidase Based Amperometric Biosensors forHistamine Detection / M. Niculescu, I. Frébort, P. Peč [et al.] // Electroanalysis. – 2000. – V. 12, № 5. – P. 369–375.

144. Telsnig Dietlind. Development of a Voltammetric Amine Oxidase-Modified Biosensor for the Determination of Biogenic Amines in Food / D. Telsnig, A. Terzic, T. Krenn // International Journal of Electrochemical Science. – 2012. – V. 7, № 8. – P. 6893–6903.

145. Ethanol biosensors based on alcohol oxidase. / A. M. Azevedo, D. M. F. Prazeres, J. M. S. Cabral, L. P. Fonseca // Biosensors & Bioelectronics. – 2005. – V. 21, № 2. – P. 235–247.

146. Akyilmaz E. A mushroom (Agaricus bisporus) tissue homogenate based alcohol oxidase electrode for alcohol determination in serum. / E. Akyilmaz, E. Dinckaya // Talanta. – 2000. – V. 53, № 3. – P. 505–509.

147. Boujtita M. Development of a disposable ethanol biosensor based on a chemically modified screen-printed electrode coated with alcohol oxidase for the

analysis of beer. / M. Boujtita, J. P. Hart, R. Pittson // Biosensors & Bioelectronics. – 2000. – V. 15, № 5-6. – P. 257–263.

148. Amperometric biosensor for ethanol detection based on alcohol oxidase immobilised within electrochemically deposited Resydrol film / L. Shkotova, A Soldatkin, M. Gonchar [et al.] // Materials Science and Engineering: C. – 2006. – V. 26, № 2-3. – P. 411–414.

149. Real-time quantification of methanol in plants using a hybrid alcohol oxidase-peroxidase biosensor. / T. Hasunuma, S. Kuwabata, E. Fukusaki, A. Kobayashi // Analytical Chemistry. – 2004. – V. 76, № 5. – P. 1500–1506.

150. Screen-printed biosensors using different alcohol oxidases / N. G. Patel, S. Meier, K. Cammann, G.-C. Chemnitius // Sensors and Actuators B: Chemical. – 2001. – V. 75, № 1-2. – P. 101–110.

151. A biosensor based on co-immobilized L-glutamate oxidase and L-glutamate dehydrogenase for analysis of monosodium glutamate in food. / A. K. Basu, P. Chattopadhyay, U. Roychudhuri, R. Chakraborty // Biosensors & Bioelectronics. – 2006. – V. 21, № 10. – P. 1968–1972.

152. Amperometric Biosensors for On-Line Monitoring of Extracellular Glucose and Glutamate in the Brain / E. Zilkha, A. Koshy, T. P. Obrenovitch [et al.] // Analytical Letters. – 1994. – V. 27, № 3. – P. 453–473.

153. Ultramicrobiosensor for the Selective Detection of Glutamate / O. M. Schuvailo, S. Gáspár, A. P. Soldatkin, E. Csöregi // Electroanalysis. – 2007. – V. 19, № 1. – P. 71–78.

154. Ammam Malika. Highly sensitive and selective glutamate microbiosensor based on cast polyurethane/AC-electrophoresis deposited multiwalled carbon nanotubes and then glutamate oxidase/electrosynthesized polypyrrole/Pt electrode. / M. Ammam, J. Fransaer // Biosensors and Bioelectronics. – 2010. – V. 25, № 7. – P. 1597–1602.

155. Li Jianping. A Cholesterol Biosensor Based on Entrapment of Cholesterol Oxidase in a Silicic Sol-Gel Matrix at a Prussian Blue Modified Electrode / J. Li, T. Peng, Y. Peng // Electroanalysis. – 2003. – V. 15, № 12. – P. 1031–1037.

156. Silica-Polyaniline Based Bienzyme Cholesterol Biosensor: Fabrication and Characterization / K. M. Manesh, P. Santhosh, A. I. Gopalan, K.-P. Lee // Electroanalysis. – 2010. – V. 22, № 20. – P. 2467–2474.

157. Tiwari Ashutosh. Electrochemical Study of Chitosan-SiO 2 -MWNT Composite Electrodes for the Fabrication of Cholesterol Biosensors / A. Tiwari, S. Gong // Electroanalysis. – 2008. – V. 20, № 19. – P. 2119–2126.

158. Cox James A. Evaluation of Polycation-Stabilized Lactate Oxidase in a Silica Sol-Gel as a Biosensor Platform / J. A. Cox, P. M. Hensley, C. L. Loch // Microchimica Acta. – 2003. – V. 142, № 1-2. – P. 1–5.

159. Development of an amperometric l-lactate biosensor based on l-lactate oxidase immobilized through silica sol–gel film on multi-walled carbon nanotubes/platinum nanoparticle modified glassy carbon electrode / J. Huang, J. Li, Y. Yang [et al.] // Materials Science and Engineering: C. – 2008. – V. 28, № 7. – P. 1070–1075.

160. Silica sol–gel immobilized amperometric biosensor for the determination of phenolic compounds / J. Li, L. S. Chia, N. K. Goh, S. N. Tan // Analytica Chimica Acta. – 1998. – V. 362, № 2-3. – P. 203–211.

161. Wang Bingquan. Organic-phase enzyme electrode for phenolic determination based on a functionalized sol–gel composite / B. Wang, S. Dong // Journal of Electroanalytical Chemistry. – 2000. – V. 487, № 1. – P. 45–50.

162. Wang B. Silica sol-gel composite film as an encapsulation matrix for the construction of an amperometric tyrosinase-based biosensor. / B. Wang, J. Zhang, S. Dong // Biosensors & Bioelectronics. – 2000. – V. 15, № 7-8. – P. 397–402.

163. Chitosan-based tyrosinase optical phenol biosensor employing hybrid nafion/sol-gel silicate for MBTH immobilization. / J. Abdullah, M. Ahmad, L. Y. Heng [et al.] // Talanta. – 2006. – V. 70, № 3. – P. 527–532.

164. Audebert P. Electrochemical probing of the activity of glucose oxidase embedded sol-gel matrixes / P. Audebert, C. Demaille, C. Sanchez // Chemistry of Materials. – 1993. – V. 5, № 7. – P. 911–913.

165. Amperometric glucose biosensor based on sol-gel organic-inorganic hybrid material. / B. Wang, B. Li, Q. Deng, S. Dong // Analytical Chemistry. – 1998. – V. 70, № 15. – P. 3170–3174.

166. Li Tong. Development of an amperometric biosensor based on glucose oxidase immobilized through silica sol–gel film onto Prussian Blue modified electrode / T. Li, Z. Yao, L. Ding // Sensors and Actuators B: Chemical. – 2004. – V. 101, № 1-2. – P. 155–160.

167. Salimi Abdollah. Glucose biosensor prepared by glucose oxidase encapsulated sol-gel and carbon-nanotube-modified basal plane pyrolytic graphite electrode. / A. Salimi, R. G. Compton, R. Hallaj // Analytical Biochemistry. – 2004. – V. 333, № 1. – P. 49–56.

168. Amperometric aqueous sol–gel biosensor for low-potential stable choline detection at multi-wall carbon nanotube modified platinum electrode / Z. Song, J.-D. Huang, B.-Y. Wu [et al.] // Sensors and Actuators B: Chemical. – 2006. – V. 115, № 2. – P. 626–633.

169. Amperometric acetylcholine biosensor based on self-assembly of gold nanoparticles and acetylcholinesterase on the sol-gel/multi-walled carbon nanotubes/choline oxidase composite-modified platinum electrode. / S. Hou, Z. Ou, Q. Chen, B. Wu // Biosensors & Bioelectronics. – 2012. – V. 33, № 1. – P. 44–49.

170. Karyakin Arkady A. Prussian Blue-based `artificial peroxidase' as a transducer for hydrogen peroxide detection. Application to biosensors / A. A. Karyakin, E. E. Karyakina // Sensors and Actuators B: Chemical. – 1999. – V. 57, № 1-3. – P. 268–273.

171. Permselective Behavior of an Electrosynthesized, Nonconducting Thin Film of Poly(2-naphthol) and Its Application to Enzyme Immobilization / R. Ciriello, T. R. I. Cataldi, D. Centonze, A. Guerrieri // Electroanalysis. – 2000. – V. 12, № 11. – P. 825–830.

172. Selective Permeation of Hydrogen Peroxide through Polyelectrolyte Multilayer Films and Its Use for Amperometric Biosensors / T. Hoshi, H. Saiki, S. Kuwazawa [et al.] // Analytical Chemistry. – 2001. – V. 73, № 21. – P. 5310–5315.

173. Application of MnO2 nanoparticles as an eliminator of ascorbate interference to amperometric glucose biosensors / J.-J. Xu, X.-L. Luo, Y. Du, H.-Y. Chen // Electrochemistry Communications. – 2004. – V. 6, № 11. – P. 1169–1173.

174. Amperometric biosensors employing an insoluble oxidant as an interference-removing agent / S. H. Choi, S. D. Lee, J. H. Shin [et al.] // Analytica Chimica Acta. – 2002. – V. 461, № 2. – P. 251–260.

175. Zhang Chengxiao. An amperometric glucose biosensor incorporating a permeable pre-oxidation layer / C. Zhang, K. Wang // Analytical Letters. – 2002. – V. 35, № 5. – P. 869–880.

176. Zhao Min. Solution to the Problem of Interferences in Electrochemical Sensors Using the Fill-and-Flow Channel Biosensor / M. Zhao, D. B. Hibbert, J. J. Gooding // Analytical Chemistry. – 2003. – V. 75, № 3. – P. 593–600.

177. Palmisano Francesco. Ascorbic acid interferences in hydrogen peroxide detecting biosensors based on electrochemically immobilized enzymes / F. Palmisano, P. G. Zambonin // Analytical Chemistry. – 1993. – V. 65, № 19. – P. 2690–2692.

178. Hall Elizabeth A. H. Redox enzyme linked electrochemical sensors: Theory meets practice / E. A. H. Hall, J. J. Gooding, C. E. Hall // Mikrochimica Acta. – 1995. – V. 121, № 1-4. – P. 119–145.

179. Gorton L. Carbon paste electrodes modified with enzymes, tissues, and cells / L. Gorton // Electroanalysis. – 1995. – V. 7, № 1. – P. 23–45.

180. Remarkably selective metallized-carbon amperometric biosensors / J. Wang, F. Lu, L. Angnes [et al.] // Analytica Chimica Acta. – 1995. – V. 305, № 1-3. – P. 3–7.

181. Zhang Yanan. Electrochemical oxidation of H2O2 on Pt and Pt + Ir electrodes in physiological buffer and its applicability to H2O2-based biosensors / Y. Zhang, G. S.

Wilson // Journal of Electroanalytical Chemistry. – 1993. – V. 345, № 1-2. – P. 253–271.

182. Electrochemical Behavior of H2O2 on Gold / M. Gerlache, Z. Senturk, G. Quarin, J.-M. Kauffmann // Electroanalysis. – 1997. – V. 9, № 14. – P. 1088–1092.

183. Application of Nanoparticles in Electrochemical Sensors and Biosensors / X. Luo, A. Morrin, A. J. Killard, M. R. Smyth // Electroanalysis. – 2006. – V. 18, № 4. – P. 319–326.

184. Welch Christine M. The use of nanoparticles in electroanalysis: a review. / C. M. Welch, R. G. Compton // Analytical and Bioanalytical Chemistry. – 2006. – V. 384, № 3. – P. 601–619.

185. Characterization of platinum nanoparticle-embedded carbon film electrode and its detection of hydrogen peroxide / T. You, O. Niwa, M. Tomita [et al.] // Analytical Chemistry. – 2003. – V. 75, № 9. – P. 2080–2085.

186. Wang Joseph. Solubilization of carbon nanotubes by Nafion toward the preparation of amperometric biosensors. / J. Wang, M. Musameh, Y. Lin // Journal of the American Chemical Society. – 2003. – V. 125, № 9. – P. 2408–2409.

187. Amperometric determination of L-malic acid in a flow injection analysis manifold using packed-bed enzyme reactors / M. I. Prodromidis, S. M. Tzouwara-Karayanni, M. I. Karayannis [et al.] // The Analyst. – 1996. – V. 121, № 4. – P. 435.

188. Lobo Maria Jesús. Amperometric biosensors based on NAD(P)-dependent dehydrogenase enzymes / M. J. Lobo, A. J. Miranda, P. Tuñón // Electroanalysis. – 1997. – V. 9, № 3. – P. 191–202.

189. Amperometric biosensor for lactate based on lactate dehydrogenase and Meldola Blue coimmobilized on multi-wall carbon-nanotube / A Pereira, M. Aguiar, A Kisner [et al.] // Sensors and Actuators B: Chemical. – 2007. – V. 124, № 1. – P. 269–276.

190. Determination of nano-molar levels of formaldehyde in drinking water using flow-injection system with immobilized formaldehyde dehydrogenase after off-line solid-phase extraction / N. Kiba, L. Sun, S. Yokose [et al.] // Analytica Chimica Acta. – 1999. – V. 378, № 1-3. – P. 169–175.

191. An electrochemical biosensor for formaldehyde / Y. Herschkovitz, I. Eshkenazi, C. . Campbell, J. Rishpon // Journal of Electroanalytical Chemistry. – 2000. – V. 491, № 1-2. – P. 182–187.

192. Bi-enzyme biosensor based on NAD+- and glutathione-dependent recombinant formaldehyde dehydrogenase and diaphorase for formaldehyde assay / O. Nikitina, S. Shleev, G. Gayda [et al.] // Sensors and Actuators B: Chemical. – 2007. – V. 125, № 1. – P. 1–9.

193. Reagentless amperometric formaldehyde-selective biosensors based on the recombinant yeast formaldehyde dehydrogenase. / O. Demkiv, O. Smutok, S. Paryzhak [et al.] // Talanta. – 2008. – V. 76, № 4. – P. 837–846.

194. Niculescu Mihaela. Glycerol Dehydrogenase Based Amperometric Biosensor for Monitoring of Glycerol in Alcoholic Beverages / M. Niculescu, S. Sigina, E. Csöregi // Analytical Letters. – 2003. – V. 36, № 9. – P. 1721–1737.

195. Eftekhari Ali. Glycerol biosensor based on glycerol dehydrogenase incorporated into polyaniline modified aluminum electrode using hexacyanoferrate as mediator / A. Eftekhari // Sensors and Actuators B: Chemical. – 2001. – V. 80, № 3. – P. 283–289.

196. Amperometric glyceride biosensor / V. Laurinavicius, B. Kurtinaitiene, V. Gureviciene [et al.] // Analytica Chimica Acta. – 1996. – V. 330, № 2-3. – P. 159–166.

197. Amperometric biosensor based on glycerol oxidase for glycerol determination / T. B. Goriushkina, L. V. Shkotova, G. Z. Gayda [et al.] // Sensors and Actuators B: Chemical. – 2010. – V. 144, № 2. – P. 361–367.

198. Amperometric detection of D-sorbitol with NAD+-D-sorbitol dehydrogenase modified carbon paste electrode / S. B. Saidman, M. J. Lobo-Castañón, A. Miranda- [et al.] // Analytica Chimica Acta. – 2000. – V. 424, № 1. – P. 45–50.

199. Campbell Carmen E. NADH Oxidation at the Honey-Comb Like Structure of Active Carbon: Coupled to Formaldehyde and Sorbitol Dehydrogenases / C. E. Campbell, J. Rishpon // Electroanalysis. – 2001. – V. 13, № 1. – P. 17–20.

200. Renewable dehydrogenase-based interfaces for bioelectronic applications. / B. L. Hassler, N. Kohli, J. G. Zeikus [et al.] // Langmuir : the ACS Journal of Surfaces and Colloids. – 2007. – V. 23, № 13. – P. 7127–7133.

201. A hyaluronic acid dispersed carbon nanotube electrode used for a mediatorless NADH sensing and biosensing / J. Filip, J. Sefčovičová, P. Tomčík [et al.] // Talanta. – 2011. – V. 84, № 2. – P. 355–361.

202. Electrochemically assisted deposition of sol–gel bio-composite with co-immobilized dehydrogenase and diaphorase / Z. Wang, M. Etienne, G.-W. Kohring [et al.] // Electrochimica Acta. – 2011. – V. 56, № 25. – P. 9032–9040.

203. Durable cofactor immobilization in sol-gel bio-composite thin films for reagentless biosensors and bioreactors using dehydrogenases. / Z. Wang, M. Etienne, F. Quilès [et al.] // Biosensors & Bioelectronics. – 2012. – V. 32, № 1. – P. 111–117.

204. Gajovic Nenad. Comparison of Two Enzyme Sequences for a NovelL-Malate Biosensor / N. Gajovic, A. Warsinke, F. W. Scheller // Journal of Chemical Technology & Biotechnology. – 1997. – V. 68, № 1. – P. 31–36.

205. Biosensors for L-malate and L-lactate based on solid binding matrix / J. Katrlík, A. Pizzariello, V. Mastihuba [et al.] // Analytica Chimica Acta. – 1999. – V. 379, № 1-2. – P. 193–200.

206. Development of a commercial amperometric biosensor electrode for the ketone D-3-hydroxybutyrate. / N. J. Forrow, G. S. Sanghera, S. J. Walters, J. L. Watkin // Biosensors & Bioelectronics. – 2005. – V. 20, № 8. – P. 1617–1625.

207. Biosensor for rapid determination of 3-hydroxybutyrate using bi-enzyme system. / R. C. H. Kwan, P. Y. T. Hon, W. C. Mak [et al.] // Biosensors & Bioelectronics. – 2006. – V. 21, № 7. – P. 1101–1106.

208. Amperometric biosensor for rapid measurement of 3-hydroxybutyrate in undiluted whole blood and plasma / C. J. McNeil, J. A. Spoors, J. M. Cooper [et al.] // Analytica Chimica Acta. – 1990. – V. 237. – P. 99–105.

209. Chaubey Asha. Application of polyaniline/sol-gel derived tetraethylorthosilicate films to an amperometric lactate biosensor. / A. Chaubey, K. K. Pande, B. D.

Malhotra // Analytical Sciences : the International Journal of the Japan Society for Analytical Chemistry. – 2003. – V. 19, № 11. – P. 1477–1480.

210. Direct electrochemistry of lactate dehydrogenase immobilized on silica sol-gel modified gold electrode and its application. / J. Di, J. Cheng, Q. Xu [et al.] // Biosensors and Bioelectronics. – 2007. – V. 23, № 5. – P. 682–687.

211. Electrochemical behavior of lactate dehydrogenase immobilized on “silica sol-gel/nanometre-sized tridecameric aluminum polycation” modified gold electrode and its application. / J. Cheng, D. Huang, J. Zhang [et al.] // The Analyst. – 2009. – V. 134, № 7. – P. 1392–1395.

212. Albareda-Sirvent M. Preliminary estimates of lactic and malic acid in wine using electrodes printed from inks containing sol–gel precursors / M. Albareda-Sirvent, A. . Hart // Sensors and Actuators B: Chemical. – 2002. – V. 87, № 1. – P. 73–81.

213. Blaedel W. J. Electrochemical oxidation of reduced nicotinamide adenine dinucleotide / W. J. Blaedel, R. A. Jenkins // Analytical Chemistry. – 1975. – V. 47, № 8. – P. 1337–1343.

214. Gorton Lo. Chemically modified electrodes for the electrocatalytic oxidation of nicotinamide coenzymes / L. Gorton // Journal of the Chemical Society, Faraday Transactions 1. – 1986. – V. 82, № 4. – P. 1245.

215. Gorton Lo. Electrochemistry of NAD(P)+/NAD(P)H, in: A.J. Bard (Ed.), Encyclopedia of Electrochemistry, Weinheim, Germany : Wiley-VCH Verlag, 2007. pp. 67–143.

216. Wang Joseph. Scanning tunneling microscopic probing of surface fouling during the oxidation of nicotinamide coenzymes / J. Wang, L. Angnes, T. Martinez // Bioelectrochemistry and Bioenergetics. – 1992. – V. 29, № 2. – P. 215–221.

217. Banks Craig E. Exploring the electrocatalytic sites of carbon nanotubes for NADH detection: an edge plane pyrolytic graphite electrode study. / C. E. Banks, R. G. Compton // The Analyst. – 2005. – V. 130, № 9. – P. 1232–1239.

218. Musameh Mustafa. Electrochemical activation of carbon nanotubes / M. Musameh, N. S. Lawrence, J. Wang // Electrochemistry Communications. – 2005. – V. 7, № 1. – P. 14–18.

219. Wooten Marilyn. Facilitation of NADH electro-oxidation at treated carbon nanotubes. / M. Wooten, W. Gorski // Analytical Chemistry. – 2010. – V. 82, № 4. – P. 1299–1304.

220. Chakraborty Sudip. Mediated electrocatalytic oxidation of bioanalytes and biosensing of glutamate using functionalized multiwall carbon nanotubes-biopolymer nanocomposite / S. Chakraborty, C. R. Raj // Journal of Electroanalytical Chemistry. – 2007. – V. 609, № 2. – P. 155–162.

221. Prieto-Simón Beatriu. Comparative study of electron mediators used in the electrochemical oxidation of NADH. / B. Prieto-Simón, E. Fàbregas // Biosensors & Bioelectronics. – 2004. – V. 19, № 10. – P. 1131–1138.

222. Comparative investigation of NADH electrooxidation at graphite electrodes modified with two new phenothiazine derivatives / V. Lates, D. Gligor, L. M. Muresan, I. C. Popescu // Journal of Electroanalytical Chemistry. – 2011. – V. 661, № 1. – P. 192–197.

223. Schlereth D. D. Surface-modified gold electrodes for electrocatalytic oxidation of NADH based on the immobilization of phenoxazine and phenothiazine derivatives on self-assembled monolayers / D. D. Schlereth, E. Katz, H.-L. Schmidt // Electroanalysis. – 1995. – V. 7, № 1. – P. 46–54.

224. Malinauskas A. Electrochemical study of the redox dyes Nile Blue and Toluidine Blue adsorbed on graphite and zirconium phosphate modified graphite / A. Malinauskas, T. Ruzgas, L. Gorton // Journal of Electroanalytical Chemistry. – 2000. – V. 484, № 1. – P. 55–63.

225. Glucose biosensor based on the incorporation of Meldola Blue / J. Kulys, H. E. Hansen, T. Buch-Rasmussen [et al.] // Analytica Chimica Acta. – 1994. – V. 288, № 3. – P. 193–196.

226. Alcohol biosensor based on alcohol dehydrogenase and Meldola Blue immobilized into a carbon paste electrode. / S. García Mullor, M. Sánchez-Cabezudo, A J. Miranda Ordieres, B. López Ruiz // Talanta. – 1996. – V. 43, № 5. – P. 779–784.

227. Amperometric determination of NADH at a Nile blue/ordered mesoporous carbon composite electrode / L. Zhu, R. Yang, X. Jiang, D. Yang // Electrochemistry Communications. – 2009. – V. 11, № 3. – P. 530–533.

228. New amperometric dehydrogenase electrodes based on electrocatalytic NADH-oxidation at poly (methylene blue)-modified electrodes / A. A. Karyakin, E. E. Karyakina, W. Schuhmann [et al.] // Electroanalysis. – 1994. – V. 6, № 10. – P. 821–829.

229. Biocatalysis and electrocatalysis at carbon paste electrodes doped by diaphorase-methylene green and diaphorase-meldola blue / J. Kulys, G. Gleixner, W. Schuhmann, H.-L. Schmidt // Electroanalysis. – 1993. – V. 5, № 3. – P. 201–207.

230. Silber A. Poly(methylene blue)-modified thick-film gold electrodes for the electrocatalytic oxidation of NADH and their application in glucose biosensors / A. Silber, N. Hampp, W. Schuhmann // Biosensors and Bioelectronics. – 1996. – V. 11, № 3. – P. 215–223.

231. Electrocatalytic detection of NADH and ethanol at glassy carbon electrode modified with electropolymerized films from methylene green / Z.-H. Dai, F.-X. Liu, G.-F. Lu, J.-C. Bao // Journal of Solid State Electrochemistry. – 2007. – V. 12, № 2. – P. 175–180.

232. Chi Qijin. Electrocatalytic oxidation of reduced nicotinamide coenzymes at Methylene Green-modified electrodes and fabrication of amperometric alcohol biosensors / Q. Chi, S. Dong // Analytica Chimica Acta. – 1994. – V. 285, № 1-2. – P. 125–133.

233. Adsorption of methylene blue dye onto carbon nanotubes: a route to an electrochemically functional nanostructure and its layer-by-layer assembled nanocomposite / Y. Yan, M. Zhang, K. Gong [et al.] // Chemistry of Materials. – 2005. – V. 17, № 13. – P. 3457–3463.

234. Adsorption behavior of methylene blue on carbon nanotubes. / Y. Yao, F. Xu, M. Chen [et al.] // Bioresource Technology. – 2010. – V. 101, № 9. – P. 3040–3046.

235. Lawrence Nathan S. Chemical adsorption of phenothiazine dyes onto carbon nanotubes: Toward the low potential detection of NADH / N. S. Lawrence, J. Wang // Electrochemistry Communications. – 2006. – V. 8, № 1. – P. 71–76.

236. Synergistic effect of mediator-carbon nanotube composites for dehydrogenases and peroxidases based biosensors. / A. Arvinte, L. Rotariu, C. Bala, A. M. Gurban // Bioelectrochemistry (Amsterdam, Netherlands). – 2009. – V. 76, № 1-2. – P. 107–114.

237. Evaluation of Meldola Blue-Carbon Nanotube-Sol-Gel Composite for Electrochemical NADH Sensors and Their Application for Lactate Dehydrogenase-Based Biosensors / A. Arvinte, A. M. Sesay, V. Virtanen, C. Bala // Electroanalysis. – 2008. – V. 20, № 21. – P. 2355–2362.

238. Methylene green electrodeposited on SWNTs-based “bucky” papers for NADH and l-malate oxidation. / C. W. Narváez Villarrubia, R. A. Rincón, V. K. Radhakrishnan [et al.] // ACS Applied Materials & Interfaces. – 2011. – V. 3, № 7. – P. 2402–2409.

239. Single-walled carbon nanotubes functionalized with poly(nile blue A) and their application to dehydrogenase-based biosensors / P. Du, S. Liu, P. Wu, C. Cai // Electrochimica Acta. – 2007. – V. 53, № 4. – P. 1811–1823.

240. Kosmulski Marek. Chemical Properties of Material Surfaces / M. Kosmulski. – New York : CRC Press, 2001. – P. 776.

241. Critical Effect of Polyelectrolytes on the Electrochemical Response of Dehydrogenases Entrapped in Sol-Gel Thin Films / Z. Wang, M. Etienne, G. W. Kohring, A. Walcarius // Electroanalysis. – 2010. – V. 22, № 17-18. – P. 2092–2100.

242. Shui Jianglan. Platinum nanowires produced by electrospinning. / J. Shui, J. C. M. Li // Nano Letters. – 2009. – V. 9, № 4. – P. 1307–1314.

243. Mechanism of Soap-Free Emulsion Polymerization of Styrene and 4-Vinylpyridine: Characteristics of Reaction in the Monomer Phase, Aqueous Phase,

and Their Interface / H. Ni, Y. Du, G. Ma [et al.] // Macromolecules. – 2001. – V. 34, № 19. – P. 6577–6585.

244. Zolotov U. A. Fundamentals of analytical chemistry / U. A. Zolotov. – M. : Vyshaya shkola, 2002. – P. 351.

245. WSXM: a software for scanning probe microscopy and a tool for nanotechnology. / I. Horcas, R. Fernández, J. M. Gómez-Rodríguez [et al.] // The Review of Scientific Instruments. – 2007. – V. 78, № 1. – P. 013705.

246. SECM-based automate equipped with a shearforce detection for the characterization of large and complex samples / M. Etienne, B. Layoussifi, T. Giornelli, D. Jacquet // Electrochemistry Communications. – 2012. – V. 15, № 1. – P. 70–73.

247. Cornish-Bowden Athel. Principles of Enzyme Kinetics / A. Cornish-Bowden. – M. : Mir, 1979. – P. 280.

248. Lineweaver Hans. The Determination of Enzyme Dissociation Constants / H. Lineweaver, D. Burk // Journal of the American Chemical Society. – 1934. – V. 56, № 3. – P. 658–666.

249. Adsorption behavior of methylene blue and its congeners on a stainless steel surface. / K. Imamura, E. Ikeda, T. Nagayasu [et al.] // Journal of Colloid and Interface Science. – 2002. – V. 245, № 1. – P. 50–57.

250. Hall SB. Electrochemical oxidation of hydrogen peroxide at platinum electrodes. Part 1. An adsorption-controlled mechanism / S. Hall, E. Khudaish, A. Hart // Electrochimica Acta. – 1997. – V. 43, № 5-6. – P. 579–588.

251. Comparisons of platinum, gold, palladium and glassy carbon as electrode materials in the design of biosensors for glutamate. / R. D. O'Neill, S.-C. Chang, J. P. Lowry, C. J. McNeil // Biosensors & Bioelectronics. – 2004. – V. 19, № 11. – P. 1521–1528.

252. Hall S. Electrochemical oxidation of hydrogen peroxide at platinum electrodes. Part II: effect of potential / S. Hall, E. Khudaish, A. Hart // Electrochimica Acta. – 1998. – V. 43, № 14-15. – P. 2015–2024.

253. In situ chemical reductive growth of platinum nanoparticles on glass slide for the mass fabrication of biosensors. / M. Yang, F. Qu, Y. Lu [et al.] // Talanta. – 2008. – V. 74, № 4. – P. 831–835.

254. Fabrication and electrical properties of platinum nanofibres by electrostatic spinning / H. Lee, S. Choi, S. M. Jo [et al.] // Journal of Physics D: Applied Physics. – 2009. – V. 42, № 12. – P. 125409.

255. Li D. Electrospinning of Nanofibers: Reinventing the Wheel? / D. Li, Y. Xia // Advanced Materials. – 2004. – V. 16, № 14. – P. 1151–1170.

256. Trasatti S. Real surface area measurements in electrochemistry / S. Trasatti, O. Petrii // Journal of Electroanalytical Chemistry. – 1992. – V. 327, № 1-2. – P. 353–376.

257. Amatore C. Charge transfer at partially blocked surfaces: A model for the case of microscopic active and inactive sites / C. Amatore, J. Saveant // Journal of Electroanalytical Chemistry. – 1983. – V. 147. – P. 39–51.

258. De Leo Manuela. 3D-Ensembles of Gold Nanowires: Preparation, Characterization and Electroanalytical Peculiarities / M. De Leo, A. Kuhn, P. Ugo // Electroanalysis. – 2007. – V. 19, № 2-3. – P. 227–236.

259. Hall S. Electrochemical oxidation of hydrogen peroxide at platinum electrodes. Part IV: phosphate buffer dependence / S. Hall // Electrochimica Acta. – 1999. – V. 44, № 25. – P. 4573–4582.

260. Menon Vinod P. Fabrication and Evaluation of Nanoelectrode Ensembles / V. P. Menon, C. R. Martin // Analytical Chemistry. – 1995. – V. 67, № 13. – P. 1920–1928.

261. Handbook of Electrochemistry / C. G. Zoski, ed. – Amsterdam : Elsevier, 2007. – P. 892.

262. Johnston David A. The electrochemistry of hydrogen peroxide on evaporated gold/palladium composite electrodes. Manufacture and electrochemical characterization / D. A. Johnston, M. F. Cardosi, D. H. Vaughan // Electroanalysis. – 1995. – V. 7, № 6. – P. 520–526.

263. Amperometric biosensors based on gold nanoparticles-decorated multiwalled carbon nanotubes-poly(diallyldimethylammonium chloride) biocomposite for the determination of choline / X. Qin, H. Wang, X. Wang [et al.] // Sensors and Actuators B: Chemical. – 2010. – V. 147, № 2. – P. 593–598.

264. Using gold nanorods to enhance the current response of a choline biosensor / X. Ren, F. Tang, R. Liao, L. Zhang // Electrochimica Acta. – 2009. – V. 54, № 28. – P. 7248–7253.

265. Identification and properties of the prosthetic group of choline oxidase from Alcaligenes sp. / M. Ohta-Fukuyama, Y. Miyake, S. Emi, T. Yamano // Journal of Biochemistry. – 1980. – V. 88, № 1. – P. 197–203.

266. Hamaker H. C. Formation of a deposit by electrophoresis / H. C. Hamaker // Transactions of the Faraday Society. – 1940. – V. 35. – P. 279–287.

267. Electrochemical Behavior and Electrocatalytic Study of the Methylene Green Coated on Modified Silica Gel / A. R. de Lucca, A. de S. Santos, A. C. Pereira [et al.] // Journal of Colloid and Interface Science. – 2002. – V. 254, № 1. – P. 113–119.

268. Oriented Mesoporous Silica Films Obtained by Electro-Assisted Self-Assembly (EASA) / A. Goux, M. Etienne, E. Aubert [et al.] // Chemistry of Materials. – 2009. – V. 21, № 4. – P. 731–741.

269. Factors affecting the preparation and properties of electrodeposited silica thin films functionalized with amine or thiol groups. / E. Sibottier, S. Sayen, F. Gaboriaud, A. Walcarius // Langmuir : the ACS Journal of Surfaces and Colloids. – 2006. – V. 22, № 20. – P. 8366–8373.

270. Schauder S. Polyol metabolism of Rhodobacter sphaeroides: biochemical characterization of a short-chain sorbitol dehydrogenase. / S. Schauder, K. H. Schneider, F. Giffhorn // Microbiology (Reading, England). – 1995. – V. 141, № 8. – P. 1857–1863.

271. Walcarius Alain. Ordered porous thin films in electrochemical analysis / A. Walcarius, A. Kuhn // TrAC Trends in Analytical Chemistry. – 2008. – V. 27, № 7. – P. 593–603.

272. Bartlett Philip N. Electrochemical deposition of macroporous platinum, palladium and cobalt films using polystyrene latex sphere templates / P. N. Bartlett, P. R. Birkin, M. A. Ghanem // Chemical Communications. – 2000. – № 17. – P. 1671–1672.

273. Macroporous ultramicroelectrodes for improved electroanalytical measurements. / R. Szamocki, A. Velichko, C. Holzapfel [et al.] // Analytical Chemistry. – 2007. – V. 79, № 2. – P. 533–539.

274. Tailored mesostructuring and biofunctionalization of gold for increased electroactivity. / R. Szamocki, S. Reculusa, S. Ravaine [et al.] // Angewandte Chemie (International Ed. in English). – 2006. – V. 45, № 8. – P. 1317–1321.

275. Multiscale-tailored bioelectrode surfaces for optimized catalytic conversion efficiency. / Y. Bon Saint Côme, H. Lalo, Z. Wang [et al.] // Langmuir : the ACS Journal of Surfaces and Colloids. – 2011. – V. 27, № 20. – P. 12737–12744.

276. Walcarius Alain. Electrocatalysis, sensors and biosensors in analytical chemistry based on ordered mesoporous and macroporous carbon-modified electrodes / A. Walcarius // TrAC Trends in Analytical Chemistry. – 2012. – V. 38. – P. 79–97.

277. Novel Three-Dimensional Electrodes: Electrochemical Properties of Carbon Nanotube Ensembles / J. Li, A. Cassell, L. Delzeit [et al.] // The Journal of Physical Chemistry B. – 2002. – V. 106, № 36. – P. 9299–9305.

278. Carbon nanotube sponges. / X. Gui, J. Wei, K. Wang [et al.] // Advanced Materials. – 2010. – V. 22, № 5. – P. 617–621.

279. Gutiérrez María C. Ice-Templated Materials: Sophisticated Structures Exhibiting Enhanced Functionalities Obtained after Unidirectional Freezing and Ice-Segregation-Induced Self-Assembly / M. C. Gutiérrez, M. L. Ferrer, F. del Monte // Chemistry of Materials. – 2008. – V. 20, № 3. – P. 634–648.

280. Engineered macroporosity in single-wall carbon nanotube films. / R. K. Das, B. Liu, J. R. Reynolds, A. G. Rinzler // Nano Letters. – 2009. – V. 9, № 2. – P. 677–683.

281. Carbon nanotube networks patterned from aqueous solutions of latex bead carriers / C. Dionigi, P. Stoliar, G. Ruani [et al.] // Journal of Materials Chemistry. – 2007. – V. 17, № 35. – P. 3681–3686.

282. A Preliminary Study on the Effect of Macro Cavities Formation on Properties of Carbon Nanotube Bucky-Paper Composites / L. F. Dumée, K. Sears, J. Schütz [et al.] // Materials. – 2011. – V. 4, № 3. – P. 553–561.

283. Yuan Zhong-Yong. Insights into hierarchically meso–macroporous structured materials / Z.-Y. Yuan, B.-L. Su // Journal of Materials Chemistry. – 2006. – V. 16, № 7. – P. 663–677.

284. Critical particle concentration in electrophoretic deposition / S. Radice, C. R. Bradbury, J. Michler, S. Mischler // Journal of the European Ceramic Society. – 2010. – V. 30, № 5. – P. 1079–1088.

285. Prodromidis Mamas I. Enzyme Based Amperometric Biosensors for Food Analysis / M. I. Prodromidis, M. I. Karayannis // Electroanalysis. – 2002. – V. 14, № 4. – P. 241–261.

286. Biosensor for the determination of sorbitol based on molecularly imprinted electrosynthesized polymers. / L. Feng, Y. Liu, Y. Tan, J. Hu // Biosensors & Bioelectronics. – 2004. – V. 19, № 11. – P. 1513–1519.

287. Analysis of sorbitol, galactitol, and myo-inositol in lens and sciatic nerve by high-performance liquid chromatography. / I. Miwa, M. Kanbara, H. Wakazono, J. Okuda // Analytical Biochemistry. – 1988. – V. 173, № 1. – P. 39–44.

288. Islam Md Shahidul. Sorbitol-based osmotic diarrhea: possible causes and mechanism of prevention investigated in rats. / M. S. Islam, E. Sakaguchi // World Journal of Gastroenterology : WJG. – 2006. – V. 12, № 47. – P. 7635–7641.

289. HPLC with pulsed amperometric detection for sorbitol as a biomarker for diabetic neuropathy. / H.-J. Sim, J.-S. Jeong, H.-J. Kwon [et al.] // Journal of Chromatography. B, Analytical Technologies in the Biomedical and Life Sciences. – 2009. – V. 877, № 14-15. – P. 1607–1611.

290. Turner A. Biosensors: Fundamentals and Applications / A. Turner, I. Karube, G. Wilson. – M. : Mir, 1992. – P. 614.

291. Pletnev M U. Cosmetics and hygiene detergents / M. U. Pletnev. – M. : Himiya, 1990. – P. 272.

292. Xu Jinhuang. Kinetics and mechanism of the reaction of aqueous iron(III) with ascorbic acid / J. Xu, R. B. Jordan // Inorganic Chemistry. – 1990. – V. 29, № 21. – P. 4180–4184.

293. Is the oxidation of L-ascorbic acid by aquated iron(III) ions in acidic aqueous solution substitution- or electron-transfer-controlled? A combined chloride, pH, temperature, and pressure dependence study / B. Baensch, P. Martinez, D. Uribe [et al.] // Inorganic Chemistry. – 1991. – V. 30, № 24. – P. 4555–4559.

294. State standard 25268-82. Confectionery Products. Methods for determination of xylitol and sorbitol. 2004.

295. Devyatin V. A. Chemical analysis methods in the production of vitamins / V. A. Devyatin. – M. : Medicina, 1964. – P. 360.

296. The International Pharmacopoeia / Geneva: World Health Organization , 1983. – P. 364.

297. Electro-oxidation of d-sorbitol on platinum in perchloric medium: A voltammetric study / I. Fonseca, M. I. S. Lopes, J. L. Santos, L. Proença // Electrochimica Acta. – 1995. – V. 40, № 17. – P. 2701–2706.

298. Electrocatalytic oxidation of d-sorbitol on platinum in acid medium: analysis of the reaction products / L. Proença, M. I. S. Lopes, I. Fonseca [et al.] // Journal of Electroanalytical Chemistry. – 1997. – V. 432, № 1-2. – P. 237–242.

299. Skvortsova L.I. Voltammetric determination of sorbite at a mechanically renewed copper electrode / L. I. Skvortsova, O. V. Karunina // Journal of Analytical Chemistry. – 2009. – V. 64, № 10. – P. 1066-1071.

300. Selective determination of D-sorbitol and D-mannitol in foodstuffs by ion chromatography with polarized photometric detection / A. Yamamoto, H. Ohmi, A.

Matsunaga [et al.] // Journal of Chromatography A. – 1998. – V. 804, № 1-2. – P. 305–309.

301. Soga Tomoyoshi. Determination of carbohydrates in food samples by capillary electrophoresis with indirect UV detection / T. Soga, M. Serwe // Food Chemistry. – 2000. – V. 69, № 3. – P. 339–344.

302. Pospíšilová Marie. Separation and determination of pharmaceutically important polyols in dosage forms by capillary isotachophoresis / M. Pospíšilová, M. Polášek, J. Procházka // Journal of Chromatography A. – 1997. – V. 772, № 1-2. – P. 277–282.

303. Bergmeyer Hans Ulrich. Methods of Enzymatic Analysis, Vol. 6, Metabolites 1: Carbohydrates / H. U. Bergmeyer. – Wiley-VCH, 1984. – P. 701.

304. D-Sorbitol/Xylitol Colorimetric method. n.d.

305. Megazyme International. D-sorbitol/xylitol assay procedure. 2011.

306. Report. Dietary Reference Intakes for Thiamin, Riboflavin, Niacin, Vitamin B6, Folate, Vitamin B12, Pantothenic Acid, Biotin, and Choline / Report. – Washington : National Academic Press, 1998. – P. 564.

307. Indirect electrocatalytic determination of choline by monitoring hydrogen peroxide at the choline oxidase-prussian blue modified iron phosphate nanostructures. / H. Zhang, Y. Yin, P. Wu, C. Cai // Biosensors & Bioelectronics. – 2012. – V. 31, № 1. – P. 244–250.

308. Zhang Zhanxia. A sensitive choline biosensor using Fe(3)O(4) magnetic nanoparticles as peroxidase mimics. / Z. Zhang, X. Wang, X. Yang // The Analyst. – 2011. – P. 4960–4965.

309. Yamada H. Properties of choline oxidase of Cylindrocarpon didymum M-1 / H. Yamada, N. Mori, Y. Tani // Agricultural and Biological Chemistry. – 1979. – V. 43, № 10. – P. 2173–2177.

310. Situmorang Manihar. Immobilisation of enzyme throughout a polytyramine matrix: a versatile procedure for fabricating biosensors / M. Situmorang, J. J. Gooding, D. Hibbert // Analytica Chimica Acta. – 1999. – V. 394. – P. 211–223.

311. A Pyruvate Oxidase Electrode Based on an Electrochemically Deposited Redox Polymer / N. Gajovic, K. Habermüller, A. Warsinke [et al.] // Electroanalysis. – 1999. – V. 11, № 18. – P. 1377–1383.

312. Ascorbic acid sensor based on ion-sensitive field-effect transistor modified with MnO_2 nanoparticles / X.-L. Luo, J.-J. Xu, W. Zhao, H.-Y. Chen // Analytica Chimica Acta. – 2004. – V. 512, № 1. – P. 57–61.

313. Woollard D C. Determination of choline in milk and infant formulas by enzymatic analysis: collaborative study. / D. C. Woollard, H. E. Indyk // Journal of AOAC International. – 2000. – V. 83, № 1. – P. 131–138.

314. Engel RW. Modified methods for the chemical and biological determination of choline / R. Engel // Journal of Biological Chemistry. – 1942. – V. 144. – P. 701–710.

315. Beattie FJR. A colorimetric method for the determination of choline and acetylcholine in small amounts / F. Beattie // Biochemical Journal. – 1936. – P. 1554–1559.

316. Simultaneous determination of free carnitine and total choline by liquid chromatography/mass spectrometry in infant formula and health-care products: single-laboratory validation. / P. Andrieux, T. Kilinc, C. Perrin, E. Campos-Giménez // Journal of AOAC International. – 2008. – V. 91, № 4. – P. 777–785.

317. Quantitation of Choline and Its Metabolites in Tissues and Foods by Liquid Chromatography/Electrospray Ionization-Isotope Dilution Mass Spectrometry / H. Koc, M.-H. Mar, A. Ranasinghe [et al.] // Analytical Chemistry. – 2002. – V. 74, № 18. – P. 4734–4740.

318. Measurement of choline and choline metabolite concentrations using high-pressure liquid chromatography and gas chromatography-mass spectrometry. / E. A. Pomfret, K. A. DaCosta, L. L. Schurman, S. H. Zeisel // Analytical Biochemistry. – 1989. – V. 180, № 1. – P. 85–90.

319. Saucerman J R. Quantitative gas chromatographic headspace determination of choline in adult and infant formula products. / J. R. Saucerman, C. E. Winstead, T.

M. Jones // Journal of the Association of Official Agricultural Chemists. – 1984. – V. 67, № 5. – P. 982–985.

320. Dorsey John G. Determination of choline in soybean meal by liquid chromatography with the ion-exchange membrane detector / J. G. Dorsey, L. C. Hansen, T. W. Gilbert // Journal of Agricultural and Food Chemistry. – 1980. – V. 28, № 1. – P. 28–32.

321. Carter Nicole. The determination of choline in vitamin preparations, infant formula and selected foods by capillary zone electrophoresis with indirect ultraviolet detection. / N. Carter, V. C. Trenerry // Electrophoresis. – 1996. – V. 17, № 10. – P. 1622–1626.

322. Holmes H C. Changes in the choline content of human breast milk in the first 3 weeks after birth / H. C. Holmes, G. J. A. I. Snodgrass, R. A. Iles // European Journal of Pediatrics. – 2000. – V. 159, № 3. – P. 198–204.

323. Horwitz William. Official Methods of Analysis of the Association of Official Analytical Chemists / W. Horwitz. – Aoac International, 2005. .

324. A sensitive enzyme-based colorimetric assay for choline-containing phospholipids / S. M. Khan, T. M. Khan, R. D. Wells [et al.] // Journal of the Science of Food and Agriculture. – 1992. – V. 58, № 3. – P. 443–445.

325. Rader Jeanne I. Extension of AOAC official method 999.14 (choline in infant formula and milk) to the determination of choline in dietary supplements. / J. I. Rader, C. M. Weaver, M. W. Trucksess // Journal of AOAC International. – 2004. – V. 87, № 6. – P. 1297–1304.

326. Amperometric choline biosensors based on multi-wall carbon nanotubes and layer-by-layer assembly of multilayer films composed of Poly(diallyldimethylammonium chloride) and choline oxidase / X. Qin, H. Wang, X. Wang [et al.] // Materials Science and Engineering: C. – 2009. – V. 29, № 4. – P. 1453–1457.

327. Pt based enzyme electrode probes assembled with Prussian Blue and conducting polymer nanostructures. / A. Curulli, F. Valentini, S. Orlanduci [et al.] // Biosensors & Bioelectronics. – 2004. – V. 20, № 6. – P. 1223–1232.

328. Polyvinylferrocenium immobilized enzyme electrode for choline analysis / H. Gülce, Y. S. Aktaş, A. Gülce, A. Yıldız // Enzyme and Microbial Technology. – 2003. – V. 32, № 7. – P. 895–899.

329. Construction and Analytical Characterization of Prussian Blue-Based Carbon Paste Electrodes and Their Assembly as Oxidase Enzyme Sensors / D. Moscone, D. D'Ottavi, D. Compagnone [et al.] // Analytical Chemistry. – 2001. – V. 73, № 11. – P. 2529–2535.

330. Reynolds E C. Contents of toothpaste - safety implications / E. C. Reynolds // Australian Prescriber. – 1994. – V. 14, № 2. – P. 49–51.

331. Dorn G A. The study of consumer properties of pastry with sugar substitutes / G. A. Dorn, O. R. Sidorova // Polzunovskiy Vestnik. – 2012. – V. 2, № 2. – P. 131–134.

332. Bahador A. Effect of xylitol on cariogenic and beneficial oral streptococci: a randomized, double-blind crossover trial. / A. Bahador, S. Lesan, N. Kashi // Iranian Journal of Microbiology. – 2012. – V. 4, № 2. – P. 75–81.